Australia's National
Science Agency

# G-PST Topic 5: The Role of Inverter-base Resources During System Restoration

Stage 3 Final Report

Prepared by Aurecon
Reference: 524175

Revision: 1C
7 June 2024

Bringing ideas to life

AUSTRALIAN ENERGY MARKET OPERATOR

# Document control record

Document prepared by:

**Aurecon Australasia Pty Ltd**

ABN 54 005 139 873

Aurecon Centre
Level 8, 850 Collins Street
Docklands, Melbourne VIC 3008

PO Box 23061
Docklands VIC 8012
Australia

**T** +61 3 9975 3000
**F** +61 3 9975 3444
**E** melbourne@aurecongroup.com
**W** aurecongroup.com



| **Document control** | | | | | | |
|---|---|---|---|---|---|---|
| **Report title** | | Final Report | | | | |
| **Document code** | | | **Project number** | | 524175 | |
| **File path** | | Https://aurecongroup.sharepoint.com/sites/524175/5_WorkingFiles/File Share/G-PST_Topic_5_Final_Report_2024-06-07/G-PST_Topic_5_Final_Report_Stage_3_2024_SME_Comments_Addressed.docx | | | | |
| **Client** | | CSIRO | | | | |
| **Client contact** | | John Ward | **Client reference** | | | |
| **Rev** | **Date** | **Revision details/status** | **Author** | **Reviewer** | **Verifier** (if required) | **Approver** |
| 0 | 2024-01-22 | First internal draft | N. Crooks | B. Badrzadeh | | B. Badrzadeh |
| 1A | 2024-02-19 | First draft report issued | N. Crooks | B. Badrzadeh | | B. Badrzadeh |
| 1B | 2024-05-15 | First copy final report issued | M. Ahmed<br>E. Piubellini | N. Crooks | | M. Fard |
| 1C | 2024-06-06 | Final report CSIRO and SME review comments addressed. | M. Ahmed | N. Crooks | | N. Crooks |
| **Current revision** | | **1C** | | | | |

| **Approval** | | | |
|---|---|---|---|
| Name | Moudud Ahmed | Name | Nathan Crooks |
| Title | Engineer, Power Systems | Title | Associate, Power Systems |

# Contents

# Figures

# Tables

# Acknowledgments

The research presented in this report was funded by CSIRO, Australia's national science agency, and carried out as part of CSIRO's contribution to the initiatives of the Global Power System Transformation (GPST) Consortium. This research supports Australia's transition to a stable, secure and affordable power system and contributes to critical research identified by the Consortium required to accelerate the decarbonisation of our electricity grid.

The research presented in this report was supported by the Australian Energy Market Operator, a stakeholder in the GPST Consortium, who provided access to confidential network and generating system models under confidentiality agreement, and subject matter expert contribution of research findings.

# Executive summary

This report is prepared as the Stage 3 part of Topic 5 of Australia's Global Power System Transformation (G-PST) Research Roadmap[1], with the intent of understanding and expanding system restoration capabilities in the National Electricity Market (NEM). As penetration of inverter-based resources (IBRs) increases throughout the NEM and existing synchronous coal and gas generators retire, providers of black start and system restart are diminishing. This project investigates the role IBRs can take in system restart, especially under high or 100% IBR penetration conditions, continuing from existing research performed through 2022 and 2023. The following key topics are the focus of the 2023-24 research program on Topic 5:

- Investigating the stability boundary conditions of restarted islands which are inclusive of multiple non-black start IBR support devices.
- Analysis of the impact of and, where possible, reasonable range for control system parameters of IBR during system restoration.
- Assessment of the impact of location of black start devices, considering proximity to load centres, synchronous generators, and non-black start IBR.
- Evaluation of the challenges and opportunities with synchronisation of two or more restarted islands, considering both synchronous and IBR-only islands during system restoration.
- Observe the impact of distributed energy resources (DER) on the system restart process, with key focus on attempting to determine thresholds for levels of DER to maintain stability during system restart.
- Recommendations on any technical requirements or regulation changes, or otherwise, that should be considered for system restoration under high or 100% penetration of IBRs.

Studies were conducted utilising detailed vendor specific or site specific electro-magnetic transient (EMT) models under confidentiality agreements with equipment manufacturers and Australian energy market operator (AEMO). Detailed network models required for system restart studies were provided by AEMO and configured to reflect a plausible future network of the North Queensland (NQLD) region, inclusive of a future renewable energy zone (REZ). Key findings across the hundreds of simulations and sensitivities performed were:

- Grid forming (GFM) black start IBR to grid following (GFL) IBR support device ratio of 1 : 10 is recommended as the (GFL) upper limit for system restoration. The 1 : 10 ratio was demonstrated as stable for both system restoration and application of a network fault during the restoration process. The 1 : 10 ratio emphasises that GFM black start IBR are extremely viable for system restoration, although energy availability (duration of support) needs to be considered for battery energy storage systems (BESS).

[1] More details can be found at https://www.csiro.au/en/research/technology-space/energy/G-PST-Research-Roadmap.

- Voltage and frequency control and protection settings of IBRs are suitable for system restoration without alteration from system normal settings, although adjustment of frequency protection and frequency droop can provide additional benefit. Changes to these settings can be used to optimise the contribution of different devices to frequency management, which is recommended to alleviate GFM black start BESS usage in order to maintain sufficient energy reserves for transient (in the 0 s to 2 s timeframe) response.
- Inertia and damping characteristics of GFM IBRs should be optimised for system restart conditions, but typical settings observed under system normal conditions do not present any immediate instability or other concern under system restart conditions.
- GFM black start device location near synchronous generators facilitates the option for soft energisation of the synchronous generator, which may create viable system restart scenarios despite a synchronous generator grid-tie transformer being too large for a GFM black start device to energise.
- Synchronisation of two separate restarted islands is viable between both synchronous only and IBR-only islands, with significant but manageable transients observed on synchronisation, but no sustained oscillations or instability present following synchronisation.
- Under- and over-voltages experienced when energising aggregated DER and load models are driven by instantaneous connection of the aggregate models. Reconnect functionality with ramped active and reactive power response of DER and load models over seconds and minutes is required to fully capture the impact to system restart and to capture how voltage management would need to be implemented.
- No control system interactions or network instabilities were observed when connecting DER, although 20% or greater of the aggregated DER was observed to disconnect following a fault. The BESS plants within the system compensated for this behaviour, but BESS energy management will need to be a key focus when managing DER during system restart in future.

Significant further research is still needed to guide the power industry on future options for system restoration in high penetration and 100% IBR networks. Future recommended work focuses on protection relays, network protection schemes, and different control structures and operating modes for IBRs such as static compensator (STATCOM) mode for solar farms (SFs) and different grid-following control implementations.

# 1 Introduction

This report is prepared as part of the Global Port System Transformation (G-PST) research Topic 5 *Restoration and Black Start – Creating new procedures for black starting and restoring a power system with high or 100% IBR penetrations*. This report provides the findings of research completed as part of the 2023-24 portion of the Topic 5 research plan, extending on the findings from the 2022-23 portion of the plan.

## 1.1 Significance

The importance of this research topic stems from the fact that a black start capability typically cannot be procured by AEMO unless that service is offered by a generator, and a service cannot be reliably offered if the capability has not been considered and assessed during the plant design. Understanding the power system restoration needs, with rapidly changing power systems and generation mix, would provide justification to support the necessary modifications in design and requirements of new IBRs yet to be connected. Retrofitting the capability after a few years will be significantly more expensive, if possible at all. The same applies to network elements, such as protective relays.

The outcome of these studies will assist the Australian power industry to develop more specific technical and regulatory requirements and incentives for the expected performance of grid-forming and grid-following inverters during system restoration. This is recognising that black start conditions are vastly different and more onerous compared to system normal conditions, and as such additional capabilities which are not needed during normal operating conditions, beyond the self-start ability, will likely be required. At the same time the objective of this research is to identify the extent to which IBR will need to emulate, or otherwise, the natural and inherent response of a synchronous machine during system restoration, avoiding expensive and unnecessary cost of additional hardware for the IBR.

## 1.2 Previous stages

The proposed 2023-24 research program aims to extend the work done in 2022-2023 using numerous power systems computer aided design (PSCAD™)/electromagnetic transient including DC (EMTDC™ ) simulation studies. The key objectives of the 2022-2023 works were to determine the capabilities and limitations of emerging black start sources and compare them to power system needs under scenarios with very few or no synchronous generators online. The first Stage (Stage 1) was based on simplified, but realistic network models, to assess the capabilities and limitations of various black start options and to develop high-level functional specifications for the use of IBR during system restoration based on results obtained from several hundreds of PSCAD™/EMTDC™ simulation studies. The second Stage (Stage 2) of the project focused on system restart capabilities, needs, constraints, and reliance on the wider power system as far as a REZ is concerned. North Queensland Renewable Energy Zone (NQREZ) was chosen as discussed with CSIRO and AEMO. The Stage 2 results confirmed viable options for using grid-forming inverters and grid-following inverters in conjunction with a synchronous condenser as additional black start providers beyond existing synchronous generators, emphasising that grid-forming inverters out-performed other black start devices.

## 1.3 Stage 3 focus areas

Stage 3, the focus of this report, aims to delve into greater details and address some of the residual questions and high priority areas from the 2021 roadmap that could not be addressed in the 2022-23 work due to time constraints. It also expands on the types of network elements analysed, with inclusion of distributed energy resources and composite loads. Wide-area PSCAD$^{TM}$/EMTDC$^{TM}$ models from the previous stage were used as re-permitted by AEMO. Stage 3 studies placed an emphasis on investigating restarted islands containing two to five generating systems, in comparison to the 2022-23 work which focussed on impacts to black starting a single device and forming a two-device island from load and generation.

### 1.3.1 Large-scale IBR

#### Grid-following inverters

The 2022-23 work focussed on the viability of energising a single grid-following inverter as a support device during system restoration. Further progress covered in this report investigated the viability of multiple grid-following inverters as support devices being utilised in the restoration process, comparing different resource types such as wind, solar and batteries, as well as varying ratios of size of black start device to supported grid-following devices. Both the device energisation, where model detail permitted it, and the stability of the formed island were studied. Sensitivity studies analysing the impact of various control system parameters on the system restart process and restarted island resilience and stability were performed to define permittable boundaries to system restoration utilising IBRs.

#### Grid-forming inverters

Grid-forming inverters have been considered in previous work on Topic 5 as black start providers, only studying their ability to facilitate restart of a black system by energising single elements (e.g., grid-following device, transformer, transmission line, load). To provide further insight and an expansion of requirements for grid-forming black start devices, the following key questions are being investigated.

- What are the boundary conditions for stability of a grid-forming inverter when operating as a black start device and restarting a system?
- How do the control system parameters of a grid-forming inverter influence the resilience and stability of a restarted island?
- How do grid-forming inverters operating as a black start device interact with other black start devices when synchronising an island to another, already energised, power system?

### 1.3.2 Bottom-up restoration

The location of black start devices plays a large role in their suitability for and the efficiency of system restart provision, often determining whether a plant is offered a System Restart Ancillary Service (SRAS) contract or not. With the expected future wide-spread installation of black-start capable IBR devices, specifically grid-forming batteries, location will continue to play a critical role in identifying the black-start devices which provide the greatest system restart benefit to the network. Proximity to the following three system aspects is considered in this report to determine how it impacts system restart capability, what failure mechanisms are observed and whether proximity to certain network elements provides greater stability during system restoration.

- Load centres.
- Areas of concentration of synchronous generators.
- Areas of concentration of non-black start IBR.

Additionally, due to the larger number and often smaller size of black-start capable IBR than traditional synchronous generators, black start devices provide the possibility to independently restart multiple smaller islands and subsequently connect them together. In contrast, traditional system restart will grow a single island until it subsequently reconnects with an existing intact network or restarts the entire system itself. Synchronising smaller islands will result in an interaction between multiple black start providers, and whether instabilities or undesirable responses are introduced is of particular interest. It is also vital to understand if there are any required change to settings or IBR mode to facilitate connection of two restarted islands.

### 1.3.3 Technical regulatory requirements

IBR-only islands have the potential for very different dynamic behaviour and requirements compared to a synchronous system, whether intact or an island. Understanding the operational boundaries of an IBR only network during system restoration gives direction to both equipment design and network operation. The following scenarios and questions are considered in this report.

- Device and generating system requirements in an IBR dominated or IBR only island.
  - Are system normal voltage and frequency control requirements suitable for system restart, and are there recommended adjustments to improve system restart viability?
  - Are fault ride through performance requirements for IBRs during system restoration too restrictive or too lenient and what are recommended alternative standards?
  - What key characteristics are required from a black-start IBR to be considered suitable for system restoration?
- Power system requirements in an IBR dominated or IBR only island.
  - Are voltage requirements for normal operation too restrictive or too lenient during system restoration and what are recommended alternative limits?

Studies attempting to answer the above questions, and more, overlap with analysis of large-scale IBR and bottom-up restoration. Analysis of the broader set of studies throughout this entire report extrapolate findings to make recommendations for changes to technical and regulatory requirements.

### 1.3.4 Impact of distributed energy resources (DER) and loads

Loads within the Australian power system have changed significantly over the last 20–30 years, with a greater uptake of inverter-based loads for greater controllability and efficiency. At the same time, DER such as rooftop photovoltaic (PV) and home battery energy storage systems (BESS) have seen widespread adoption by households. Changes to normal network operations due to DER and changing load mix have already taken effect. Traditional non-inverter loads (such as induction motors) have an inherent damping characteristic[2] which is critical during conventional system restart to form a stable island. IBRs such as DER, in comparison, are prone to instabilities under weak system strength conditions and do not exhibit the same damping behaviour. With the increase of inverter-based loads and DER, how the system responds during restart needs to be understood, both from an operational perspective as well as for the impact to power system transient behaviour. This report focuses on the power system transient behaviour driven by composite loads, comprising representation of inverter-based load, and DER during network contingency events as well as how much of the load and DER is disconnected or 'shaken off' from such events. This report investigates how load and DER impact island stability and interrogates the conventional system restart ideology of 'minimum load'.

[2] Damping characteristic in this context refers to negative feedback in the relationship between frequency and real power, and between voltage and reactive power, generally leading to stable behaviour.

# 2 Methodology

## 2.1 Modelling

### 2.1.1 Network

Network modelling was maintained consistent with that used for 2022-2023 Stage 2 G-PST Topic 5 studies [1]. North Queensland (NQLD) network model was used for this investigation, as presented in Figure 1.


**Figure 1 Network considered for system restart studies performed [2].**

Source: 2023-27 Powerlink Queensland Revenue Proposal – Map of Powerlink's Transmission Network

Two wide-area EMT models were provided to Aurecon thanks to AEMO under confidentiality agreement. These include the wide-area system intact EMT model generally used for system strength studies and other operational and planning investigations by AEMO and network service providers (NSPs). Another wide-area EMT model which was intended for black start studies conducted by AEMO was also received. This model includes a smaller portion of the network, but each component is represented with a greater level of details commensurate with the level of details required for black start studies. The latter model does not include any IBRs or dynamic reactive support plant, and smaller non-black start synchronous generators were excluded. Furthermore, this model does not include a representation of all substations and transmission lines in North Queensland power system as it is recognised that not all these sections are involved in early stages of system restoration and even during the system build-up. The two models were merged to form a single system restart model of North Queensland inclusive of detailed transmission network as well as site-specific plant models.

For black start studies the otherwise commonly used bus-branch representation of the substation should be replaced with more detailed breaker-node modelling, to account for which specific breakers are closed in a substation during the restoration process and which substation at the other end of the line they are connecting to. The merged model was updated to reflect breaker-node modelling for realistic energisation sequences.

The level of detail required for and considered in system restart studies are summarised for key elements in the following sub-sections.

### Transformers

A transformer model can be divided into two parts: representation of windings and representation of the iron core. The first part is linear, the second one is nonlinear, and both are frequency dependent. Each part plays a different role, depending on the study for which the transformer model is required. For EMT black start studies the transformer winding can be represented with the same level of detail as a phasor-domain model where the frequency dependency of the winding is neglected.

The three main nonlinear phenomena associated with the iron core are saturation, hysteresis and eddy current losses. In general, hysteresis loops of modern transformers have a negligible influence on the magnitude of the magnetising current. The information necessary for modelling hysteresis characteristic is not generally provided, and therefore excluded for transformer modelling for black start studies. Eddy current losses can be neglected for frequencies of up 2-3 kHz, and hence excluded from the transformer model required for black start studies. The transformer saturation characteristics  plays a significant role in black start studies.

Saturation characteristics can be incorporated from test data/manufacturer’s curves or by estimating the key parameters from transformer geometry. The former approach is a simple and convenient way of determining worst case inrush currents at the design stage. This is because with this approach, the frequency dependency of the losses is neglected. The latter approach provides marginal accuracy gain, however, the information required for this type of modelling is often only available to the transformer manufacturer.

Studies were conducted utilising, where information was available, site-specific generator models inclusive of magnetising current saturation information using the Jiles Atherton model of magnetic hysteresis. Remnant flux within the iron core of the transformer can significantly influence the inrush current when energising a transformer. To reflect worst-case conditions during studies, the remnant flux within the transformer was set to 0.8 pu, -0.8 pu and 0 pu for each of the three phases respectively.

### Overhead transmission lines

Transmission lines are nonlinear in nature due to frequency dependency both in conductors (skin effect) and in the ground or earth return path. Two main approaches exist to represent transmission lines in EMT modelling. The simplest method is to use Π-sections. The second and more detailed method is to use a distributed transmission line. The Π section model is a lumped parameter model based on series resistor inductor (RL) elements and parallel capacitance to ground (CG) elements. This model can be adopted to study the transient behaviour when the end-to-end length of the line is shorter than a couple of kilometre (km), or when studies need to be run for several tens of seconds. This model can also be used when tower geometry is unknown.

The distributed transmission line models are based on the principle of traveling waves. Relative to the Π models, distributed parameter models are more accurate but more computationally intensive.

A Bergeron model is a constant distributed-parameter model at the specified frequency whereas the frequency-dependent distributed parameter model (both Mode and Phase model) is fitted for a given frequency range, hence more accurate. The parameters of the Bergeron model are constant and applicable for a single frequency and thus may be used when no frequency dependency is to be represented. However, this model may be quite sensitive to the model frequency specified by the user.

With the extent of data available for network planning studies and phasor-domain load flow cases, a Π model or a Bergeron model can be readily developed (the latter model would need to be converted from the Π model via a phasor-domain to an EMT conversion tool). These models are generally appropriate for short lines if harmonic resonance is not a matter of concern. With a Π or Bergeron model the line impedances need to be explicitly entered in the model. Note that for black start studies, the negative- and zero-sequence impedances, and mutual impedances of double circuit transmission lines are critical, and need to be entered in the EMT model should either of the PI or Bergeron models be used.

Of the three distributed line models (Π, Bergeron, and frequency dependent distributed parameter model) the frequency-dependent (phase) model is the most accurate and should be used whenever harmonic resonance needs to be investigated. The use of frequency-dependent (phase) model is envisaged for all transmission lines involved in the system restoration if tower geometry is given.

With frequency-dependent models of the line, the sequence impedances are not often required in the model but are instead calculated automatically through a line constant routine based on given tower geometry and conduct data.

The following information is generally sought in order to represent a frequency-dependent transmission line model:

- Transmission line conductor diameter and resistance per-unit (pu) length (can also be selected from a user-defined list for standard/commonly used conductors).
- Total length of each transmission line.

- Phase transformation data.
- Spacing between conductors in a phase bundle.
- Spacing between phases.
- Shield wire diameter and resistance pu length.
- Height of each conductor and shield wire at the tower and sag to midspan, or average height of each conductor and shield wire above ground.
- Tower dimensions.
- Ground resistivity.
- Line transposition (if applicable).

Energisation studies performed in this research program are based on frequency dependant (phase) model transmission lines for all restart paths, with only short transmission lines within generating system being represented by Π sections or Bergeron line models in the absence of more detailed information.

#### Surge arresters

The primary reason for inclusion of surge arrester in black start studies is that system restoration can impose excessive temporarily over voltage (TOV) lasting for several seconds. Such TOV can compromise insulation of the surge arrester. Modelling surge arresters for voltages in the range 1.0-1.3 pu, and assessment of TOV resulting from switching transients is critical.

Surge arresters exhibit a nonlinear voltage versus current (V-I) characteristic such that they have an extremely high resistance during normal system operation and a relatively low resistance during transient over-voltages.

The commonly used frequency-independent surge arrester model is appropriate for simulations involving low frequency transients and most switching frequencies. This is because the frequency dependency will only become relevant at very high frequency over-voltages associated with lightning strikes or transients associated with gas insulated substations (GIS).

Surge arrester models were included at all transmission substations considered for energisation. More detailed surge arrester information was not available for models of generating systems.

### 2.1.2 Synchronous generators

Dynamic models of existing synchronous generators with focus on black start studies were sourced from AEMO. These models account for different operating modes such as droop and isochronous modes for the governor, and large fans and pumps used in power station auxiliaries. Mode switchover was applied to these generators during the restoration process where necessary, for example switching from isochronous to droop mode when other generators are brought online, or engaging the power system stabiliser (PSS) when generator loading increases above a predefined level. Black start synchronous generators included the following critical information:

- Machine modelling:
  - Two q-axis damper windings, and distribution of saturation on d-axis.
- Control systems:

– Automatic Voltage Regulator (AVR)
– Power System Stabiliser (PSS)
– Limiters, such as under and over-excitation limiters or ratio of the voltage to frequency (V/Hz) limiters.
– Synchronous and isochronous control models.

- Protection systems:
  – Protection functions such as under- and over-excitation protection, out-of-step (OOS) and loss-of-excitation (LOE).

Models of synchronous generators that are non-critical from a system restoration perspective were treated with only the same level of detail as those used for system intact studies, and typically did not contain all control modes and protection systems present in black start synchronous generator models.

### 2.1.3 Grid-following inverters

#### Battery energy storage systems

Battery energy storage systems utilised vendor specific EMT models but are not site-specific to the Far North Queensland (FNQLD) region being analysed. All inverter and power plant controller parameters are accessible and were adjusted to reflect a plant connection suitable for the NQLD 275 kV network. Table 1, summarises base settings of key parameters for the grid-following (GFL) BESS with further sensitivity studies conducted to assess the impact of each of these variables.

**Table 1 GFL internal default settings.**

| VARIABLE | VALUE | UNITS |
|---|---|---|
| **Plant base** | 163.8 | MVA |
| **Rated active power** | 100 | MW |
| **Voltage droop on active power base[3]** | 4.0 | % |
| **Voltage droop dead band on nominal voltage** | 0.0 | % |
| **Frequency droop on active power base** | 2.4 | % |
| **Frequency deadband on nominal frequency** | 0.03 | % |

The vendor-specific EMT model included protection flags and internal monitor signals which were inspected when analysing results. The model contained flags to set the enable time of the power plant controller (PPC) and had inbuilt connect functionality when grid conditions are suitable (e.g., voltage within 0.9 pu – 1.1 pu and frequency within 49.9 Hz – 50.1 Hz) which were set to enable the plant operation when energised from the network. The model possessed a fast-start feature to

[3] A 4.0% droop slope implies that a 0.04 per unit deviation in voltage from the setpoint would result in a 1.0 per unit reactive power setpoint.

initialise the model and reach steady-state conditions as quickly as possible for generator connection studies and is a model specific feature, not an accurate representation of physical inverters. To work around the delayed initialisation not completely addressed by the fast-start feature, additional limits were temporarily set to prevent the plant from overshooting setpoint targets on start-up and to reflect more realistic black start control behaviour. The model utilised included full IGBT switching detail to capture potential impacts on plant and network harmonics.

### Wind farms

Wind farm (WF) models utilised were vendor specific EMT models but were not site-specific to the NQLD region being analysed. Four WFs of two different original equipment manufacturers (OEMs) with different power ratings were used and summarised in the Table 2. An aggregated 33 kV reticulation network was considered for all models, and accessible parameters in the WF model were adjusted to reflect a suitable plant connection for the NQLD 275 kV network. The OEM models included protection flags and internal monitor signals which were inspected when analysing results. The WFs models do not have an in-built system restart feature and cannot readily be initialised at an arbitrary simulation time, always assuming initialisation occurs at 0s with the intent of reaching steady state, as suitable for grid connection studies. As such, to represent black start, the wind turbine models were connected to an artificial voltage source to facilitate start-up while initially isolated from the wider network. The artificial voltage source was disconnected when the turbines were connected to the network. It is acknowledged that this does not reflect actual plant turbine energisation behaviour and represents an assumption that the WF can start-up. Voltage, current and frequency are monitored prior to energisation to ensure the conditions are acceptable for a WF to start up following energisation. The WF main grid transformer and HV network is hard energised, being energised from the network through a closing circuit breaker, through a standard system restart process. The voltage, current and frequency quantities are monitored to evaluate whether or not conditions are acceptable to pick up the windfarm.

**Table 2 GFL WF plant information.**

| VARIABLE | 190MVA GFL WF | 304MVA GFL WF | 180MVA WF | 452.89MVA WF |
|---|---|---|---|---|
| **Plant base (MVA)** | 190 | 304 | 100 | 452.89 |
| **Rated active power (MW)** | 190 | 304 | 180 | 452.89 |
| **Voltage droop on active power base** | 5.0% | 5.0% | 5.0% | 6.0% |
| **Voltage droop dead band on nominal voltage** | ±0.015 | ±0.015 | ±0.015 | ±0.015 |

### Solar farms

Similar to the WFs, the SF models utilised are vendor specific EMT models but are also not site-specific to the NQLD region being analysed. The SF models, also similarly to the WF models, do not have an in-built system restart feature and cannot readily be initialised at an arbitrary simulation time, always assuming initialisation occurs at 0s with the intent of reaching steady state for grid connection studies. As such, the SF models used an artificial voltage source and  the main grid transformer and HV network is hard energised as for the WFs..

**Table 3 GFL SF internal default settings.**

| VARIABLE | VALUE | UNITS |
|---|---|---|

| | | |
|---|---|---|
| **Plant base** | 121 | MVA |
| **Rated active power** | 110 | MW |
| **Voltage droop on active power base** | 4.0 | % |
| **Voltage droop dead band on nominal voltage** | ±0.015 | % |
| **Frequency droop on active power base** | 1.7 | % |
| **Frequency deadband on nominal frequency** | 0.03 | % |

### Static Var Compensators

Two static var compensators (SVCs) were used and both of them site-specific to the NQLD region being analysed. The nameplate rating of each SVC is 230 MVA and 150 MVA respectively. The SVC models utilised had an in-built reconnect feature when voltage and frequency recovered to suitable levels allowing it to be initialised at an arbitrary simulation time. Therefore, unlike the solar farms or WFs, no artificial voltage source ware connected to facilitate start-up while isolated from the wider network, in contrast the representation of SVC energisation more accurately reflected a physical SVC system start-up.

## 2.1.4 Grid-forming inverters

A grid-forming (GFM) BESS was utilised as a black start device. Models of GFM BESS, provided under a confidentiality agreement with an OEM, were used for this purpose with settings configured to reflect a future planned connection in NQLD. Table 4 summarises the base settings of key parameters for the GFM BESS with further sensitivity studies performed to assess the impact of changing key variables on the stability of networks restarted while already near stability limits.

**Table 4 GFM internal default settings.**

| VARIABLE | VALUE | UNITS |
|---|---|---|
| **Plant base** | 349 | MVA |
| **Rated active power** | 300 | MW |
| **Damping constant** | 8 | |
| **Inertia constant** | 4 | s |
| **Maximum overload current** | 1 | pu |
| **Voltage Q(V) droop**[4] | 10.0 | % |
| **Voltage deadband on nominal voltage** | 0.0 | % |
| **Governor frequency droop** | 2.517 | % |
| **Governor frequency deadband on nominal frequency** | 0.03 | % |

[4] A 10.0% droop slope implies that a 0.10 per unit deviation in voltage from the setpoint would result in a 1.0 per unit reactive power setpoint.

Black start of the GFM BESS was conducted by soft energising the inverter and main grid transformers to the plant's connection point – the inverters ramped the voltage up from 0 pu to nominal output. System restoration sequences were progressed from the black started GFM BESS.

### 2.1.5 Load modelling

Load modelling in all base scenarios utilised a static active and reactive power load known as a "constant impedance, constant current, constant power (ZIP)" model. The ZIP model has the ability to reflect voltage and frequency dependency according to the following two equations.

$$P = P_0(1 + K_{PF} \times dF) \times \left(\frac{V}{V_0}\right)^{NP} \quad (1)$$

Where,

| | | |
|---|---|---|
| $P$ | = | Equivalent load active power |
| $P_0$ | = | Active power at rated voltage |
| $K_{PF}$ | = | Frequency index (rate of change of active power to frequency) |
| $dF$ | = | Change in frequency |
| $V$ | = | Load voltage |
| $V_0$ | = | Rated voltage |
| $NP$ | = | Voltage index (rate of change of active power to voltage) |

$$Q = Q_0\left(1 + K_{QF} \times dF\right) \times \left(\frac{V}{V_0}\right)^{NQ} \quad (2)$$

Where,

| | | |
|---|---|---|
| $Q$ | = | Equivalent load reactive power |
| $Q_0$ | = | Reactive power at rated voltage |
| $K_{QF}$ | = | Frequency index (rate of change of reactive power to frequency) |
| $dF$ | = | Change in frequency |
| $V$ | = | Load voltage |
| $V_0$ | = | Rated voltage |
| $NQ$ | = | Voltage index (rate of change of reactive power to voltage) |

Sensitivity studies were performed considering the use of the composite load model which aggregates both static and, in contrast to the ZIP model, dynamic loads. It consists of four different motor types, electronic load and static load lumped behind an equivalent distribution impedance, as presented in Figure 2.

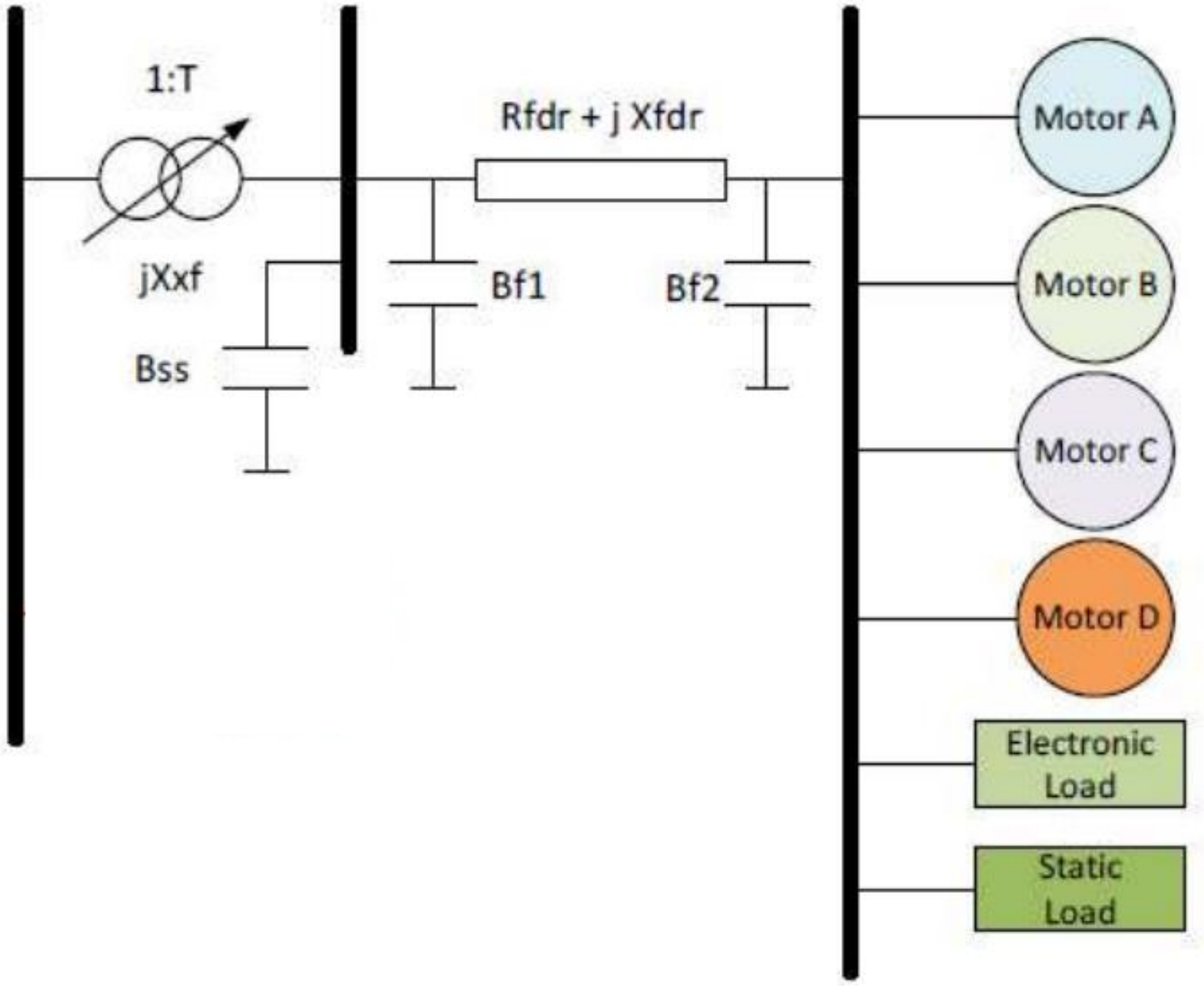


**Figure 2 Composite load model structure.**

Source: PSS®E models for load and distributed PV in the NEM, Figure 3 [3]

According to the model development and validation report produced by AEMO [3] subsequent to the development of the composite load model, it provides better dynamic alignment with system response than ZIP models and especially in a black-start environment it is expected to capture load dynamics better owing to the representation of motor models and electronic load. Additionally, the composite load model captures protection settings on loads and reflects their disconnection behaviour when exposed to adverse network conditions. The composite load model does not yet however include a reconnection feature to ramp it back up following a trip or when energised from a black system. This prevents the composite load model from being used to reflect load connection behaviour as it occurs in reality. Despite the lack of reconnect feature, the composite load model does include a start-up time which, in the black start studies performed, prevents protection from disconnecting the load before it is energised. Loads are represented as aggregated in (system intact) network studies and the start-up time feature of the composite model results in the entire load being connected simultaneously, whereas on the physical system a portion of the load would reconnect and ramp up over time. Implementation and validation of a reconnect feature in the composite load model would be of great value to future black start studies.

### 2.1.6 Distributed energy resources (DER)

A DER model is often bundled together with the composite load model but for the purpose of system restart studies was considered independently to isolate the different impacts of load and DER. The DER model primarily reflects aggregated tripping of rooftop photovoltaics (PV) due to voltage and frequency excursions outside normal operating bands. The DER model does not include a reconnect feature that would represent the ramp-up type behaviour of DER which occurs (in reality) following a disturbance. As such, it could not be used to study energisation of load during a black-start. An example of the recovery ramp expected from rooftop PV, the dominant form of DER in Australia, is presented in Figure 3 and it is a recommended here as a future improvement to the DER model. Ongoing DER modelling improvements is another area of the G-PST, Topic 9, which is able to take these system restart improvements into account.

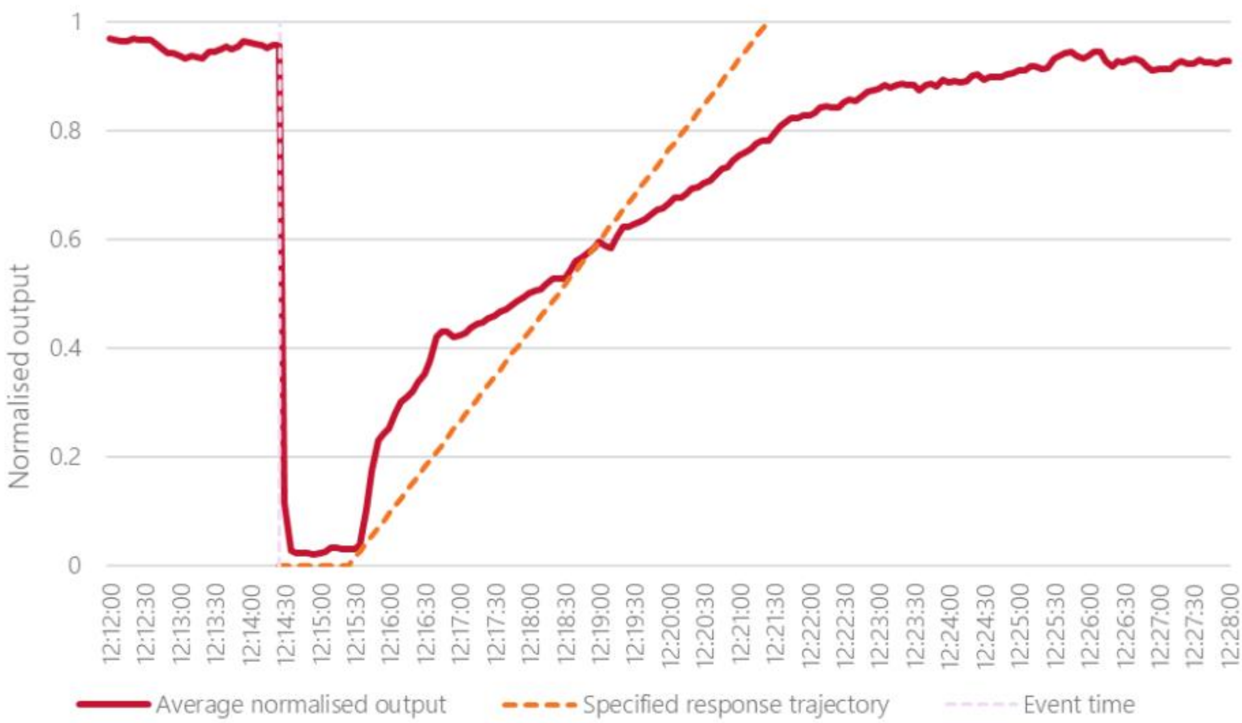


**Figure 3 Normalised generation profile for inverters following disconnection due to over-voltage [4]**

Source: Behaviour of distributed resources during power system disturbances, Figure 26 [4]

The DER model start-up time feature does not bypass protection settings completely. In particular, when DER is connected after 50s or more of zero voltage, as in a system restart study, the protection (model) trips immediately upon being enabled. To work around the protection behaviour during black conditions, the DER models were temporarily connected to a (artificial) voltage source that provides a normal voltage. The voltage source was disconnected just prior to the DER model being connected to the energised network. Although such modelling does not provide any understanding of the DER connection behaviour following system restart, it nevertheless facilitates analysis of DER's impact on the stability of a restarted island following a disturbance. Accurately representing DER tripping behaviour during system restart is important, since switching events can cause temporary over- and under- -voltage and -frequency, and sudden increases in observed load. The amount of DER "shaken off" during switching events are studied here to determine the maximum permissible amount of DER that can be supported without risking the stability of a restarted island.

## 2.2 Analysis

The following section outlines scenarios and sensitivity studies completed in Stage 3 to define feasible system restoration options and conditions, as well as recommendations on generator system restart technical requirements, accounting for IBR.

### 2.2.1 Restarted island stability boundaries

Boundary conditions of restarted island stability were investigated in the initial steps of Stage 3 research, as learnings around the boundary of restarted island stability feed into sensitivities studies on control system parameters, island resiliency, island synchronisation and other works included in the scope of this investigation. Previous works on Topic 5 from Stage 2 determined that in most restarted islands with IBR, the key limiting factor for viable restart scenarios was availability of reactive power control to maintain voltages. Further works were expanded on Stage 2 to identify alternative boundary points and failure mechanisms of a system restoration utilising IBR. The following two general circumstances were investigated, in the listed order:

1. Scaling of the MVA capacity of the black start device to create a greater capacity ratio between the GFM black start device and GFL support devices.
2. Pick-up of multiple IBR grid-following plants using a single black start device, to better quantify requirements for the MVA ratio between the black start device and support service devices.
   - Investigation attempting to identify the MVA ratio of black start device to GFL support device at which appears either (i) control system interactions between plants, or (ii) control system instability with the network.

During early stages of system restoration, black start devices are typically connected to stabilising load or generation by energising only single elements, such as individual transmission lines or transformers. When loss of a single element can cause a system restart scenario to collapse it is considered “N” level system security. System normal requirements require “N-1” level system security where a single network element, whether generator, load, line, transformer, or other network device, can be lost and the system will remain stable and not have any additional network element disconnect. High winds, tree branches and the general impact of major weather events are the most common cause of faults on the power system and could even be the initial cause of a black system event. Because it is quite possible that a network fault may occur during system restoration, when practical during the restoration process a “N-1” level of system security should be restored. Both “N” level and “N-1” level system security, from a system dynamic perspective, were assessed during system restoration for each system restart pathway investigated. Table 5, below, provides a list of all scenarios assessed for “N” level system security, while additional fault sensitivity studies were performed to investigate “N-1” system security.

**Table 5 Stability boundary scenario list**

| SCENARIO ID | BLACK START DEVICE | SUPPORT DEVICES | SUPPORT DEVICE / BLACK START RATIO |
|---|---|---|---|
| **A** | 87.5 MVA GFM BESS | • 163.8 MVA GFL BESS | 1.872 |
| **B** | 350 MVA GFM BESS | • 163.8 MVA GFL BESS<br>• 190 MVA WF | 1.011 |

| | | | |
|---|---|---|---|
| **C** | 87.5 MVA GFM BESS | • 163.8 MVA GFL BESS<br>• 190 MVA WF | 4.043 |
| **D1** | 87.5 MVA GFM BESS | • 163.8 MVA GFL BESS<br>• 190 MVA WF<br>• 304 MVA WF | 7.518 |
| **D2** | 87.5 MVA GFM BESS | • 163.8 MVA GFL BESS<br>• 190 MVA WF<br>• 304 MVA WF | 7.518 |
| **E** | 350 MVA GFM BESS | • 163.8 MVA GFL BESS<br>• 190 MVA WF<br>• 304 MVA WF | 1.879 |
| **F** | 47.04 MVA GFM BESS | • 163.8 MVA GFL BESS<br>• 190 MVA WF<br>• 304 MVA WF | 13.98 |
| **G** | 36.7 MVA GFM BESS | • 163.8 MVA GFL BESS<br>• 190 MVA WF<br>• 304 MVA WF | 17.92 |
| **H** | 35.75 MVA GFM BESS | • 163.8 MVA GFL BESS<br>• 190 MVA WF<br>• 304 MVA WF | 18.4 |
| **I** | 87.5 MVA GFM BESS | • 163.8 MVA GFL BESS<br>• 121 MVA SF<br>• 304 MVA SF | 6.73 |
| **J** | 87.5 MVA GFM BESS | • 163.8 MVA GFL BESS<br>• 121 MVA SF<br>• 452.89 MVA WF | 8.43 |
| **K** | 87.5 MVA GFM BESS | • 163.8 MVA GFL BESS<br>• 121 MVA SF<br>• 180 MVA WF | 5.3 |
| **L** | 87.5 MVA GFM BESS | • 163.8 MVA GFL BESS<br>• 190 MVA WF<br>• 304 MVA SF<br>• 230 MVA SVC<br>• 150 MVA SVC | 11.86 |
| **M** | 87.5 MVA GFM BESS | • 230 MVA SVC<br>• 163.8 MVA GFL BESS<br>• 190 MVA WF<br>• 304 MVA SF | 10.15 |
| **N** | 36.7 MVA GFM BESS | • 230 MVA SVC<br>• 163.8 MVA GFL BESS<br>• 190 MVA WF<br>• 304 MVA WF | 24.2 |

For all studied scenarios, the following figure, Figure 4, represents the restarted system with grey objects indicating network connections left out of service, and green objects denoting various alternative restarted elements listed in Table 5 across alternative scenarios.

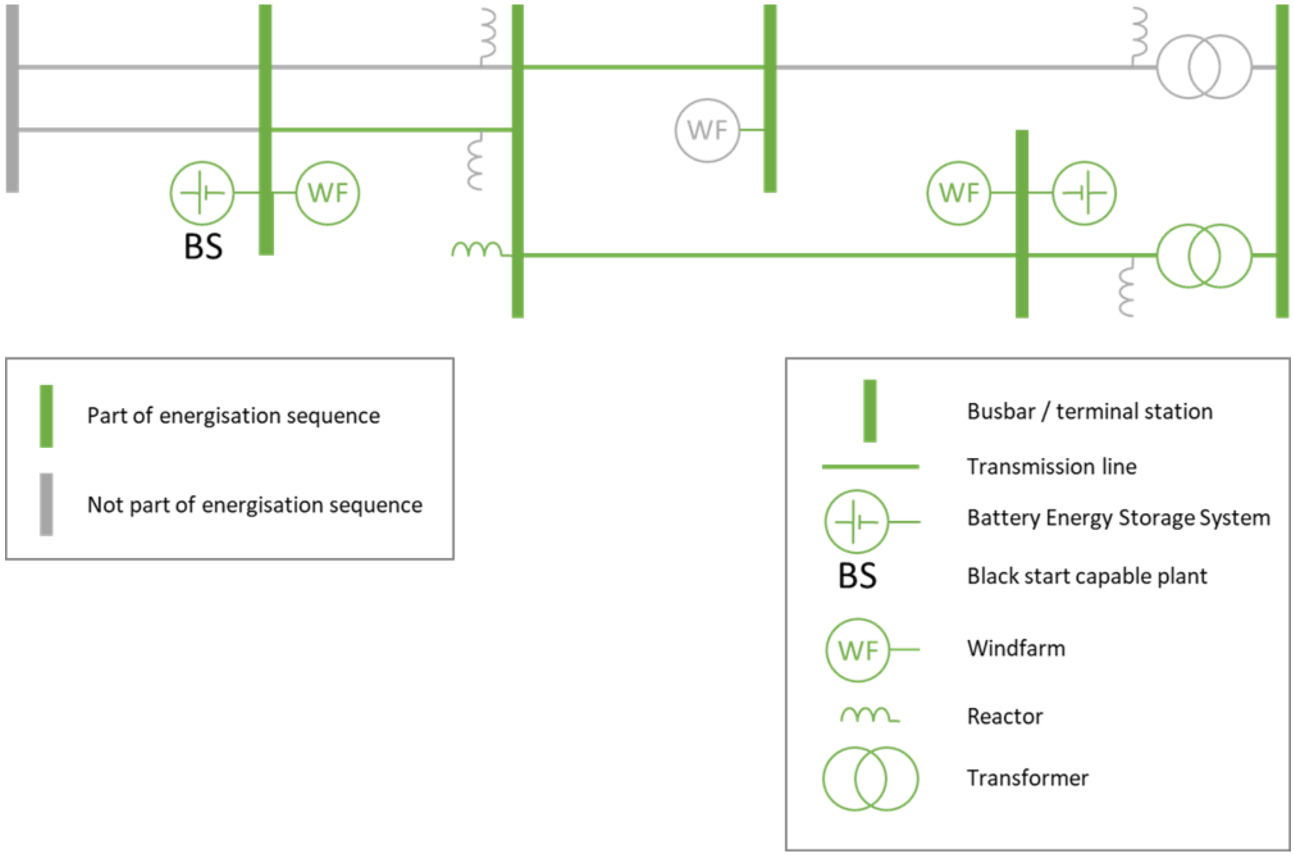


Figure 4 Restarted network used for sensitivity studies.

### Restarted island stress-testing

To stress test the restarted network, a 275 kV to 132 kV transmission level transformer was energised following the establishment of a stable island. Once the smallest size of GFM IBR/BESS? that was able to support a restarted island was identified, comprehensive point-on-wave switching was performed to identify the worst-case conditions for energisation of the transmission level transformer. In particular, the transformer was energised at 10-degree phase angle increments along the voltage waveform, with the system response at the transformer and nearby plants monitored to investigate voltage and harmonic behaviour, as well as potential plant tripping.

A sensitivity study was also performed by the energisation of two parallel transformers to evaluate whether sympathetic inrush current to the transformers would impact the transient response of the system.

### Assumptions and simplifications

The following simplifying assumptions were implemented in the model to minimise effort expended and simulation times required, having been justified through results and findings from G-PST works performed throughout 2021-2022.

- GFL BESS model under-voltage protection was set to unrealistically long delay values (that is, the protection was effectively disabled) to prevent the plant from tripping offline while network was being energised to reach the plant, as no reconnect logic was implemented in the model, and it would therefore remain offline once tripped.

- WF and SF models utilised did not have flexible start-up options and the models were required to be initialised with a (phantom) voltage source and switched from the voltage source to connect to the network, following energisation of the plant's main grid transformer.
- Time between energisation of transmission lines was between 1 to 5 seconds to speed up simulations. Previous studies performed in either 2022-2023 Stage 2 works, or within this project's scope of works, utilising a minimum of 10 seconds between energisation steps proved that energisation was possible. Reducing the time between energisation steps facilitated reaching a viable island sooner.

### 2.2.2 Control system parameter sensitivity tests

To understand the impact of alternative IBR control system parameters on restarted island stability, a range of sensitivity tests have been investigated. The following list outlines the control system parameters individually adjusted and analysed through sensitivity studies. Only a subset of possible control system parameters was studied due to limitations of: OEM technical support, model documentation, and variety and maturity of models. Results of the sensitivity studies performed feed into recommendations for generating system and power system technical requirements for system restoration.

- Black start device sensitivities investigated include
  - Inverter level frequency control settings,
  - Inverter level inertia and damping constants,
  - PPC level voltage control settings, and
  - PPC level frequency control settings.
- Support service device sensitivities investigated include
  - PPC level frequency control settings.

### 2.2.3 Black-start IBR location

The majority of studies and analysis covered in this G-PST Topic 5 focus on areas of high concentration of IBR technologies, both black start capable and incapable. The failure mechanisms, viable conditions, generator behaviour and network phenomena of a black start IBR close to an area with a high penetration of black start incapable IBR, typically a REZ, has been outlined above through Sections 2.2.1 and 2.2.2. A black start device close to an area of high IBR penetration is treated as a baseline for comparison with the following scenarios, where the black start IBR is proximal to:

- An area with high penetration of black start incapable IBRs (this is baseline for comparison, already described in the previous sections)
- A large industrial load and,
- One or more synchronous generators.

Formation of an island – energisation from the black start IBR to pick-up stabilising load or generation was studied. The difference in network dynamics, failure mechanisms and system restart viability are compared across the three scenarios outlined above.

### 2.2.4 Island resynchronisation

Greater penetration of smaller black start capable IBR throughout the network may facilitate the ability to restart several separate islands and reconnect them to restore the wider network, rather than the more traditional approach of growing a single island until it either connects to an intact system or an entire network is restored. Joining a synchronous generator-controlled island and a grid-forming BESS controlled island was investigated. When resynchronising two islands, the island presented in Figure 4 was used as GFM (BESS) controlled, IBR-only island, while Figure 5 represents the network used to form a synchronous generator-controlled island. The islands are separated by several transmission-level terminal stations, with two locations studies for the synchronisation point: one close to the synchronous generator island, and the other close to the IBR-only island. The synchronisation point was closest to the black start device in both cases, and on the opposite side of the black start device to load and generating systems.

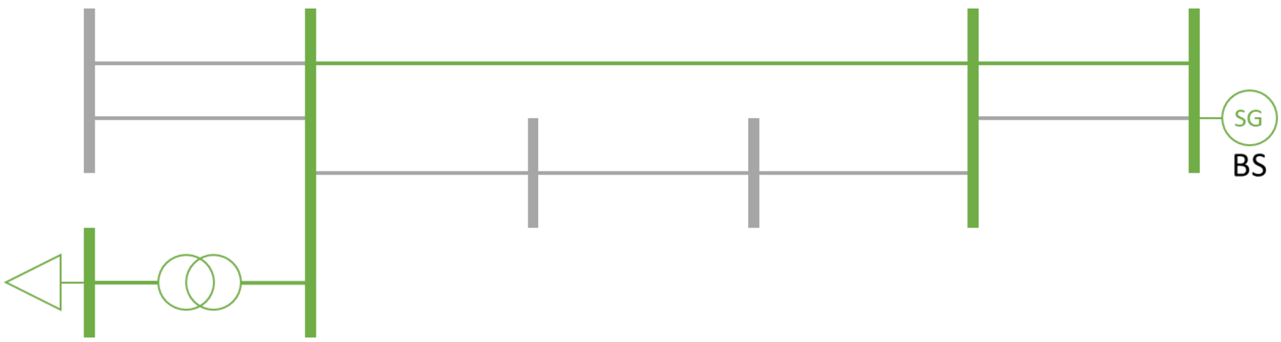


Figure 5 Synchronous generator-controlled island.

The main issue of concern when synchronising and connecting two islands, each supported by a standalone black start device, is how the two black start devices interact. Both devices are responsible for maintaining frequency and voltage within an island, and their controls may fight against each other when electrically connected.

Additionally, synchronous generators and grid-forming IBR black start devices possess different operating modes across black start and normal operations. Analysis of the impact of the different operating modes are performed, with like-for-like comparison between system responses primarily looking at the magnitude of and time to damping network oscillations. The following different modes and operating conditions are studied.

- Synchronous generator
  - Isochronous mode with power system stabiliser disabled.
  - Isochronous mode with power system stabiliser enabled.
  - Synchronous mode with power system stabiliser enabled.
- Grid-forming BESS
  - Due to lack of distinct modes available for configuration within the utilised GFM BESS, black start compared to system normal modes could not be investigated.

### 2.2.5 Load modelling

The impact of composite load models (CMPL) was investigated for an IBR-only island. The network utilised for the analysis is presented in Figure 6, below, which highlights that the load is located on the opposite side of the black start device compared to the concentration of non-black-start IBRs. The configuration is more typical of renewable energy zones being located remotely from load centres throughout the NEM. Approximately 100 MW of industrial load and 100 MW of domestic load were investigated. The domestic load was energised before the industrial load until a total of approximately 200 MW of load was in service. 100 MW of domestic load equates to 160,000 households based on mean demand at 15 kWh daily usage per household [5].

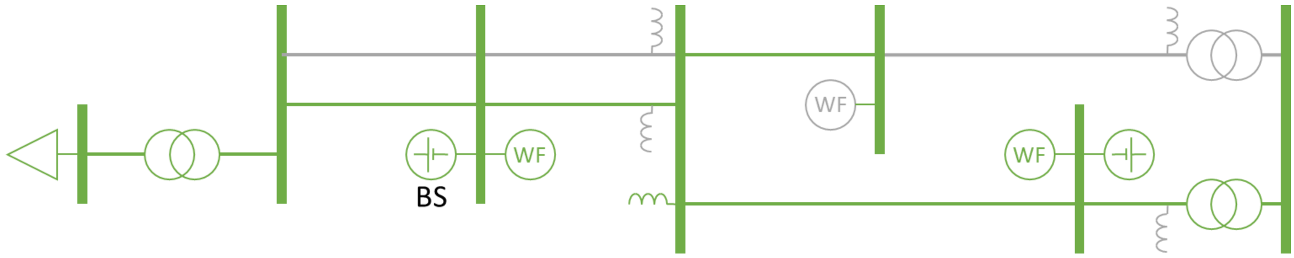


Figure 6 Network utilised for load model and DER comparison.

These studies focus on energisation transients within a formed island when subjected to switching events or faults. Additionally, the composite load model reflects load disconnections dynamically, in contrast to the ZIP model that represents steady state scaling dependence on frequency as linear and on voltage as following a power law (the exponent depending on whether constant voltage, power or impedance is assumed). The amount of load disconnected throughout a range of typical events is examined and the response of the CMPL is compared with the ZIP load model.

### 2.2.6 Distributed energy resources

Distributed energy resources were analysed in a similar fashion to (though in separate scenarios from) the load modelling, where DER models are located near the load location demonstrated in Figure 6. The DER analysis focuses on the impact of disconnecting rooftop PV during network transients. An IBR-only island inclusive of domestic load was the area of focus for studies performed. Only an already established restarted island was examined, as the DER model lacks the ability to reflect DER reconnection behaviour (recall that this is outlined in greater detail in Section 2.1.6). The islands are subjected to additional line switching events, transformer energisation events, and network faults. The volume of DER was increased in steps of 20 MVA, 5 MVA in each of four instances of the DER model located at distribution busbars, to determine the maximum amount of DER that can be supported without destabilising the restarted island.

# 3 Results

## 3.1 Restarted island stability boundaries

### 3.1.1 MVA ratio of black start to support device

Two conditions were considered during system restart studies of multiple IBR times devices:

- Less stringent "N" level system security – the ability for a scenario to facilitate system restart without any subsequent network fault. Summary of results is presented in Table 6.
  - No faults are applied under "N" level system security studies. Only the system restoration process and transformer energisation sensitivity were performed.
  - A maximum GFM black start device to GFL support device ratio of 1 : 18 (GFM : GFL) was observed.
  - A GFM black start device could not support more than 18 times its MVA rating in GFL support devices due to insufficient reactive power absorption capability of the GFM black start device to compensate for line charging of transmission lines energised to reach nearby generating systems.
  - Analysis with different technology types and OEMs was stable up to a ratio of 1 : 12, but studies should always be performed for system restart scenarios to confirm if site-specific conditions could reduce the required GFM ratio.
- More stringent "N-1" level system security – the ability for a scenario to both facilitate system restart and endure a subsequent network without collapsing or developing an instability. Summary of results is presented in Table 7.
  - A maximum GFM black start device to GFL support device ratio of 1 : 10 was observed, with a 1 : 11 ratio and higher showing tripping or network instability following a fault.

**Table 6 Stability boundary scenario summary**

| SCENARIO ID | BLACK START DEVICE | SUPPORT DEVICES | SUPPORT DEVICE / BLACK START RATIO | COMMENTS |
|---|---|---|---|---|
| **A** | 87.5 MVA GFM BESS | • 163.8 MVA GFL BESS | 1.872 | • Stable |
| **B** | 350 MVA GFM BESS | • 163.8 MVA GFL BESS<br>• 190 MVA WF | 1.011 | • Stable<br>• FRT retriggering observed in GFL BESS |
| **C** | 87.5 MVA GFM BESS | • 163.8 MVA GFL BESS<br>• 190 MVA WF | 4.043 | • Stable<br>• FRT retriggering observed in GFL BESS |
| **D1** | 87.5 MVA GFM BESS | • 163.8 MVA GFL BESS<br>• 190 MVA WF<br>• 304 MVA WF | 7.518 | • FRT retriggering observed in GFL BESS |
| **D2** | 87.5 MVA GFM BESS | • 163.8 MVA GFL BESS<br>• 190 MVA WF | 7.518 | • Stable |

| | | | | |
|---|---|---|---|---|
| | | • 304 MVA WF | | |
| **E** | 350 MVA GFM BESS | • 163.8 MVA GFL BESS<br>• 190 MVA WF<br>• 304 MVA WF | 1.879 | • Stable<br>• GFL BESS start-up failure due to localised under-voltage<br>• FRT retriggering observed in GFL BESS |
| **F** | 47.04 MVA GFM BESS | • 163.8 MVA GFL BESS<br>• 190 MVA WF<br>• 304 MVA WF | 13.98 | • Stable |
| **G** | 36.7 MVA GFM BESS | • 163.8 MVA GFL BESS<br>• 190 MVA WF<br>• 304 MVA WF | 17.92 | • Stable |
| **H** | 35.75 MVA GFM BESS | • 163.8 MVA GFL BESS<br>• 190 MVA WF<br>• 304 MVAWF | 18.4 | • Failed to restart |
| **I** | 87.5 MVA GFM BESS | • 163.8 MVA GFL BESS<br>• 121 MVA SF<br>• 304 MVA WF | 6.73 | • Stable<br>• Minimum Number of INV 39 |
| **J** | 87.5 MVA GFM BESS | • 163.8 MVA GFL BESS<br>• 121 MVA SF<br>• 452.89 MVA WF | 8.43 | • Stable<br>• Minimum Number of INV 39 |
| **K** | 87.5 MVA GFM BESS | • 163.8 MVA GFL BESS<br>• 121 MVA SF<br>• 180 MVA WF | 5.3 | • Stable<br>• Minimum Number of INV 39 |
| **L** | 87.5 MVA GFM BESS | • 163.8 MVA GFL BESS<br>• 190 MVA WF<br>• 304 MVA WF<br>• 230 MVA SVC<br>• 150 MVA SVC | 11.86 | • Stable<br>• Minimum Number of INV 79 |
| **M** | 87.5 MVA GFM BESS | • 230 MVA SVC<br>• 163.8 MVA GFL BESS<br>• 190 MVA WF<br>• 304 MVA WF | 10.15 | • Stable<br>• Minimum Number of INV 91 |
| **N** | 36.7 MVA GFM BESS | • 230 MVA SVC<br>• 163.8 MVA GFL BESS<br>• 190 MVA WF<br>• 304 MVA WF | 24.2 | • Failed to restart<br>• Minimum Number of INV 91 |

**Table 7 Fault study scenario summary**

| SCENARIO ID | BLACK START DEVICE | SUPPORT DEVICES | FAULT TYPE | SUPPORT DEVICE / BLACK START RATIO | COMMENTS |
|---|---|---|---|---|---|
| **A1** | 87.5 MVA GFM BESS | • 163.8 MVA GFL BESS<br>• 121 MVA SF | 2PHG & Zf=0.00001 ohm | 6.73 | • Stable |

| | | | | | |
|---|---|---|---|---|---|
| | | • 304 MVAWF | | | |
| **A2** | 87.5 MVA GFM BESS | • 163.8 MVA GFL BESS<br>• 121 MVA SF<br>• 304 MVAWF | 2PHG & Zf=10 ohm | 6.73 | • Stable |
| **B1** | 87.5 MVA GFM BESS | • 163.8 MVA GFL BESS<br>• 121 MVA SF<br>• 452.89 MVA WF | 2PHG & Zf=0.00001 ohm | 8.43 | • Stable |
| **B2** | 87.5 MVA GFM BESS | • 163.8 MVA GFL BESS<br>• 121 MVA SF<br>• 452.89 MVA WF | 2PHG & Zf=10.0 ohm | 8.43 | • Stable |
| **C1** | 87.5 MVA GFM BESS | • 163.8 MVA GFL BESS<br>• 121 MVA SF<br>• 180 MVA WF | 2PHG & Zf=0.00001 ohm | 5.31 | • Stable |
| **C2** | 87.5 MVA GFM BESS | • 163.8 MVA GFL BESS<br>• 121 MVA SF<br>• 180 MVA WF | 2PHG & Zf=10 ohm | 5.31 | • Stable |
| **D1** | 87.5 MVA GFM BESS | • 230 MVA SVC<br>• 163.8 MVA GFL BESS<br>• 190 MVA WF<br>• 304 MVA WF | 2PHG & Zf=0.00001 ohm | 10.15 | • Unstable after fault |
| **D2** | 89.4 MVA GFM BESS | • 230 MVA SVC<br>• 163.8 MVA GFL BESS<br>• 190 MVA WF<br>• 304 MVA WF | 2PHG & Zf=10 ohm | 9.93 | • Stable<br>• Identified as minimum GFM MVA for stability |
| **E1** | 87.5 MVA GFM BESS | • 163.8 MVA GFL BESS<br>• 190 MVA WF<br>• 304 MVA WF<br>• 230 MVA SVC<br>• 150 MVA SVC | 2PHG & Zf=0.00001 ohm | 11.86 | • Stable |
| **E2** | 87.5 MVA GFM BESS | • 163.8 MVA GFL BESS<br>• 190 MVA WF<br>• 304 MVA WF<br>• 230 MVA SVC<br>• 150 MVA SVC | 2PHG & Zf=10 ohm | 11.86 | • Unstable after the fault |

### 3.1.2 Failure mechanisms or system restart risks

Across the studies summarised in Table 6 and Table 7, several different failure mechanisms were observed across different scenarios:

- Generating system protection activation, disconnecting the associated generating system.
- GFL IBR FRT retriggering – multiple consecutive cycling of activation and clearance of a device's FRT mode which can cause spiking of reactive power and subsequently network voltage disturbances in the range of 10 to 0.1 Hz.
- Sustained active power oscillations.

### Generating system protection activation [failure mechanism]

Some scenarios observed activation of protection settings, typically following a fault within the network. Scenario D1 is an example where activation of generating system protection occurred on the GFM BESS black start device. Limited documentation for both the GFM and GFL devices made it difficult to isolate the type of protection and exact cause, but commonly it was observed to be under-voltage protection activating. Under- and over- voltage protection are typically the most common protection types on IBRs to activate, and a greater range of voltage protection settings was already identified in Stage 2 studies from 2022 – 20223 as a recommended area of improvement for system restart participants.

### Grid-following inverter FRT retriggering [failure mechanism]

In a single scenario, D1, the grid-following BESS support device was observed to experience fault ride through retriggering on energisation. An example is presented in Figure 7, with full results observable in Appendix A Scenario D1. Two solutions were investigated:

- Increasing the MVA capacity of the GFM BESS.
- Increasing the network voltage prior to GFL support device energisation.

Both solutions removed the observed GFL FRT retriggering. It is understood that the increase in GFM BESS MVA introduces more voltage control during the system restoration and raised the network voltage. The GFL support device settings may require retuning for FRT conditions, as reduced voltage stability can result in existing hysteresis or FRT thresholds being too tight and may cause the observed FRT retriggering behaviour.

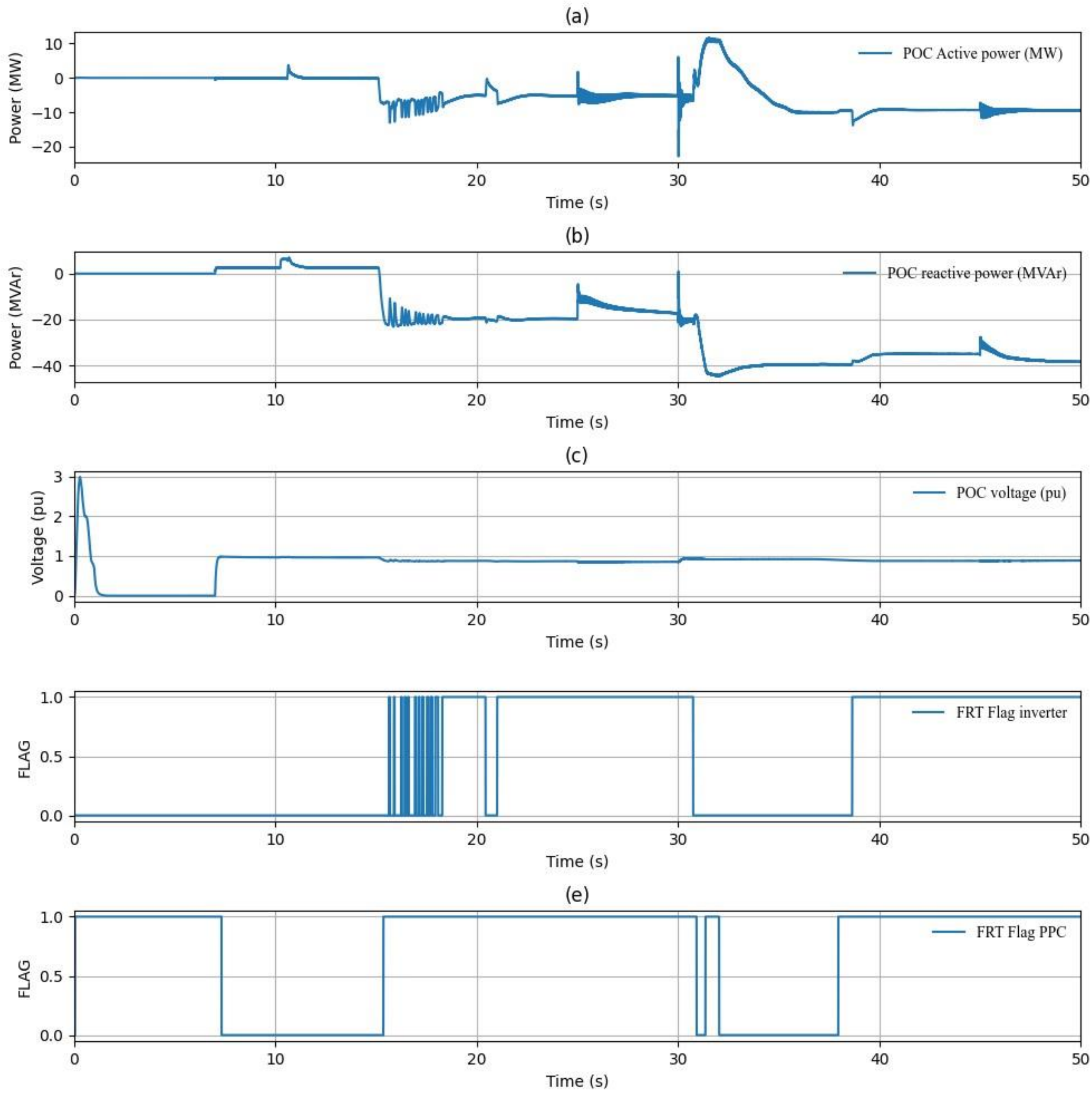


**Figure 7 Grid-following BESS FRT re-strike**

### Network active power oscillations [risk]

Sustained network active power oscillations were observed following establishment of a sizeable IBR-only island: upwards of 300 MVA of GFL IBRs and an 87.5 MVA GFM BESS. The oscillations observed were in the order of 1 MW magnitude and 5 – 10 Hz frequency. Such scale of active power magnitude is not of concern for network operation or stability but is a flag of potential control system interaction which could be exacerbated in some site-specific conditions. Studies were performed to try and isolate the source of oscillations, with them still being observed in a system containing only a GFM BESS and a single GFL windfarm, as presented in Figure 8.

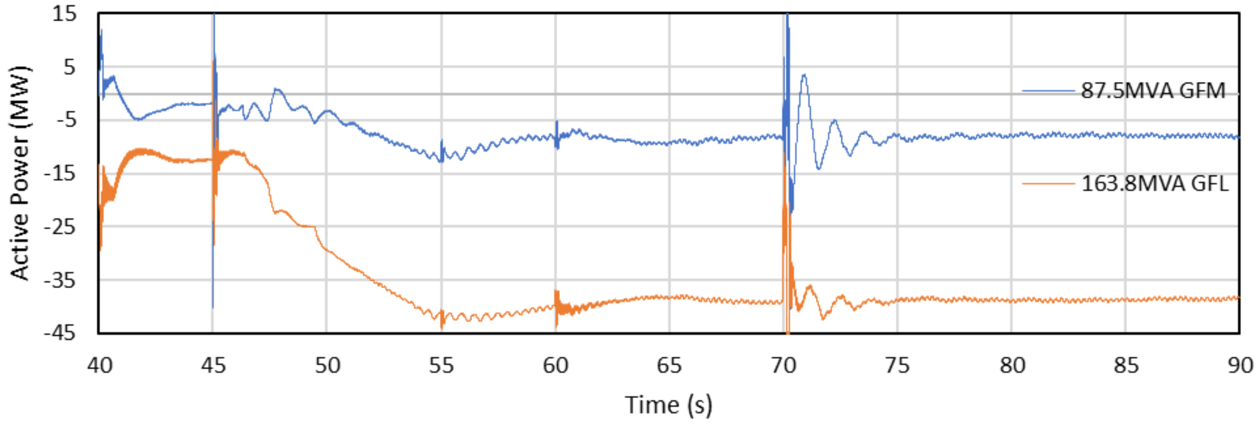


Figure 8 Active power oscillations occurring between the GFL and GFM BESS

Further sensitivities were performed to evaluate if the frequency droop settings on the GFM BESS and GFL IBRs could be adjusted to mitigate the behaviour. Results of the sensitivity are shown in Figure 9 and Figure 10, with frequency droop having no impact on mitigating oscillations.

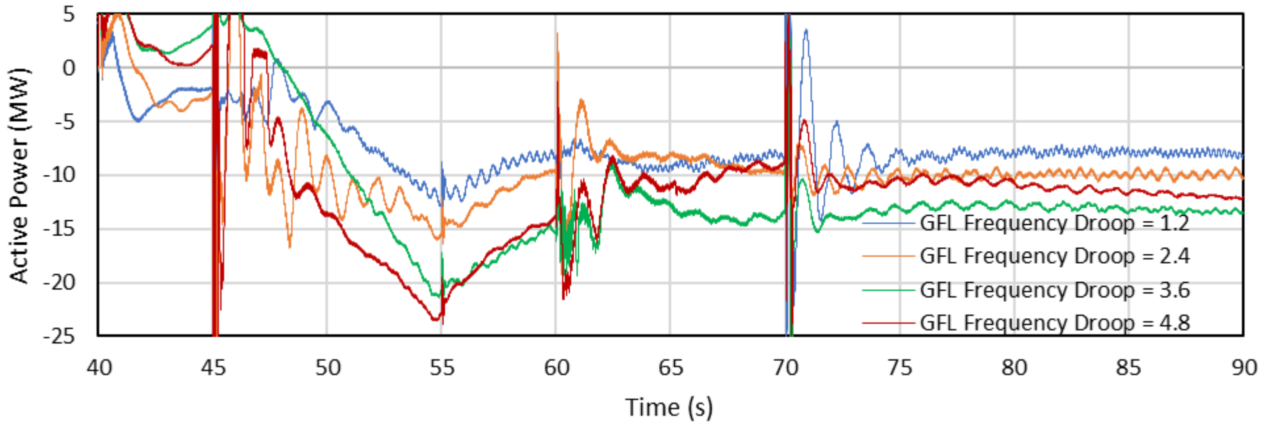


Figure 9 GFM active power – oscillations with changing GFM BESS frequency droop settings.

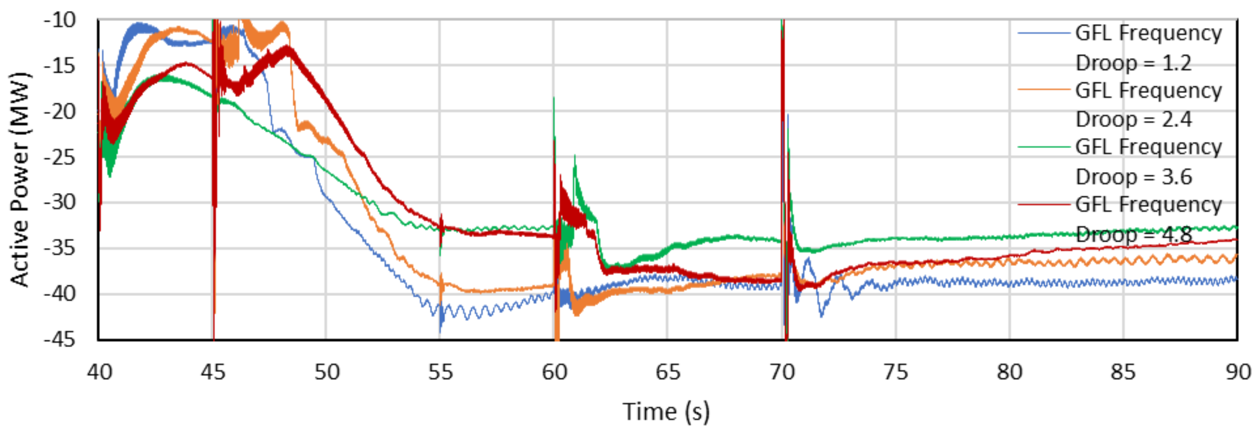


Figure 10 GFL active power – oscillations with changing GFL BESS frequency droop settings.

Studies were conducted with a sweep of GFM BESS MVA capacities, which confirmed that oscillations were more present for scenarios with low amounts of GFM BESS and that a greater GFM BESS to GFL IBR ratio reduced the observed magnitude of oscillations. The sweep of results is presented in Figure 11 and Figure 12.

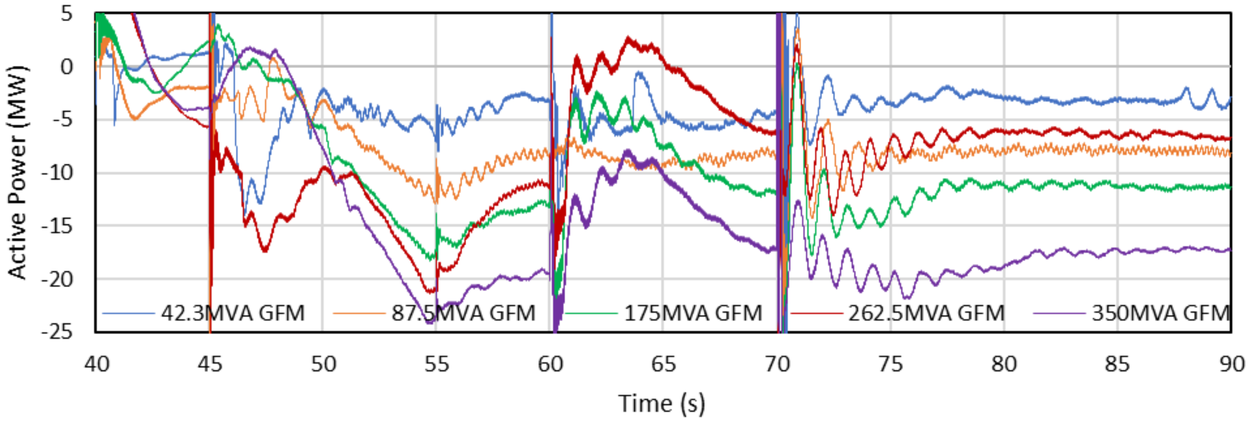


Figure 11 GFM active power – oscillations with changing GFM BESS size.

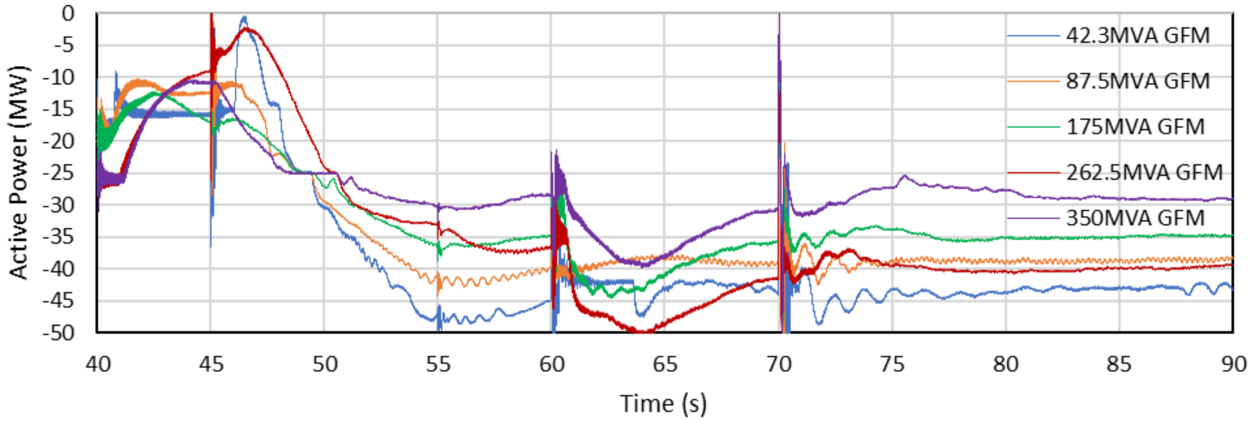


Figure 12 GFL active power – oscillations with changing GFM BESS size.

### 3.1.3 Grid-following inverter frequency control

Scenario D2 facilitated a restarted island containing the following devices:

- 87.5 MVA grid-forming BESS, used a black start device
- 163.8 MVA grid-following BESS
- 190 MVA grid-following WF
- 304 MVA grid-following WF

The grid-forming BESS acted as a swing machine, designed to adjust active and reactive power output to maintain frequency near 50 Hz and voltage near 1.0 pu at the 275 kV connection point. The two grid-following windfarms were dispatched at 15 MW and 30 MW respectively, and the grid-following BESS was dispatched at -25 MW (that is, charging, a net load) to minimise the loading on the grid-forming BESS. However, during the simulation it was observed that the grid-following BESS responded far more significantly to frequency changes, and by the end of the simulation the grid-following BESS active power output settled at -47 MW, leaving the grid-forming BESS at near 0 MW output. An example of the plant response is presented in Figure 13 below. The behaviour was unexpected but beneficial to the restart process, as greater headroom on the black start device is likely to provide it with capacity to sustain larger transient responses and maintain island stability. Further investigation outlined in Section 3.2 revealed the following:

- The GFM BESS has two controls responding to frequency:
  - Inverter frequency droop which primarily responds to short-duration transients (for example less than 2s timeframe).
  - PPC active power – frequency P(f) droop which provides sustained frequency response over longer durations (for example greater than 2s).
- The GFL devices within the system have a single P(f) droop on their PPC.

The GFL device P(f) droop on the PPC was set to have greater active power response for a smaller frequency change than the GFM P(f) droop on the GFM PPC. The resultant system behaviour was that for shorter duration transients the GFM BESS provided the majority of the active power response to maintain frequency, while over a longer period of time (for example, 10s), the GFL devices in the network provided more active power to maintain frequency than the GFM BESS.

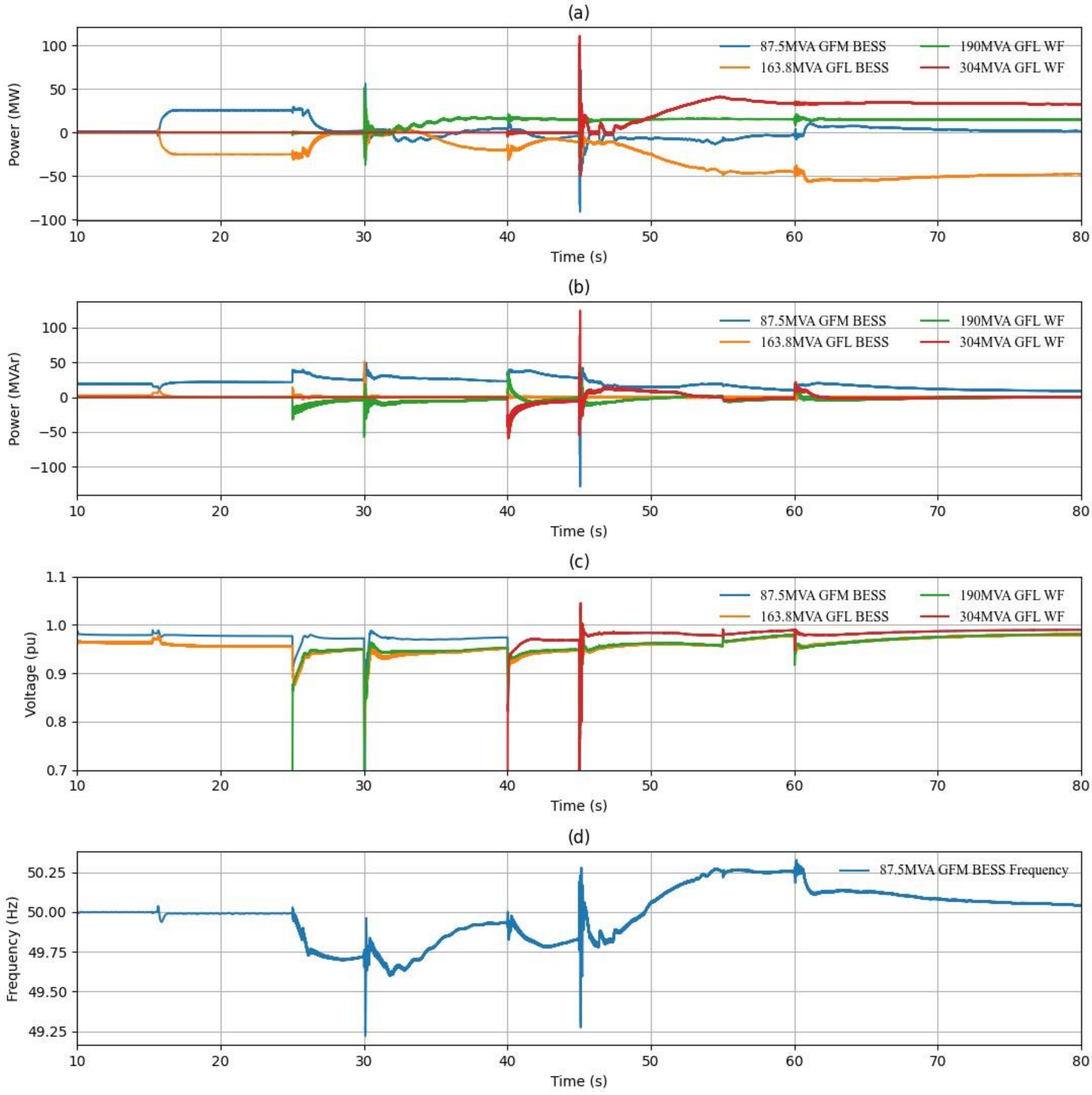


**Figure 13 Scenario D2 generating device response to frequency.**

### 3.1.4 Transformer energisation sensitivity

Point-on-wave switching was implemented when energising a transmission level 275 kV to 132 kV transformer to identify the worst-case conditions and ensure that a restarted island could ride through the event. No resonance or over-voltage conditions were observed, with the two key challenges identified are under-voltage and high harmonic voltage distortion in the 2nd order harmonic.

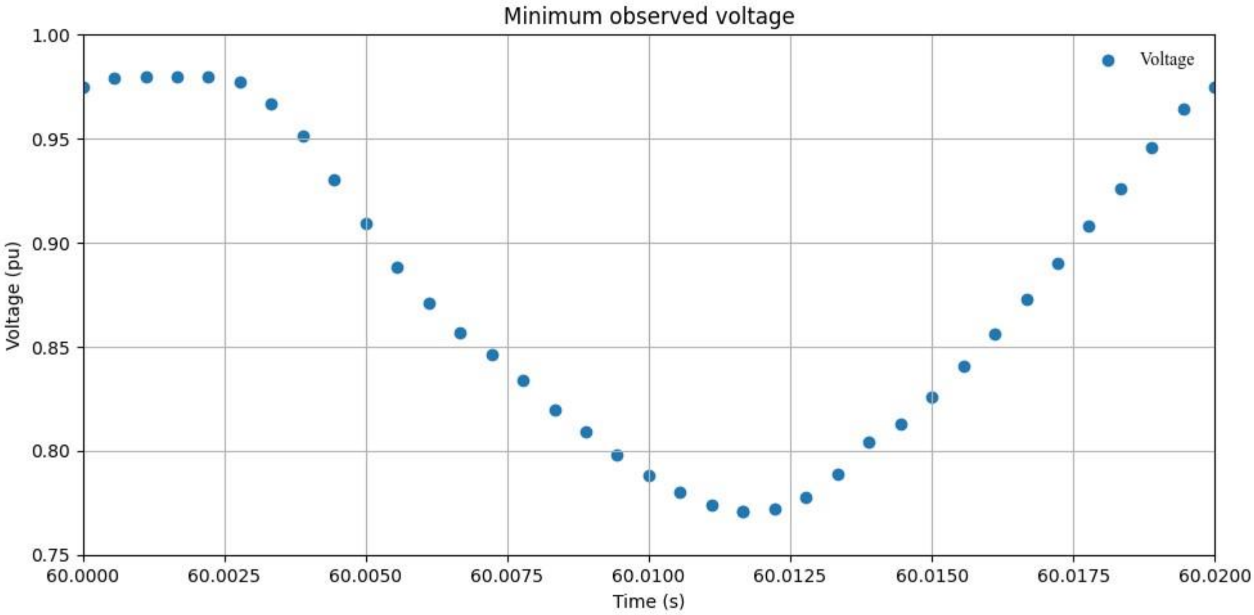


**Figure 14 Transformer energisation minimum observed voltage for all switching times.**

The worst-case conditions were identified from Figure 14, and the worst-case conditions are utilised to calculate the 3-phase RMS voltage & 2nd order harmonics for each phase are presented respectively in Figure 15 and Figure 16 below.

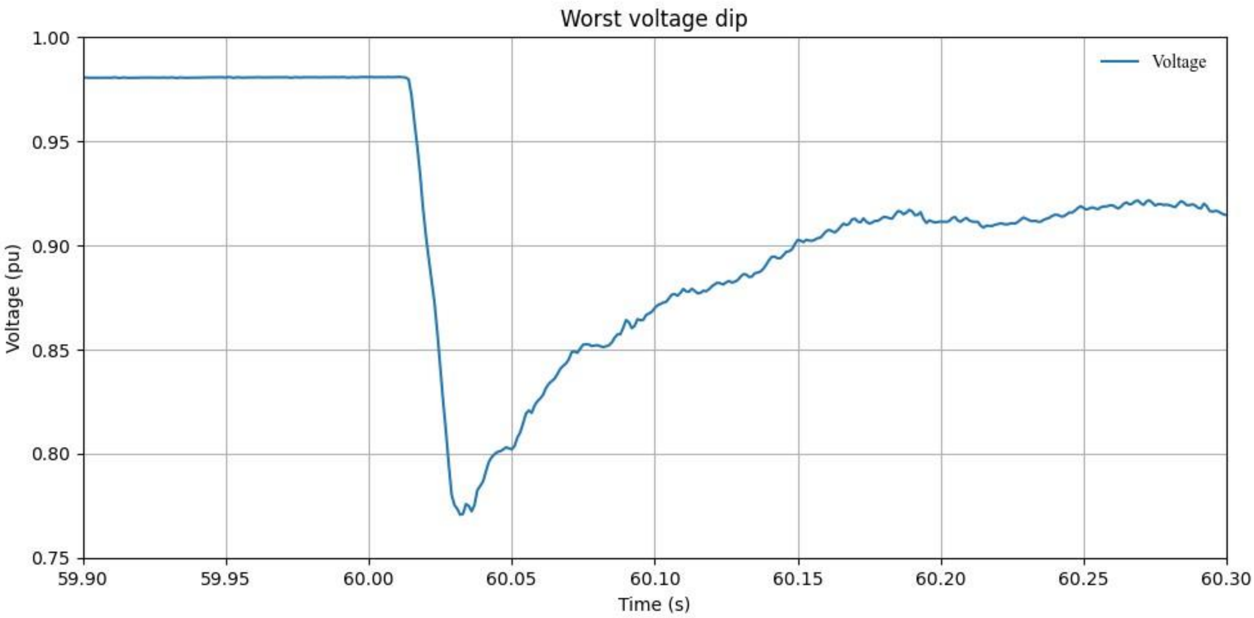

Figure 15 Worst case voltage dip on energisation at 275kV side of transformer.

Figure 14 is used to identify that the worst-case observed voltage dip on the 275kV side of the transformer was approximately 0.2 pu in magnitude, dropping the voltage to approximately 0.78 pu. Voltage remained below 0.9 pu for approximately 130 ms. The minimum access standard for S5.2.5.4 of the National Electricity Rules (NER) [6] requires plants can operate between 0.7 pu and 0.8 pu for at least 2 seconds. As such system normal requirements are more than adequate to facilitate system restart, in terms of voltage dips driven by transformer energisation during system restart.

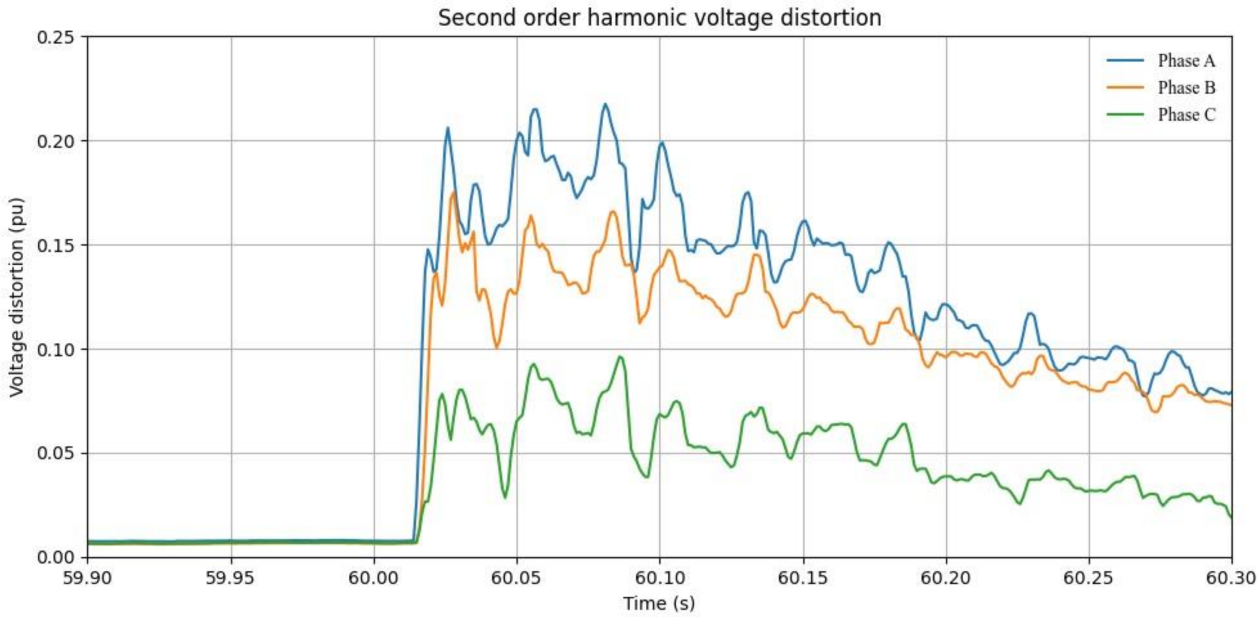


Figure 16 Worst case 2nd order harmonics on energisation at 275kV side of transformer.

Figure 16 highlights that second order harmonic voltage distortion peaks above 20% for more than 100 ms. The high second order harmonic distortion is of potential concern for some protection relays which may operate when exposed to such high levels. Further investigation is recommended utilising detailed relay models to determine whether the high second order harmonics would cause activation of the protection relays or not.

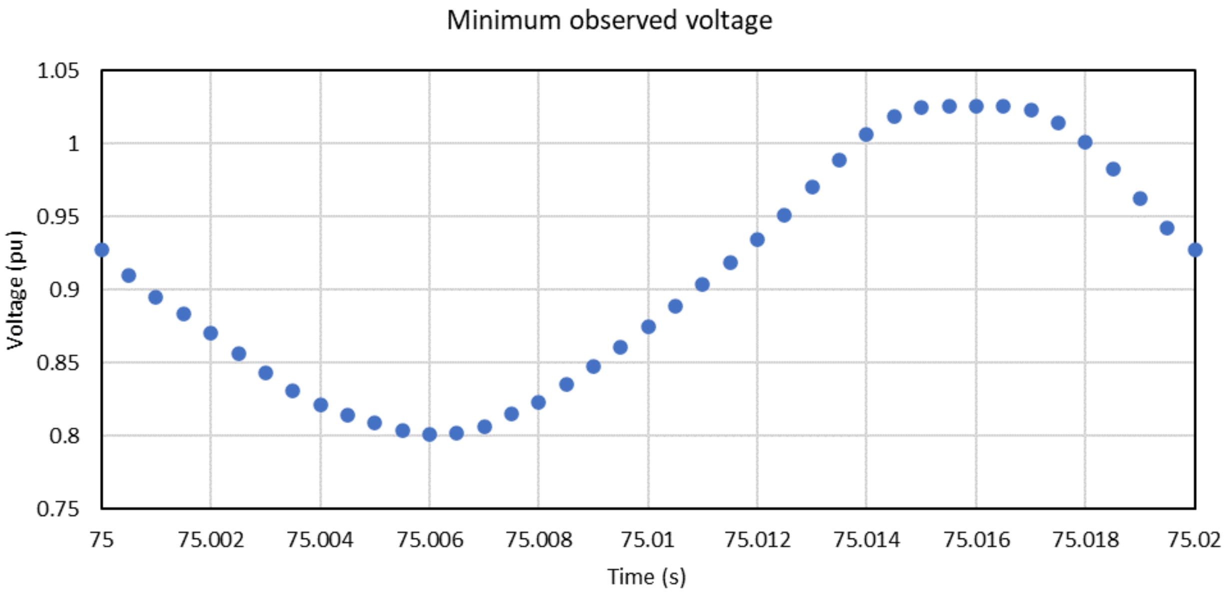


**Figure 17 Transformer energisation minimum observed voltage for all switching times with parallel transformer energised.**

Point-on-wave switching was also used to investigate the impact of energising a second transformer in parallel to an already energised transformer with the intent of determining the impact of sympathetic inrush current. Figure 17 indicates that the worst-case voltage dip on the 275kV side of the transformer is approximately 0.22 pu in magnitude, reaching a minimum of approximately 0.8 pu. Figure 18 shows that the voltage remained below 0.9 pu for approximately 70ms, which was also within the minimum access standards of S5.2.5.4 of the NER [6] for system normal conditions, and no material difference was observed when considering sympathetic inrush current.

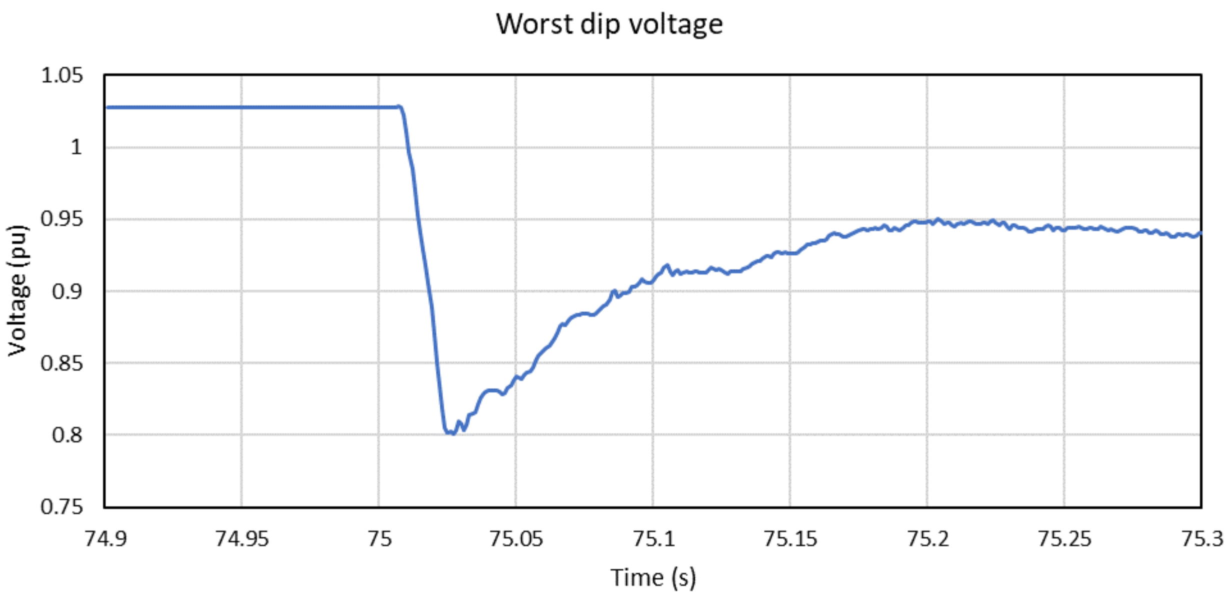


**Figure 18 Worst case voltage dip on energisation at 275kV side of transformer with parallel transformer energised.**

Figure 19 displays similar second order harmonic voltage distortion behaviour as with one transformer. In this case however, the second order harmonic distortion peaks just below 20%.

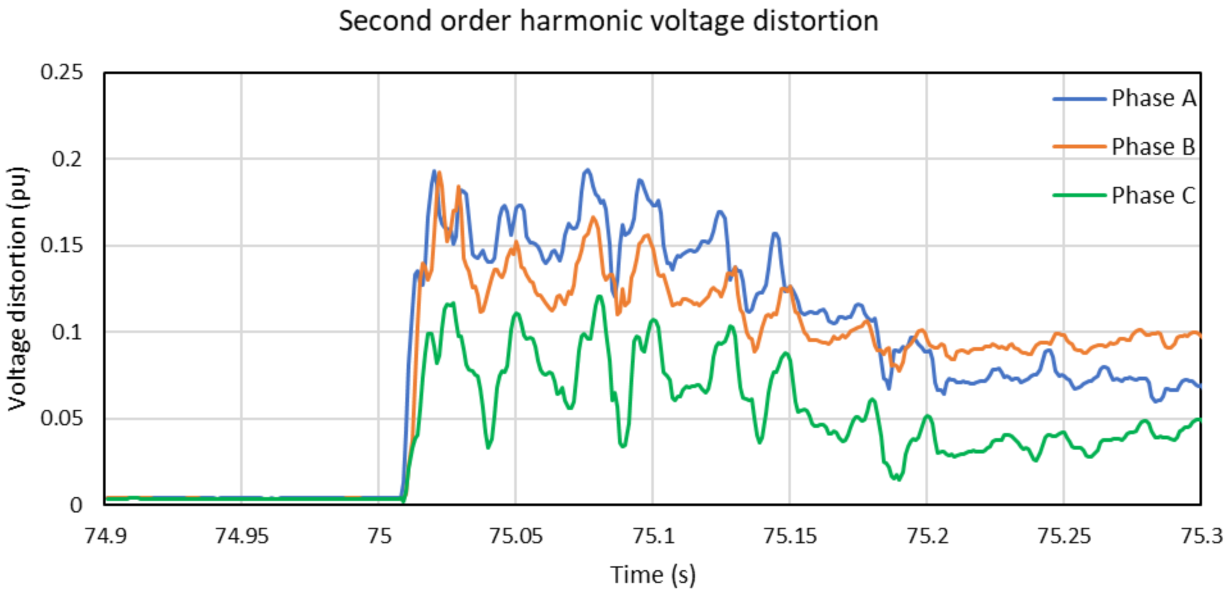


**Figure 19 Worst case 2nd order harmonics on energisation at 275kV side of transformer with parallel transformer energised.**

## 3.2 Control system parameter sensitivity tests

### 3.2.1 GFM inverter frequency control sensitivities

The sensitivity of system restart performance to grid-forming inverter frequency control was investigated to understand its impact on the formed island and its stability. The inverter frequency droop parameter that was adjusted is an internal governor and turbine droop setting, which is a component of a virtual synchronous machine implementation of grid-forming control. The plant active power – frequency P(F) droop setting was not altered as this characteristic is usually managed at the power plant controller (PPC) level, not at the inverter level for IBRs. Six different values of inverter level droop were investigated. Studies were performed utilising reduced MVA capacity of the GFM black start device as a base and all available grid-following devices to form a sizable IBR-only island. Two scenarios were investigated utilising a larger GFM black start device to confirm the impact this had on the  frequency response. All studies performed are summarised in Table 8.

**Table 8 GFM frequency control sensitivity studies summary**

| SCENARIO ID | BLACK START DEVICE | SUPPORT DEVICES | BLACK START DEVICE INVERTER DROOP SETTING |
|---|---|---|---|
| **A** | 87.5 MVA GFM BESS | • 163.8 MVA GFL BESS<br>• 190 MVA WF<br>• 304 MVA WF | 2.517% |
| **B** | 87.5 MVA GFM BESS | • 163.8 MVA GFL BESS<br>• 190 MVA WF<br>• 304 MVA WF | 2.0% |
| **C** | 87.5 MVA GFM BESS | • 163.8 MVA GFL BESS<br>• 190 MVA WF<br>• 304 MVA WF | 3.0% |

| | | | |
|---|---|---|---|
| **D** | 87.5 MVA GFM BESS | • 163.8 MVA GFL BESS<br>• 190 MVA WF<br>• 304 MVA WF | 3.5% |
| **E** | 350 MVA GFM BESS | • 163.8 MVA GFL BESS<br>• 190 MVA WF<br>• 304 MVA WF | 3.5% |
| **F** | 87.5 MVA GFM BESS | • 163.8 MVA GFL BESS<br>• 190 MVA WF<br>• 304 MVA WF | 1.0% |
| **G** | 350 MVA GFM BESS | • 163.8 MVA GFL BESS<br>• 190 MVA WF<br>• 304 MVA WF | 1.0% |
| **H** | 87.5 MVA GFM BESS | • 163.8 MVA GFL BESS<br>• 190 MVA WF<br>• 304 MVA WF | 10% |

Droop values less than 1.0% were not studied in a system restart environment, as sanity check studies performed showed instability below this value even in a single machine infinite bus (SMIB) environment.

The GFM BESS active power response for the difference scenarios in Table 8 is displayed in Figure 20.

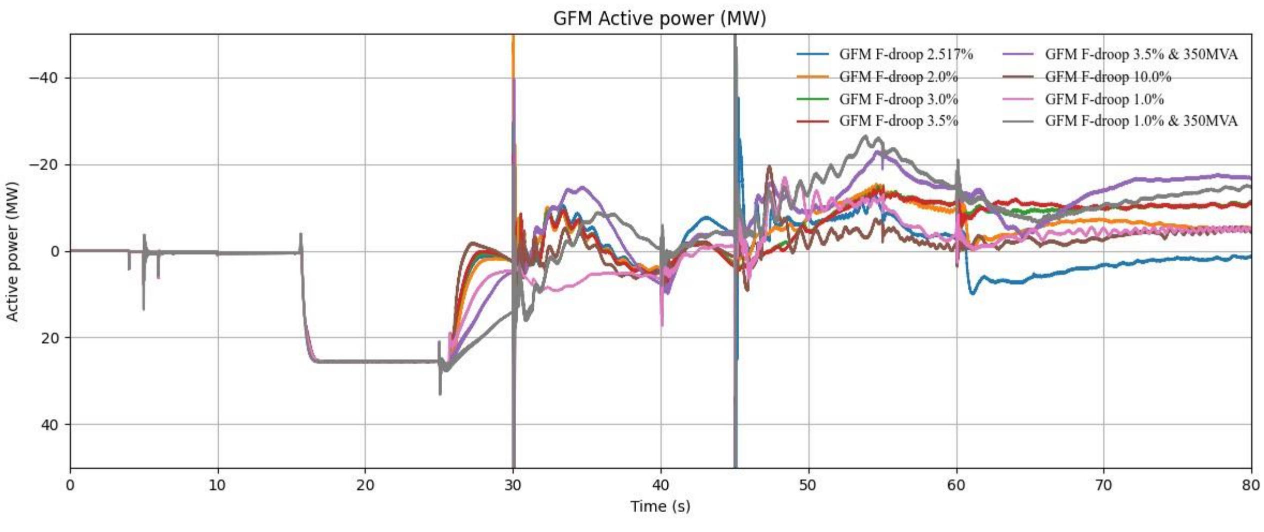


**Figure 20 GFM active power response with different GFM inverter frequency droop settings.**

The inverter frequency droop settings do not have a significant impact to sustained frequency response of the plant. The inverter frequency droop predominately contributes to fast control response when managing transients in the 0 s to 2 s timeframe. The GFM plant has a power plant controller (PPC) which also possesses frequency control and is slower acting. Based on simulation results, the PPC frequency control is understood to drive the steady-state response of the GFM BESS. Hence the inverter-level frequency droop behaviour is based upon interactions with network transients and the GFL support devices within the network, but it does not improve either network stability or the settled steady-state frequency.

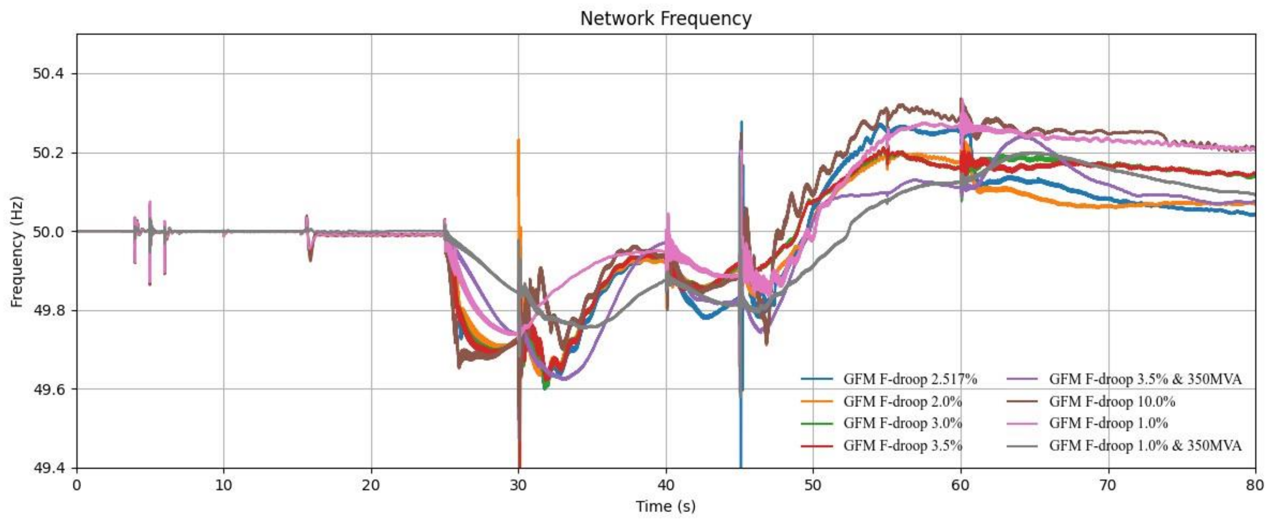


**Figure 21 Network frequency with different GFM inverter frequency droop settings.**

The network frequency for the same studies is presented in Figure 21 where smaller droop values (smaller frequency deviations required for a given active power response) result in a lower settled steady-state frequency (that is, closer to the 50Hz nominal target) at the end of the simulation. The smaller droop values appear to result in a more aggressive short-term frequency response that lowers the frequency through 60 s to 61 s and results in a lower steady-state error when frequency stabilises.

### 3.2.2 GFM inertia and damping constant sensitivity studies

Sensitivity analysis of the GFM inertia and damping constant was performed to understand the impact when a multi-machine IBR-only island is formed. Upper and lower bounds for the inertia constant (for satisfactory performance) were identified, with values outside the range of 2 – 8 showing instability or tripping of the GFM BESS. Tuning of damping constants is typically dependent on the inertia value, with overly large damping constants causing a slow recovery to the target output. The tested range of damping constants did not show any instability and it is therefore understood to have less impact on stability during system restoration than the inertia constant. The complete list of scenarios investigated is summarised in Table 9, with GFM active and reactive power response presented in Figure 22 and Figure 23 respectively, and network frequency in Figure 24.

**Table 9 GFM inertia and damping constant sensitivity studies summary**

| SCENARIO ID | BLACK START DEVICE | SUPPORT DEVICES | BLACK START DEVICE INERTIA (H) CONSTANT | BLACK START DEVICE DAMPING (D) CONSTANT | COMMENTS |
|---|---|---|---|---|---|
| **A** | 36.7 MVA GFM BESS | 163.8 MVA GFL BESS<br>190 MVA WF<br>304 MVA WF | 1 | 5 | GFM Tripped |
| **B** | 36.7 MVA GFM BESS | 163.8 MVA GFL BESS<br>190 MVA WF<br>304 MVA WF | 2 | 5 | |
| **C** | 36.7 MVA GFM BESS | 163.8 MVA GFL BESS<br>190 MVA WF | 3 | 5 | |

| | | | | | |
|---|---|---|---|---|---|
| | | 304 MVA WF | | | |
| **D** | 36.7 MVA GFM BESS | 163.8 MVA GFL BESS<br>190 MVA WF<br>304 MVA WF | 5 | 5 | |
| **E** | 36.7 MVA GFM BESS | 163.8 MVA GFL BESS<br>190 MVA WF<br>304 MVA WF | 8 | 4 | |
| **F** | 36.7 MVA GFM BESS | 163.8 MVA GFL BESS<br>190 MVA WF<br>304 MVA WF | 8 | 5 | |
| **G** | 36.7 MVA GFM BESS | 163.8 MVA GFL BESS<br>190 MVA WF<br>304 MVA WF | 8 | 6 | |
| **H** | 36.7 MVA GFM BESS | 163.8 MVA GFL BESS<br>190 MVA WF<br>304 MVA WF | 10 | 5 | GFM tripped at 45s<br>304MVA GFL WF energised at 45s |
| **I** | 36.7 MVA GFM BESS | 163.8 MVA GFL BESS<br>190 MVA WF<br>304 MVA WF | 10 | 3 | GFM tripped at 45s<br>304MVA GFL WF energised at 45s |

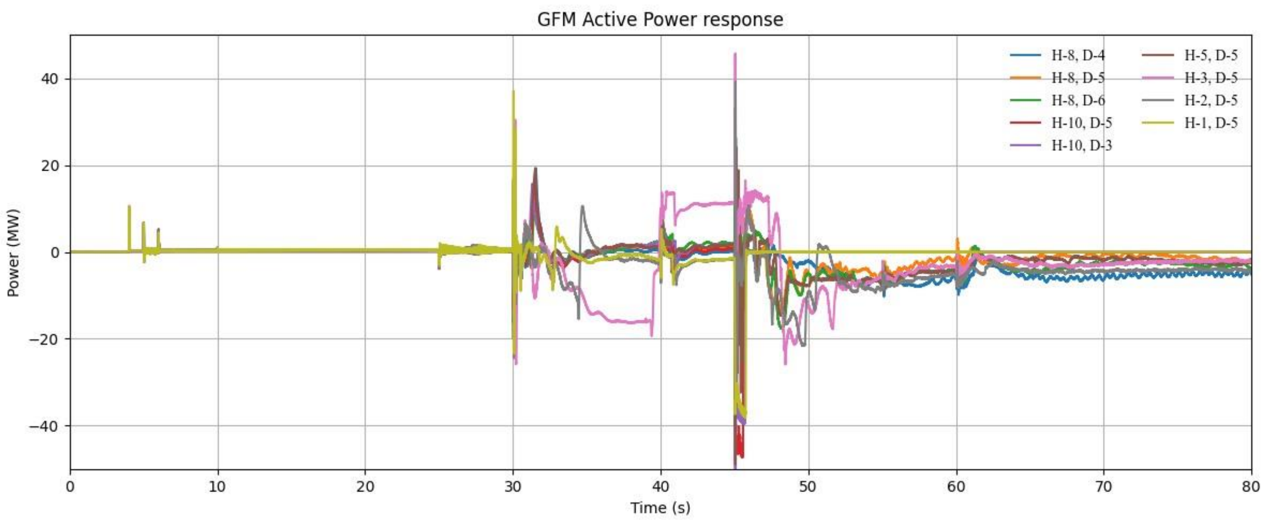


**Figure 22 GFM active power response with different inertia (H) and damping (D) constants.**

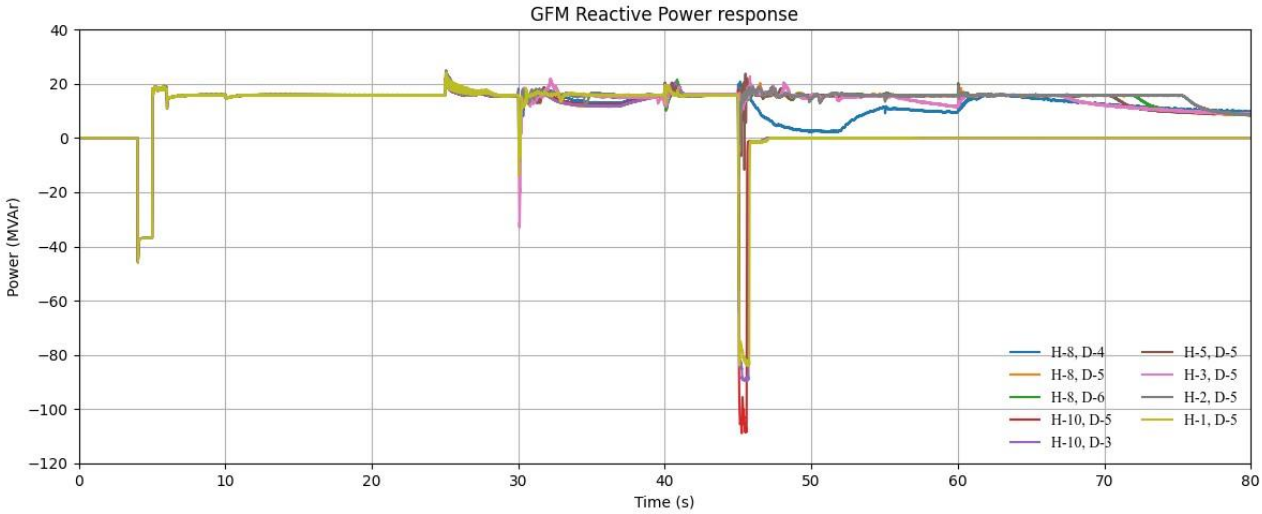


**Figure 23 GFM reactive power response with different inertia (H) and damping (D) constants.**

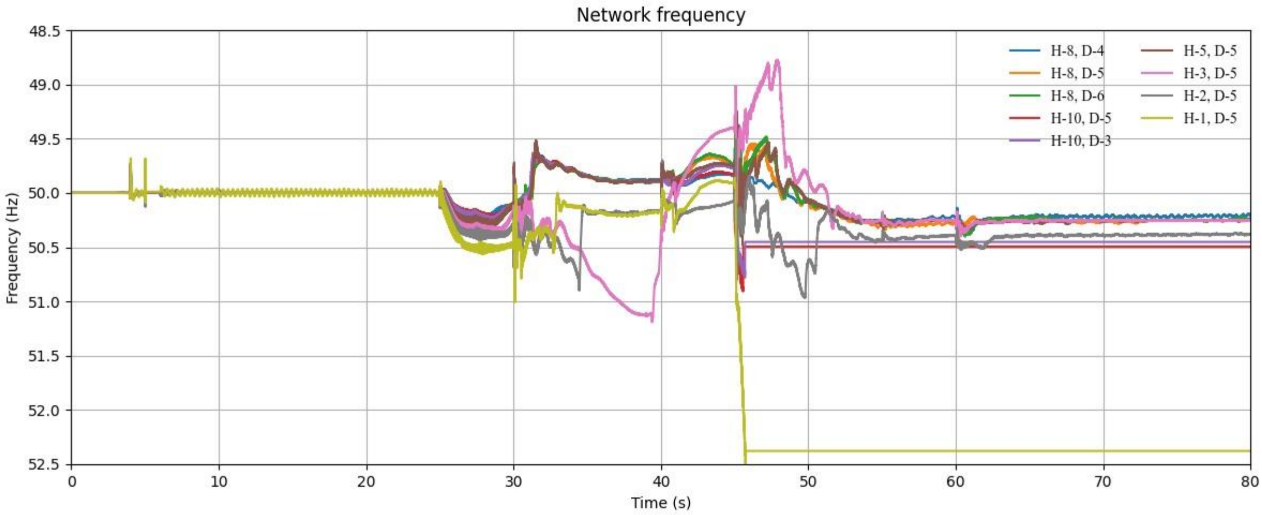


**Figure 24 Network frequency with different inertia (H) and damping (D) constants.**

### 3.2.3 GFL plant level frequency control sensitivity tests

Sensitivity analysis of grid-following device frequency control parameters was performed to understand how they can minimise loading on the grid-forming black start device and provide greater island stability and resilience. The network studied had approximately 49 MW of generation, with the GFL BESS charging and dispatched at a target of -25 MW. As can be observed in Figure 25 which presents the GFL BESS active power response, the plant never settles to its target (load) value due to frequency, , settling above nominal frequency (shown in Figure 26). Smaller GFL frequency droop settings (e.g. 2% compared to 4%) was expected to result in greater active power contribution from the GFL support devices. Study results showed that the active power output of GFL support devices was primarily dependent on the point in time at which frequency change was arrested following a network switching event and is a complex interaction between the GFM inertia response and GFL IBRs frequency droop response. Smaller GFL frequency droop was observed to reduce the magnitude of frequency swings following a network event. If GFL frequency droop was too small, it resulted in overshoot of the GFL support device active power response and subsequently resulted in unstable oscillations. The list of studies performed is outlined in Table 10.

**Table 10 GFL frequency control sensitivity studies summary**

| SCENARIO ID | BLACK START DEVICE | SUPPORT DEVICES | GFL DEVICE PPC FREQUENCY DROOP | COMMENTS |
|---|---|---|---|---|
| **A** | 87.5 MVA GFM BESS | 163.8 MVA GFL BESS<br>190 MVA WF<br>304 MVA WF | 2.4% | |
| **B** | 87.5 MVA GFM BESS | 163.8 MVA GFL BESS<br>190 MVA WF<br>304 MVA WF | 3.0% | |
| **C** | 87.5 MVA GFM BESS | 163.8 MVA GFL BESS<br>190 MVA WF<br>304 MVA WF | 1.7% | |
| **D** | 87.5 MVA GFM BESS | 163.8 MVA GFL BESS<br>190 MVA WF<br>304 MVA WF | 4.0% | |
| **E** | 87.5 MVA GFM BESS | 163.8 MVA GFL BESS<br>190 MVA WF<br>304 MVA WF | 0.1% | Instability observed with smaller droop settings |

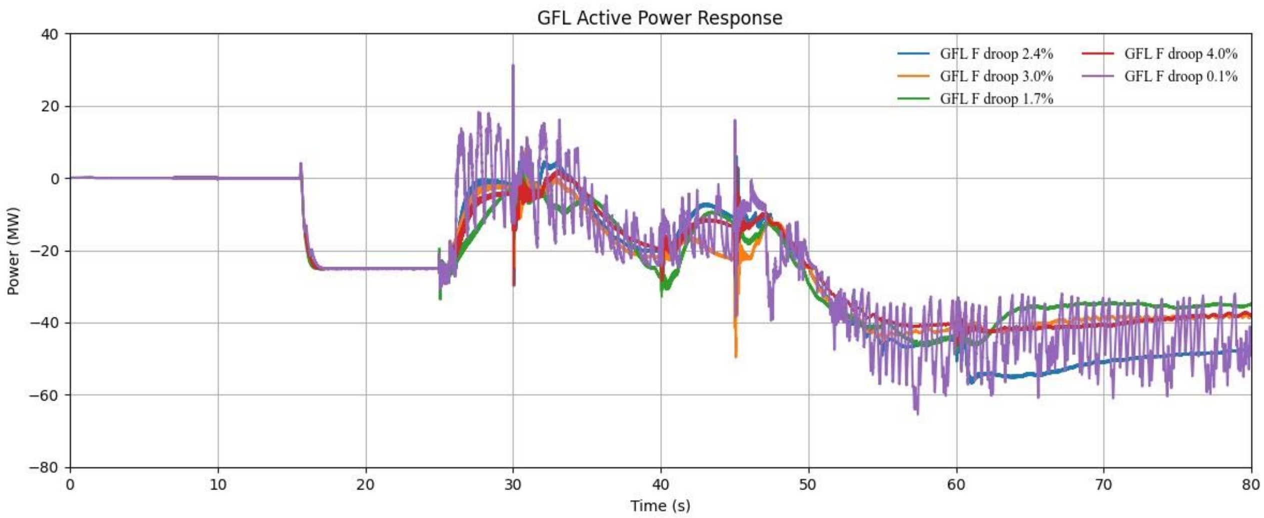


**Figure 25 GFL active power response with different frequency droop settings of GFL**

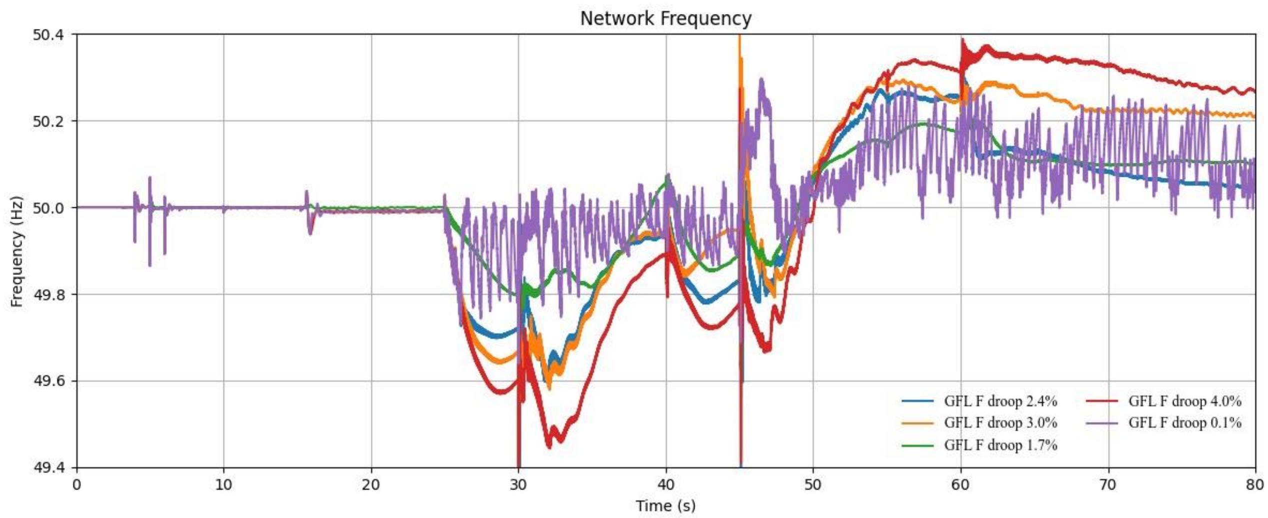


**Figure 26 Network frequency with different frequency droop settings of GFL**

### 3.2.4 GFM voltage control sensitivity tests

Voltage management and sufficient reactive power capability was identified as a key factor in system restart viability through Stage 2 findings over 2022 – 2023 and studies performed in Section 3.1. Analysis of the GFM voltage control settings, specifically considering voltage droop control, was performed to understand its significance on system restart stability – whether it could prevent voltage collapse, over-voltages or other voltage related concerns. Studies performed did not present any material difference in viability of system restoration, with even large voltage droop settings (voltage deviation permitted per unit reactive power response) still resulting in sufficient reactive power provision to maintain network voltages above 0.95 pu in steady-state conditions. The list of studies and range of voltage droop settings considered is summarised in Table 11, with reactive power and voltage response across the studies for the GFM BESS presented in Figure 27 and Figure 28.

**Table 11 GFM voltage control sensitivity studies summary**

| SCENARIO ID | BLACK START DEVICE | SUPPORT DEVICES | GFM DEVICE PPC VOLTAGE DROOP | COMMENTS |
|---|---|---|---|---|
| **A** | 87.5 MVA GFM BESS | 163.8 MVA GFL BESS<br>190 MVA WF<br>304 MVA WF | 1.0% | |
| **B** | 87.5 MVA GFM BESS | 163.8 MVA GFL BESS<br>190 MVA WF<br>304 MVA WF | 3.0% | |
| **C** | 87.5 MVA GFM BESS | 163.8 MVA GFL BESS<br>190 MVA WF<br>304 MVA WF | 5.0% | |
| **D** | 87.5 MVA GFM BESS | 163.8 MVA grid-following battery<br>190 MVA WF<br>304 MVA WF | 7.0% | |
| **E** | 87.5 MVA GFM BESS | 163.8 MVA GFL BESS | 9.0% | |

| | | | |
|---|---|---|---|
| | | 190 MVA WF<br>304 MVA WF | |
| **E** | 87.5 MVA GFM BESS | 163.8 MVA GFL BESS<br>190 MVA WF<br>304 MVA WF | 10.0% |

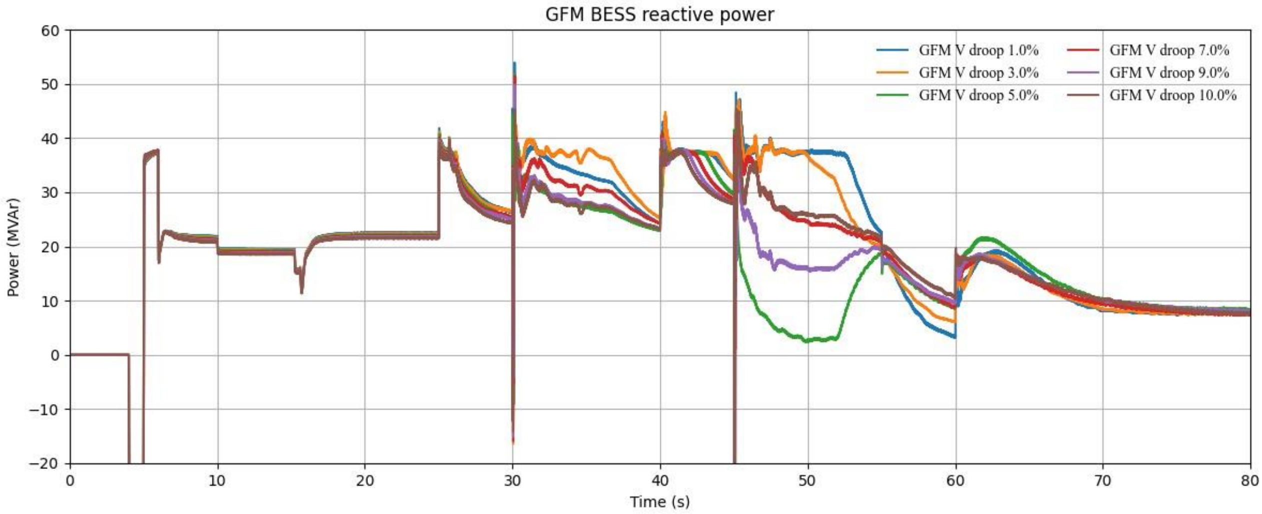


**Figure 27 GFM reactive power response with different voltage droop settings of GFM**

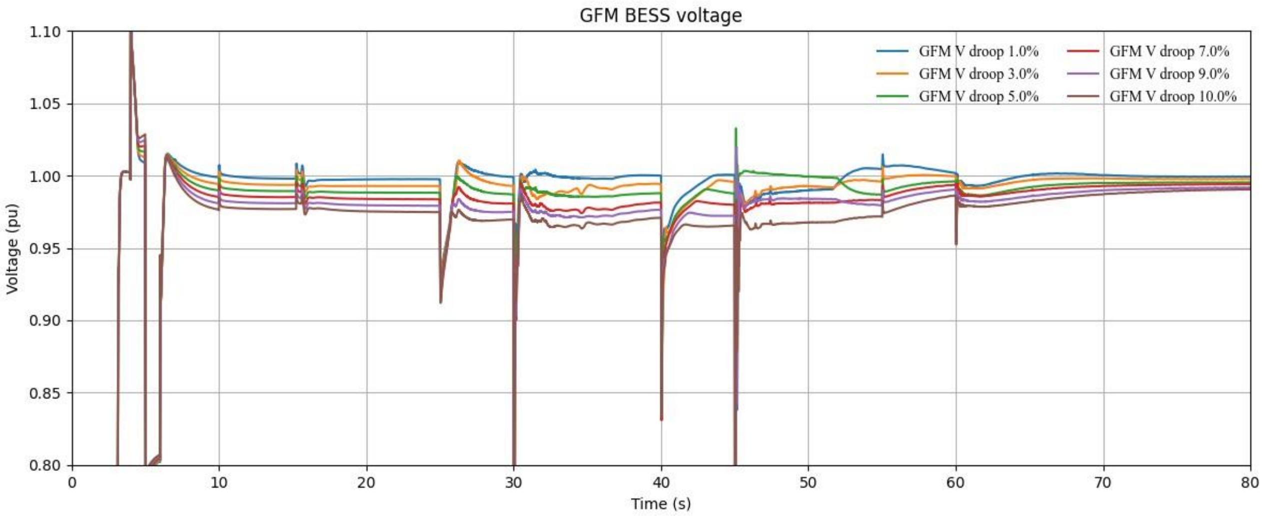


**Figure 28 GFM voltage response with different voltage droop settings of GFM**

## 3.3 Black-start IBR location studies

Studies were conducted considering a GFM black start device connected to a 275 kV busbar at the same terminal station as a synchronous generator and, in a separate study, an industrial load. The GFM black start device was separated by a main grid-tie transformer to the synchronous generator auxiliary load, and to the industrial load. Studies performed identified that energisation of the synchronous generator grid-tie transformer caused an over-voltage spike at the GFM connection point not observed in studies where the GFM is connected remote to the synchronous generator and is presented in Figure 29. The high inrush currents on the transformer energisation also caused the GFM black start device to go unstable if its capacity was too small, as presented in Figure 30 where a 87.5 MVA GFM is unstable while the 350 MVA GFM shown in Figure 29 remains stable and in-service.

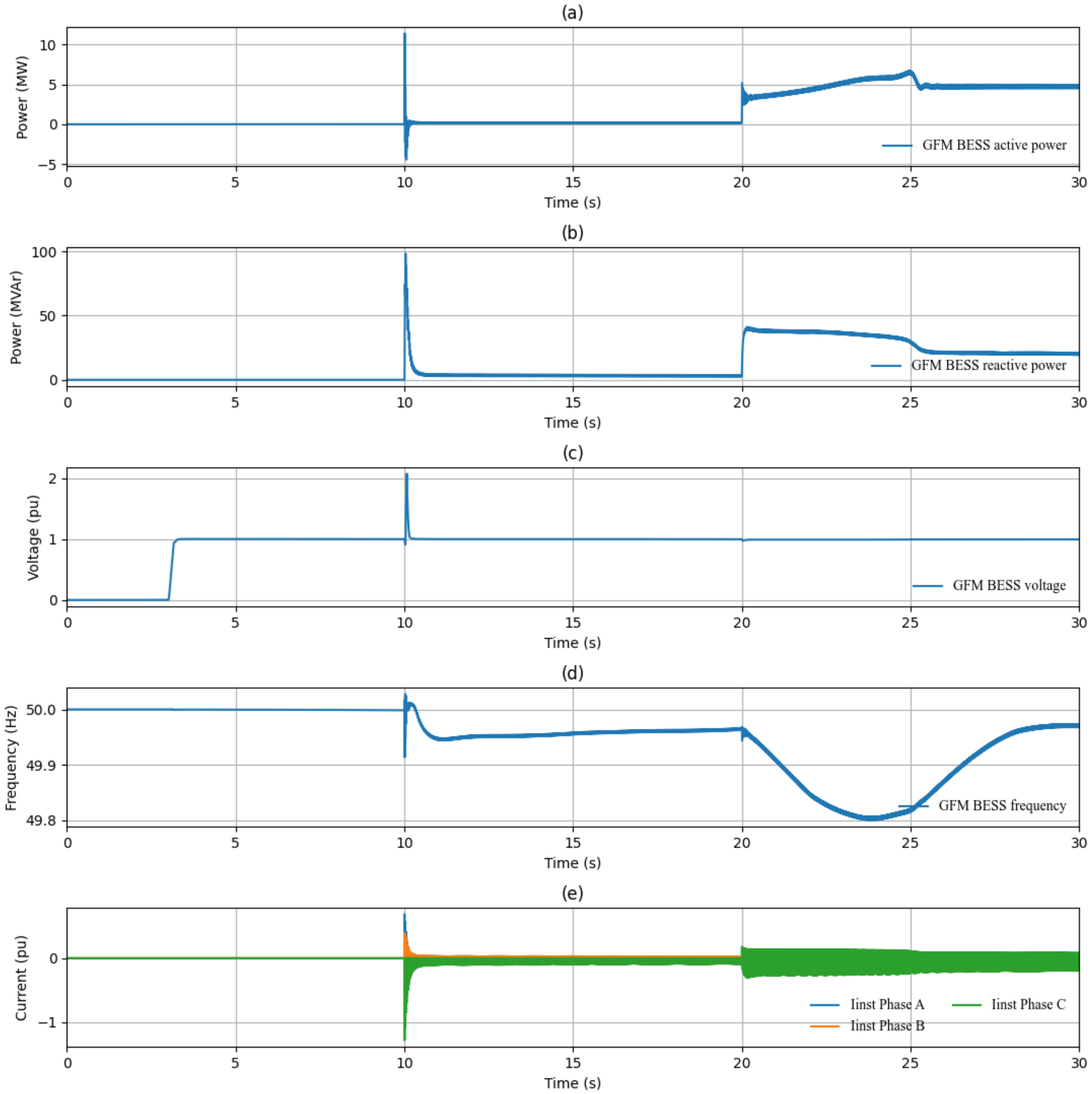


**Figure 29 350 MVA GFM BESS response to hard-energisation of synchronous generator grid-tie transformer at 10s**

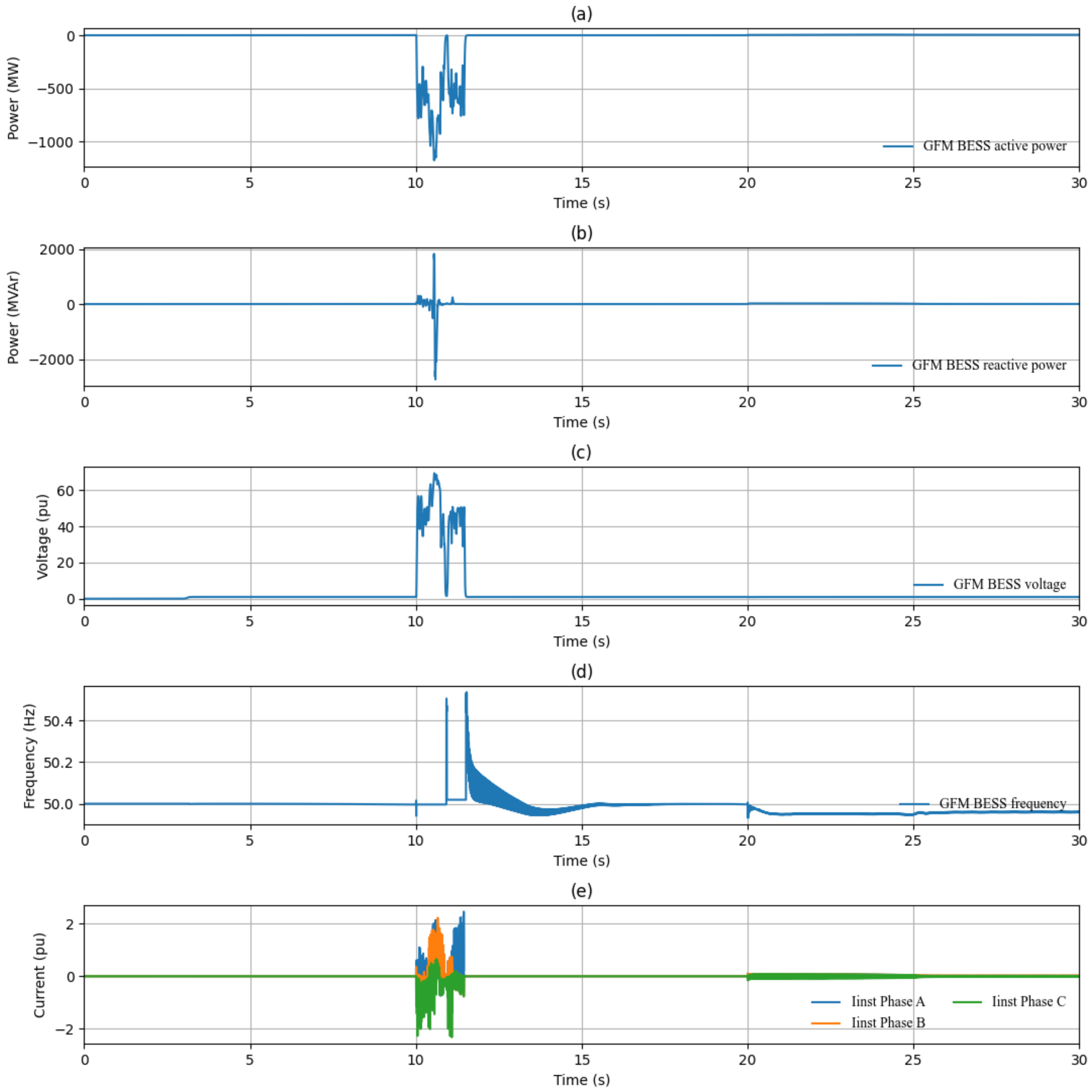


**Figure 30 87.5 MVA GFM BESS response to hard-energisation of synchronous generator grid-tie transformer at 10s**

Soft energisation was investigated as a means of connecting the synchronous generator without instability driven by transformer inrush currents. Soft energisation involves the GFM BESS black start device ramping voltage up from 0 pu while already connected to the synchronous generator and grid-tie transformer. Soft energisation is not a viable option for GFM black start devices located several terminal stations away from a synchronous generator. As shown in Figure 31, soft energisation is able to pick-up the synchronous generator without over-voltage spikes or network collapse with a significantly smaller GFM BESS black start device.

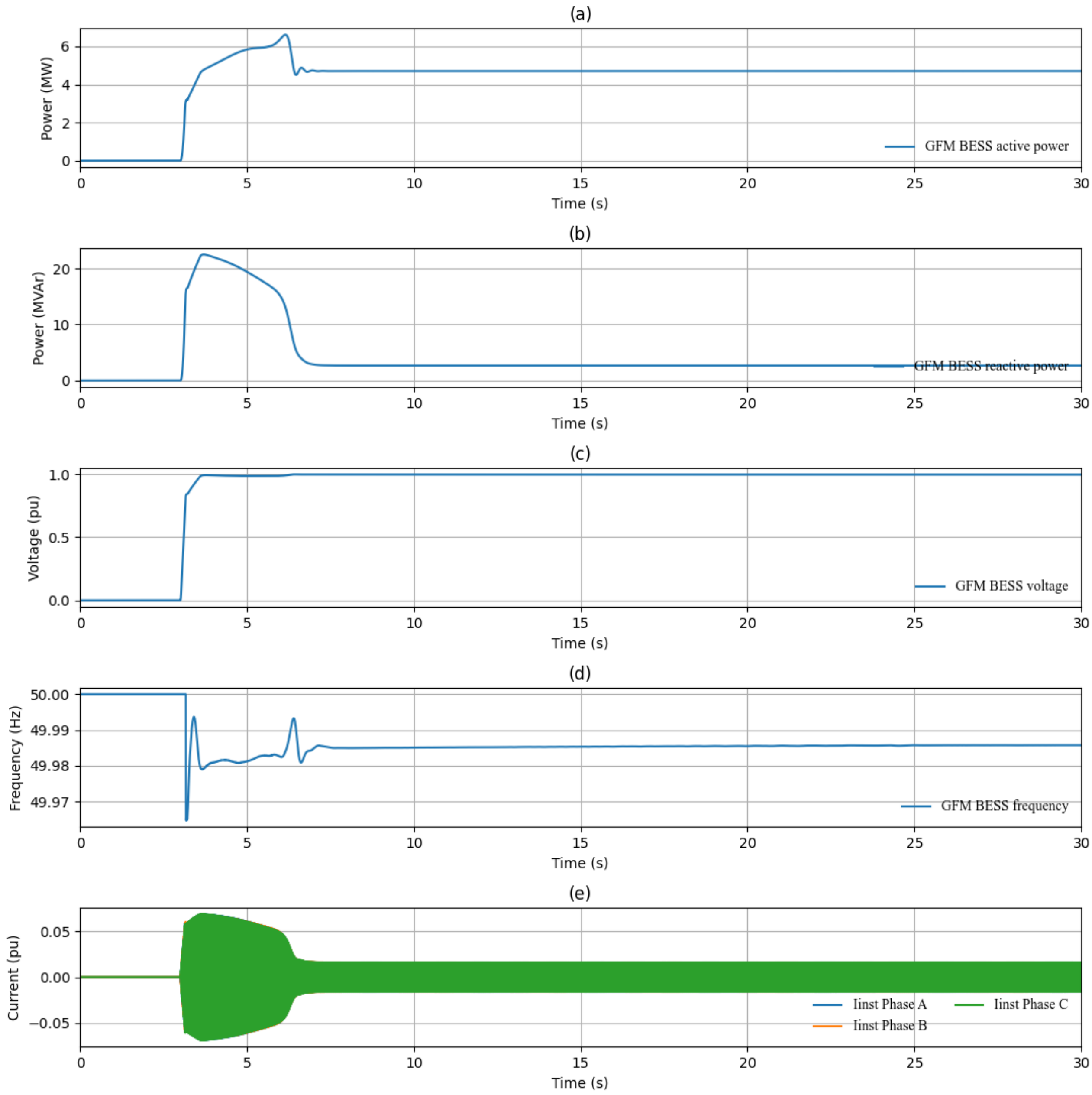


**Figure 31 87.5 MVA GFM BESS response to soft-energisation of synchronous generator grid-tie transformer and pick-up of synchronous generator auxiliary load**

A GFM BESS black start device proximal to industrial load exhibited instabilities on energisation which could not be resolved. Frequency deviation and oscillatory behaviour was observed. This was potentially attributed to the specific industrial load grid-tie transformer used and highlights that system restart requires site-specific assessment to confirm viable restart options. It is understood that energisation of a load is inefficient for a GFM BESS black start device due to limited energy availability of BESS. Practically, a GFM BESS would energise a generating system before a load to ensure sufficient energy is available to maintain the restarted system.

## 3.4 Island synchronisation

### 3.4.1 Successful synchronisation

Island synchronisation studies here demonstrate that it is possible to synchronise and join two smaller islands, one composed of IBRs only and the other composed of synchronous generators.

Significant transients are observed when synchronising two islands, driven by voltage phase angle and magnitude mismatches between the islands. Phase synchronising breakers were used to minimise the mismatches but due to challenges aligning the voltage and phase angle between two islands within simulation timeframes of one to two minutes, residual mismatches up to 0.01 pu and 10° were still observed.

Transients observed when synchronising the two islands resulted in active power swings of 0.4 pu or greater on the black start devices in each island: a synchronous generator and GFM BESS. Voltage did not dip below 0.8 pu for scenarios utilising a phase synchronising breaker and remained within existing under-voltage ride through requirements under clause S5.2.5.4 of the NER [6]. No disconnection or protection activation was observed for scenarios where phase synchronising breakers were utilised.

A summary of the studied scenarios are shown in Table 12 with black start device responses and network frequency shown in Figure 32 and Figure 33. Additional figures can be observed in Appendix C .

**Table 12 Island synchronisation studies summary**

| SCENARIO ID | IBR ISLAND | SG ISLAND | SYNCHRONISING BREAKER CLOSE TIME | COMMENTS |
|---|---|---|---|---|
| **A** | • 87.5 MVA GFM BESS<br>• 163.8 MVA GFL BESS<br>• 190 MVA WF<br>• 304 MVA WF | 350 MVA SG<br>Island load=125 MW and 60 MVAr | 65s | • System synchronised<br>• Large transient on synchronisation<br>• No devices tripped<br>• No phase synchronising breaker used |
| **B** | • 87.5 MVA GFM BESS<br>• 163.8 MVA GFL BESS MVA WF<br>• 304 MVA WF | 350 MVA SG<br>Island load=125 MW and 60 MVAr | 75s | • System synchronised<br>• Large transient on synchronisation<br>• No devices tripped<br>• No phase synchronising breaker used |
| **C** | • 87.5 MVA GFM BESS<br>• 163.8 MVA GFL BESS<br>• 121 MVA SF<br>• 452.89 MVA WF | 350 MVA SG<br>Island load=125 MW and 60 MVAr | 93.94 | • System synchronised<br>• Large transient on synchronisation<br>• Phase synchronising breaker used |
| **D** | • 87.5 MVA GFM BESS<br>• 163.8 MVA GFL BESS<br>• 190 MVA WF<br>• 304 MVA WF<br>• 230 MVA SVC<br>• 150 MVA SVC | 350 MVA SG<br>Island load=125 MW and 60 MVAr | 96.54 | • System synchronised<br>• Large transient on synchronisation<br>• Phase synchronising breaker used |

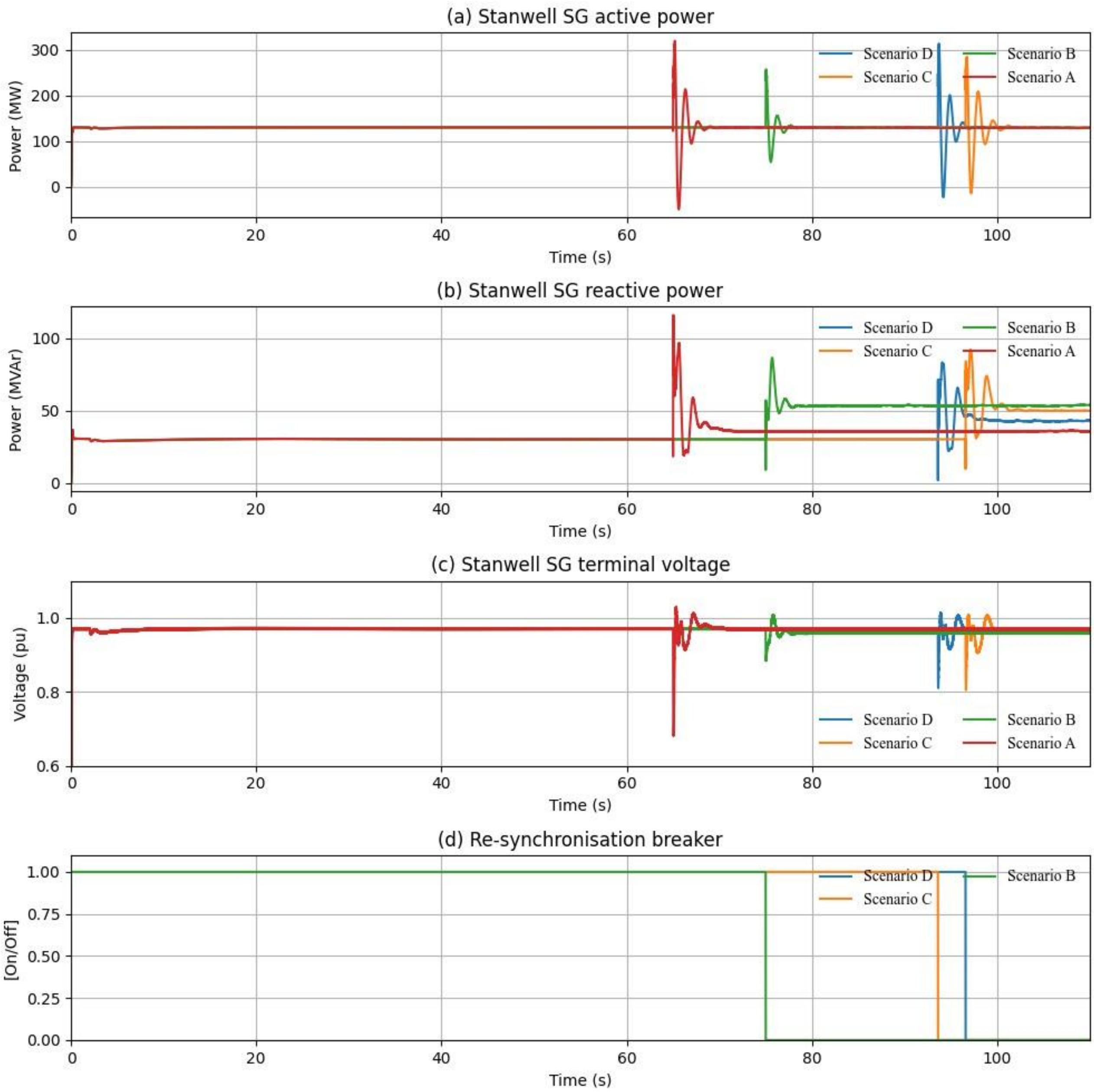


**Figure 32 Synchronous generator island response.**

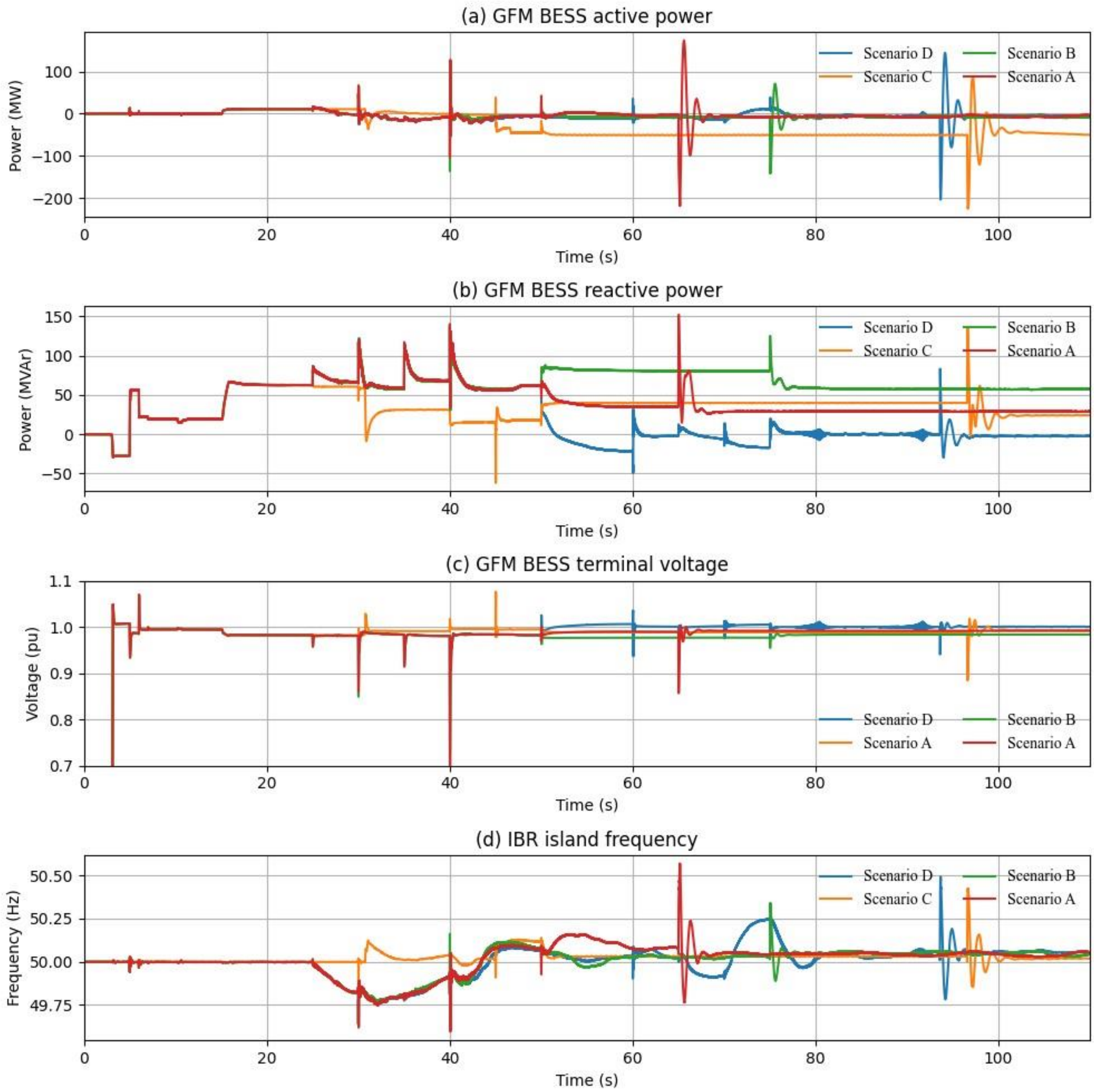


**Figure 33 IBR-only island response.**

### 3.4.2 Mode change sensitivity tests

Studies investigating the impact of the following modes and mode changes on a synchronous generator when synchronising two islands was performed.

- Isochronous mode (constant frequency, no frequency deviation permitted) with power system stabiliser disabled.
- Isochronous mode with power system stabiliser enabled.
- Synchronous mode (with frequency to active power droop response) with power system stabiliser enabled.

It has been observed that operation of a synchronous generator requires its PSS to be enabled to support loading levels up to approximately 50% of the plant capacity. A PSS is not always enabled when operating in isochronous mode as the PSS is tuned for system normal and synchronous mode operating conditions. Above 50% loading, isochronous mode should be disabled and the machine returned to synchronous mode operation. Studies showed that a synchronous generator operating in isochronous mode was able to synchronise with an IBR-only island whether a PSS was enabled or disabled. The PSS enabled in isochronous mode does add additional transients to the synchronous generator response, which is expected given the PSS is tuned for system normal operation and synchronous mode operation.

Due to the GFM BESS model lacking settings to perform mode changes, GFM BESS black start mode changes were not investigated. All IBR models, both GFM and GFL, utilised also did not posses power oscillation damper (POD) control settings which are equivalent to a PSS on a synchronous generator.

A summary of studies is presented in Table 13, with synchronous generator performance for stable scenarios presented in Figure 34 and Figure 35.

**Table 13 Island synchronisation model change sensitivity studies summary**

| SCENARIO ID | IBR ISLAND | SG ISLAND | SG OPERATING MODE | COMMENTS |
|---|---|---|---|---|
| **A** | • 87.5 MVA GFM BESS<br>• 163.8 MVA GFL BESS<br>• 121 MVA SF<br>• 452.89 MVA WF | 350 MVA SG<br>Island load=125 MW and 60 MVAr | ISO & PSS enabled | • System synchronised.<br>• No devices tripped |
| **B** | • 87.5 MVA GFM BESS<br>• 163.8 MVA GFL BESS<br>• 121 MVA SF<br>• 452.89 MVA WF | 350 MVA SG<br>Island load=125 MW and 60 MVAr | ISO and PSS disabled | • System synchronised.<br>• No devices tripped |
| **C** | • 87.5 MVA GFM BESS<br>• 163.8 MVA GFL BESS<br>• 121 MVA SF<br>• 452.89 MVA WF | 350 MVA SG<br>Island load=125 MW and 60 MVAr | SYNC & PSS enabled | • Frequency drifted pre-synchronisation. Unstable after re-synchronisation breaker on. |

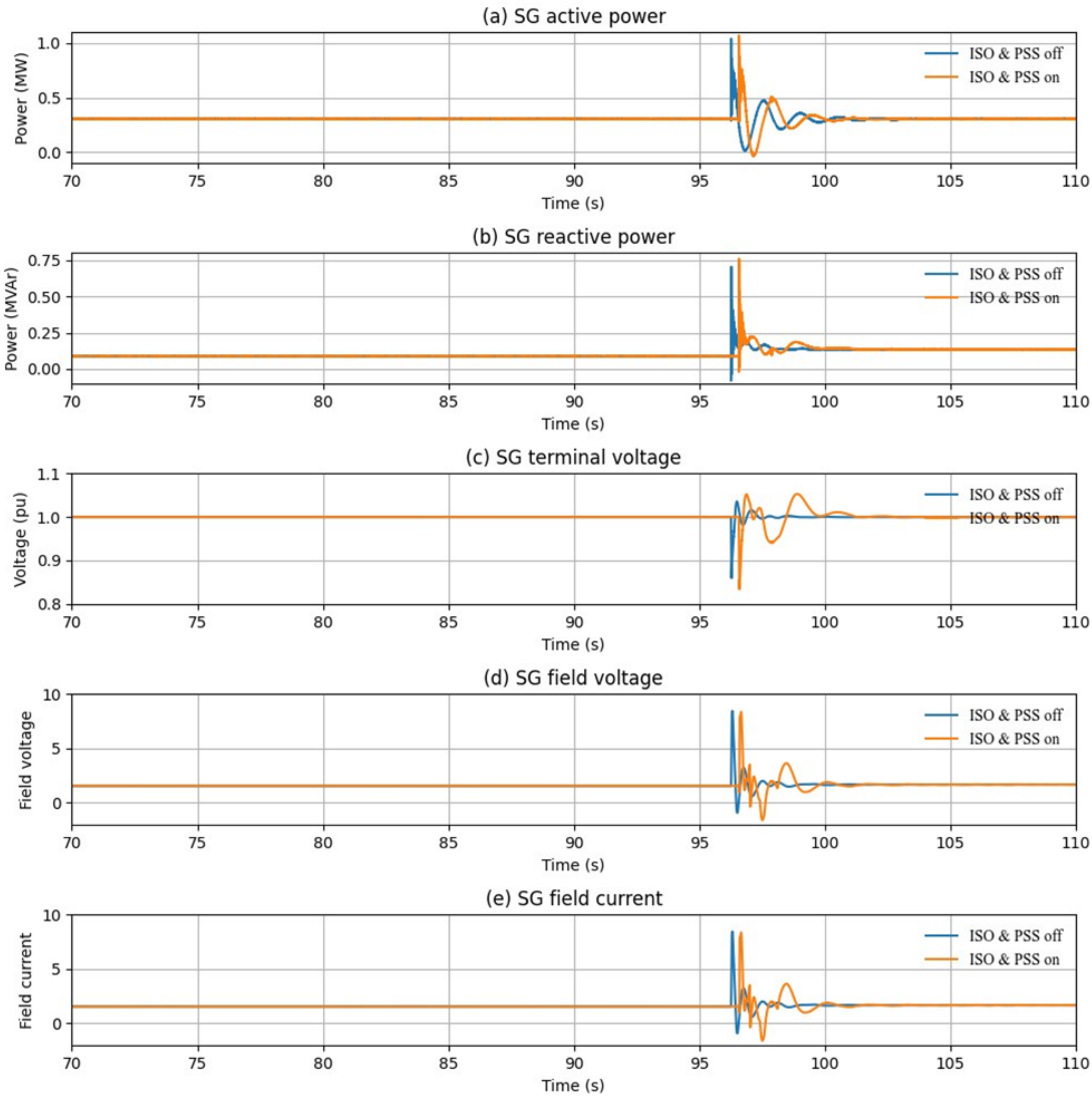


**Figure 34 Synchronous generator response with different operating modes (part 1)**

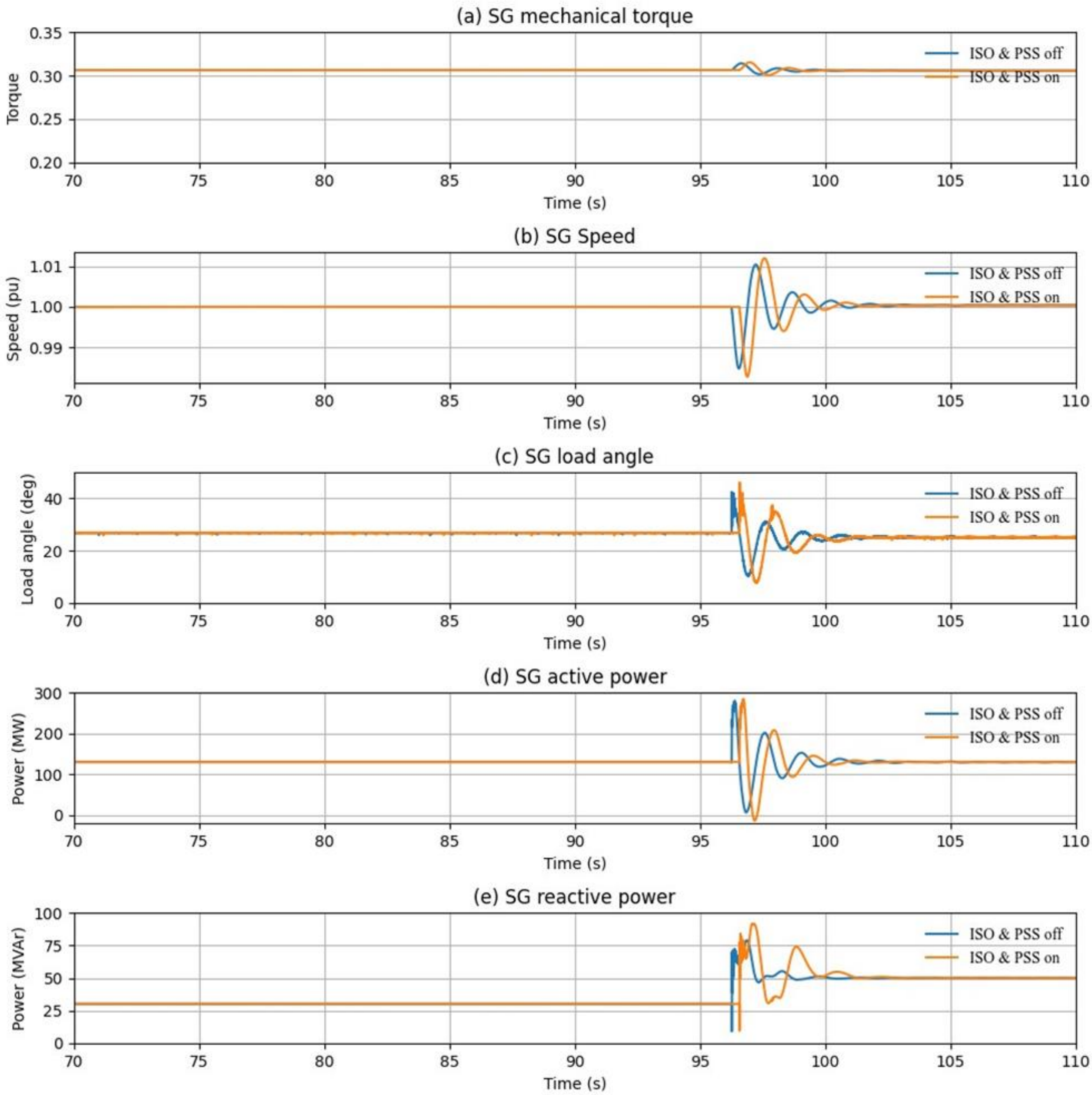


**Figure 35 Synchronous generator response with different operating modes (part 2)**

## 3.5 Distributed energy resources and load modelling

### 3.5.1 Impact of composite load model

Composite load models (CMPL) were studied across three residential load locations and one industrial location, for a total load up to 240.9 MW being considered. The key challenge encountered with connection of loads was under-voltage conditions, a challenge present regardless of the type of load model used. Significant adjustment to the sequence and timing of energisation of capacitor and inductor banks were required to maintain voltage suitable to pick-up load models and prevent under-voltage or over-voltage load “shake-off”. No material load “shake-off” was observed from credible faults studied, with only sustained under-voltage conditions resulting in temporary load reduction. Scenarios where voltage is also close to load tripping thresholds within the model can result in connect/disconnect triggering as there is no recovery deadband within the DER model. An example of a marginal difference in under-voltage driving re-triggering behaviour and reduction of load is presented in Figure 36.

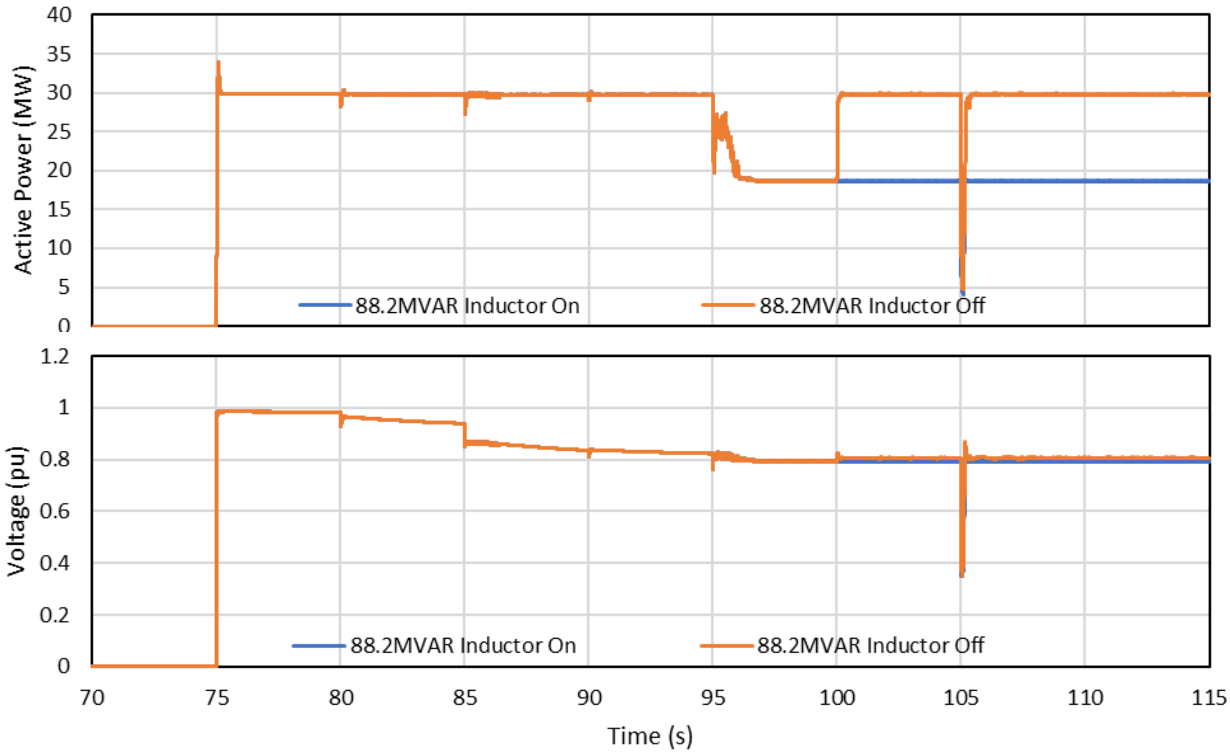


**Figure 36 CMPL response under sustained under-voltage load, with and without transmission inductor bank.**

The inclusion of the CMPL models did not introduce any new instabilities or phenomena during the system restart process. The CMPL models typically improved system restart stability when connected, similar to ZIP load model impact. An example of stable network response with CMPL is provided in Figure 37, below.

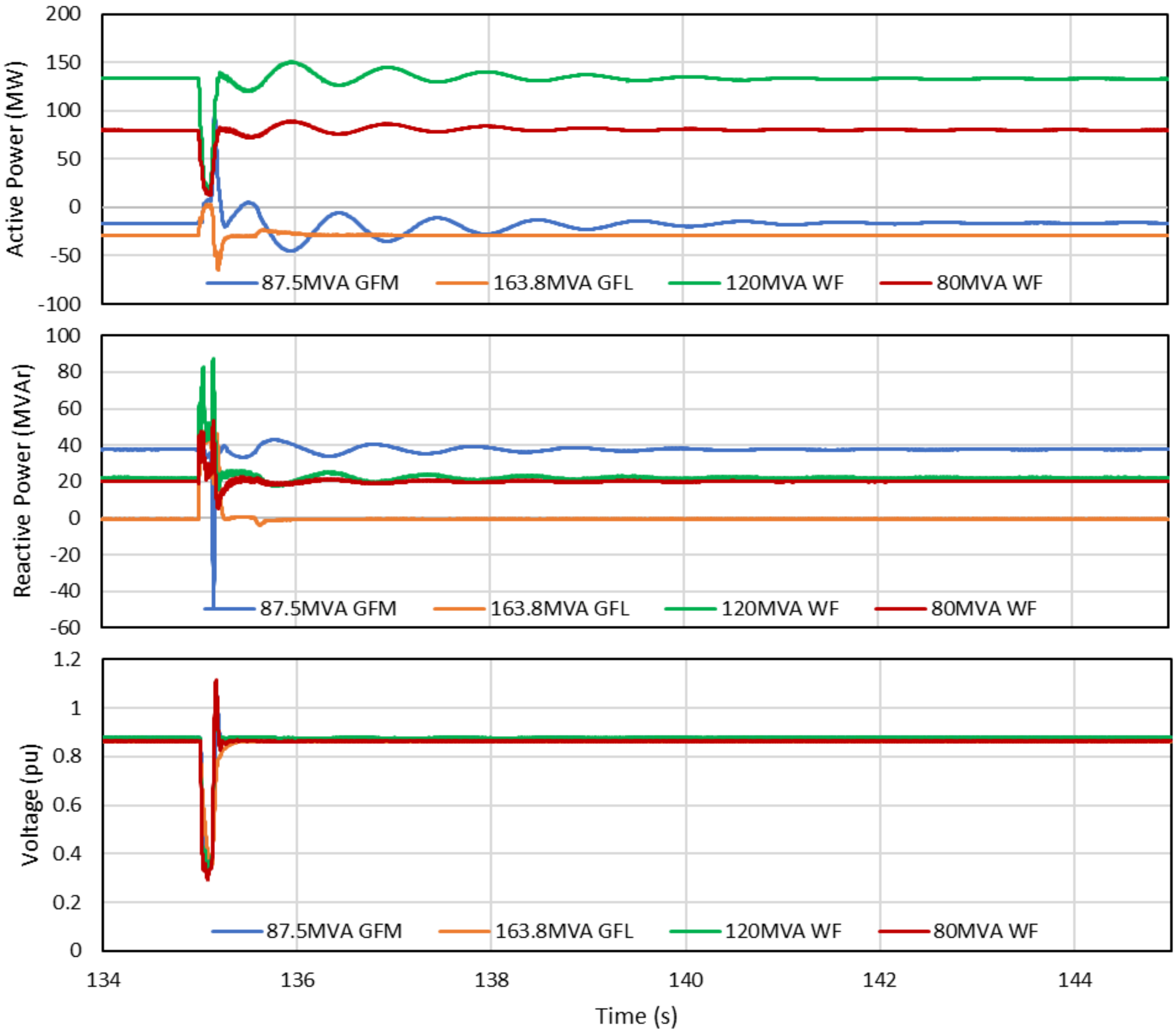


**Figure 37 Example of stable plant performance using CMPL following a two phase to ground (2PHG) fault**

A sensitivity analysis was performed by moving the fault location closer to the load models. No material change in fault depth and associated network performance was observed due to this.

Studies performed with the ZIP load model did not exhibit any instabilities. The CMPL had two key observed differences compared to the ZIP load model which highlighted it's need for use in system restart:

- ZIP load active and reactive power reduce as voltage reduces while CMPL remains at constant active and reactive power output until disconnection voltage thresholds are reached. An example is provided in Figure 38.
  - ZIP load models can be configured to have constant active and reactive power output regardless of voltage but would then not reflect active and reactive power reduction during under-voltage conditions which could easily occur during system restart.
  - ZIP load models inherently resist voltage and frequency oscillations when positive voltage and frequency coefficients are specified. An increase in voltage causes an increase in reactive power loading which opposes the voltage rise. CMPL does not exhibit the same

behaviour within normal voltage levels and would have less damping effect on network voltage and frequency oscillations.

- CMPL exhibits an active power swing on fault clearance not seen in the ZIP load model. Active power swings on fault clearance are typically reflective of synchronous machine behaviour and it is most likely driven by the different motor model components of the CMPL which aren't present in the ZIP load model. No problems were observed in the network with the active power swing, but it could result in frequency changes or under-voltages on fault clearance and is worth monitoring under system restart conditions.

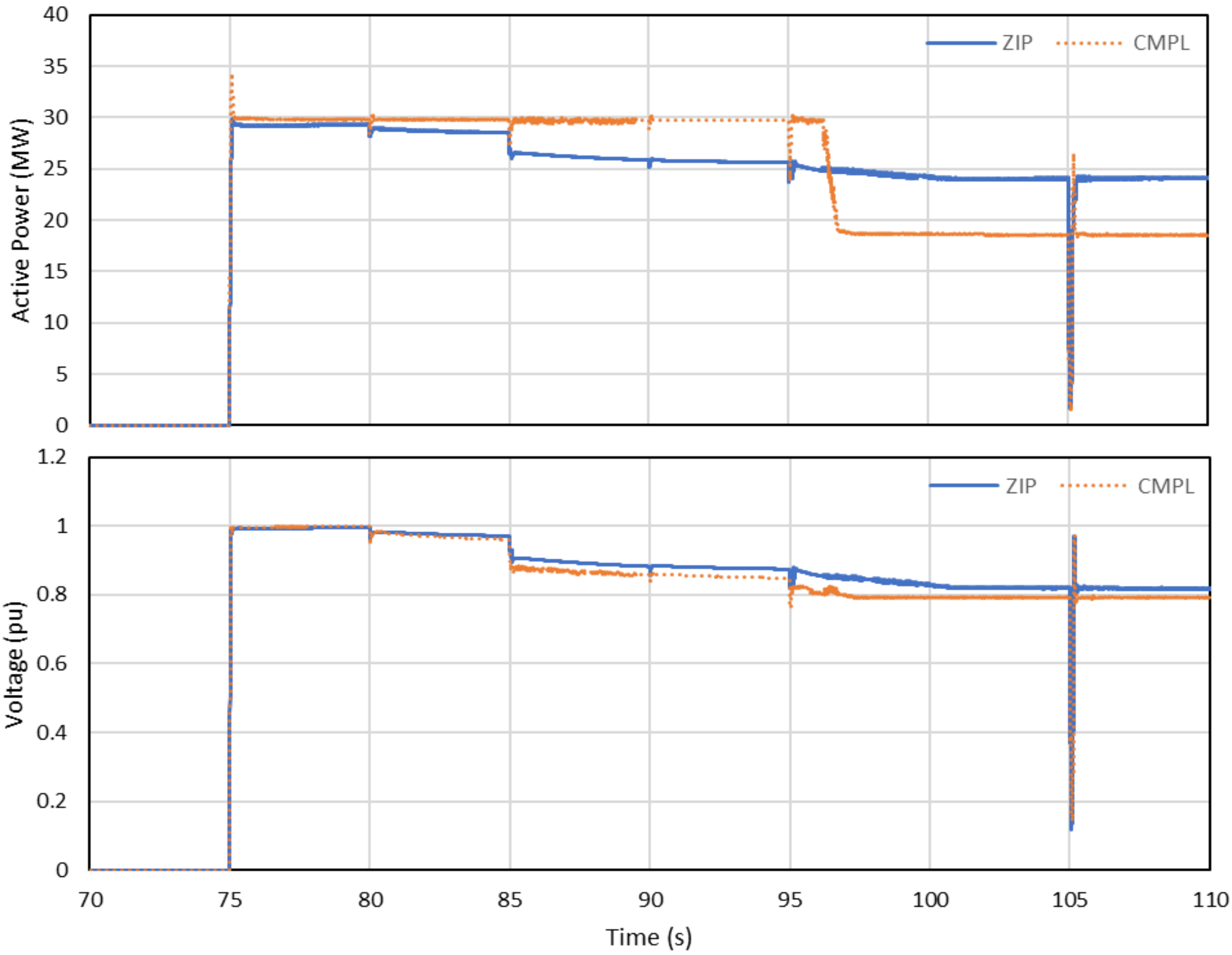


**Figure 38 Composite load model and ZIP load model system restart response for active power and voltage.**

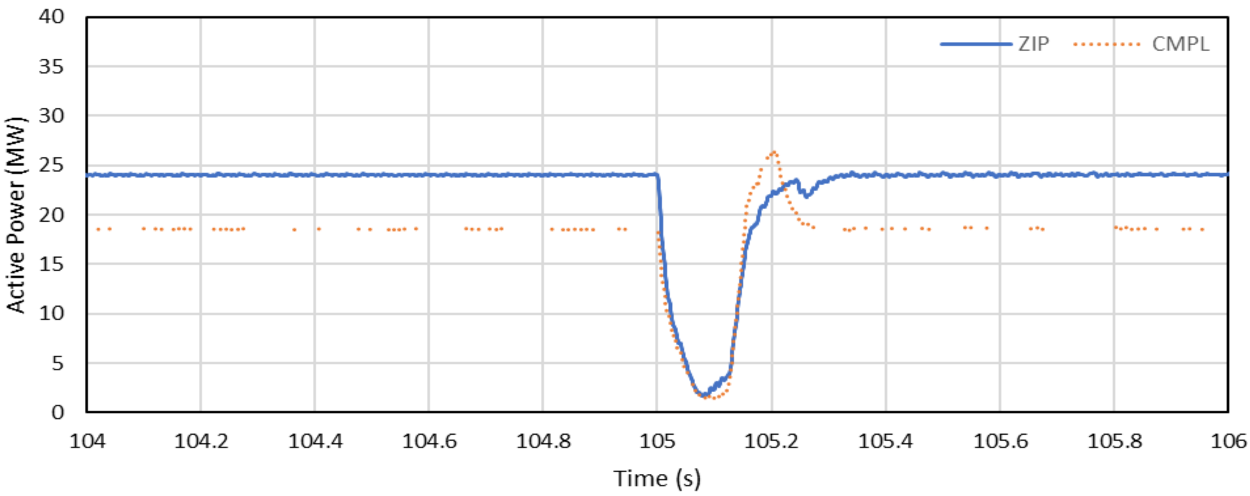

Figure 39 Composite load model and ZIP load model system restart active power response for an unbalanced fault. Figure is a zoomed version of Figure 38.

### 3.5.2 Impact of DER disconnection

Distributed energy resources were aggregated and connected to a 132 kV busbar, proximal to the composite load models. As with load modelling, the key challenge identified with DER modelling was voltage management. Capacitor or inductor banks on the transmission network had to be connected and disconnected at various times to maintain suitable voltage to support DER and contradicted with actions needed to maintain voltage for loads. Due to the aggregation of the DER model, all DER was modelled (unrealistically) as switched in immediately and there were temporary periods of high or low voltage before capacitor or inductor banks were switched to manage voltage. In reality, DERs would ramp up over a period of up to 10 minutes, which provides system operators sufficient time to perform voltage management operations. Additionally, transformer online tap changers would operate to maintain voltages on the low voltage network where domestic loads and DER are located.

DER was observed to have material levels of disconnection, upwards of 20%, during a fault, which wouldn't all recover upon fault clearance. An example of the observed disconnection is presented in Figure 40.

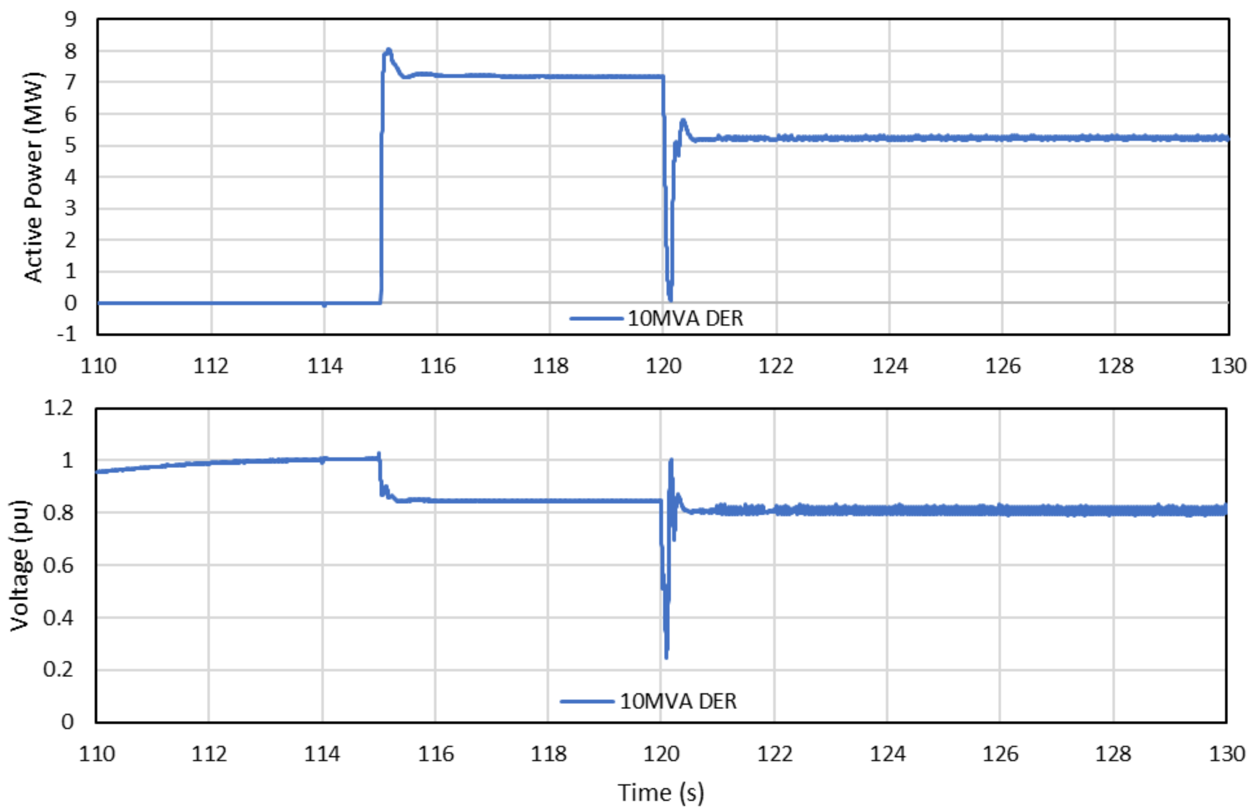


Figure 40 Stable plant performance and partial DER trip using CMPL and DER following a three phase to ground (3PHG) fault

Up to 40 MVA of DER was connected in an IBR-only environment without any observed instabilities. Numerical model issues which could not be resolved within available time were encountered preventing higher levels of DER being integrated.

## 3.6 Rise and settling time analysis

Rise and settling times of generating systems are evaluated under the NER [6] to define and confirm generating system performance. To define rise and settling times needed for system restart, rise and settling times of generating system performance and network characteristics, such as voltage, were examined across a range of study scenarios. Performance during and following a fault was considered:

- Reactive current response during a fault
- Active power, reactive power and voltage response following fault clearance

All studies performed are based off variations of restart Scenario D2, with Table 14, Table 15 and Table 16 providing summaries of the following:

- Table 14 – GFM black start device active power, reactive power and voltage settling times following clearance of a fault.
- Table 15 – GFL support device active power, reactive power and voltage settling times following clearance of a fault.
- Table 16 – GFM black start device reactive current rise and settling times during a fault.

Findings across the three groups of studies highlighted that active power, reactive power, voltage and reactive current rise times and settling times, whether during or following fault clearance, do not exceed requirements under NER [6] clause S5.2.5.5 and S5.2.5.13 for faults and voltage control, consecutively. Settling times for GFM black start device reactive power were observed as potentially longer than existing NER [6] minimum access requirements and may require relaxation for system restart conditions as no instabilities were observed due to longer settling times.

**Table 14 GFM rise and settling time response to fault during system restoration.**

| SCENARIO | GFM CAPACITY (MVA) | ACTIVE POWER RISE TIME (MS) | REACTIVE POWER RISE TIME (MS) | VOLTAGE RISE TIME (MS) | ACTIVE POWER SETTLING TIME (MS) | REACTIVE POWER SETTLING TIME (MS) | VOLTAGE SETTLING TIME (MS) |
|---|---|---|---|---|---|---|---|
| **Base scenario** | 42 | 143 | 71 | 76 | 1035 | 6771 | 541 |
| **Base scenario** | 87.5 | 145 | 10 | 70 | 1156 | 1638 | 320 |
| **Base scenario** | 175 | 143 | 39 | 68 | 1189 | 1753 | 257 |
| **Base scenario** | 262.5 | 142 | 40 | 60 | 2736 | 1439 | 258 |
| **Base scenario** | 350 | 39 | 58 | 68 | 1109 | 1218 | 257 |
| **GFM F droop increased by 2** | 87.5 | 146 | 9 | 61 | 413 | 2392 | 288 |
| **GFM F droop increased by 3** | 87.5 | 150 | 12 | 58 | 427 | 2035 | 326 |
| **GFM F droop increased by 4** | 87.5 | 149 | 11 | 60 | 427 | 1956 | 289 |
| **GFL WF offline** | 87.5 | 30 | 38 | 61 | 282 | 1700 | 259 |
| **With CMPL** | 87.5 | 115 | 18 | 53 | 2214 | 297 | 295 |
| **With CMPL and DER** | 87.5 | 17 | 33 | 23 | 3145 | 529 | 322 |
| **With CMPL and DER, inductor switched out** | 87.5 | 7 | 21 | 13 | 3179 | 6262 | 1100 |
| **With CMPL and DER, long fault** | 87.5 | 107 | 15 | 26 | 1145 | 323 | 330 |

| | | | | | | | |
|---|---|---|---|---|---|---|---|
| **With CMPL and DER, alternate fault** | 87.5 | 27 | 19 | 81 | 723 | 441 | 410 |

**Table 15 GFL rise and settling time response to fault during system restoration.**

| SCENARIO | GFM CAPACITY (MVA) | ACTIVE POWER RISE TIME (MS) | REACTIVE POWER RISE TIME (MS) | VOLTAGE RISE TIME (MS) | REACTIVE CURRENT RISE TIME (MS) | ACTIVE POWER SETTLING TIME (MS) | REACTIVE POWER SETTLING TIME (MS) | VOLTAGE SETTLING TIME (MS) |
|---|---|---|---|---|---|---|---|---|
| **Base scenario** | 42 | 151 | 23 | 74 | 104 | 3184 | 670 | 534 |
| **Base scenario** | 87.5 | 153 | 22 | 73 | 101 | 2582 | 552 | 311 |
| **Base scenario** | 175 | 136 | 23 | 65 | 93 | 3210 | 311 | 269 |
| **Base scenario** | 262.5 | 9 | 23 | 56 | 92 | 3675 | 323 | 245 |
| **Base scenario** | 350 | 26 | 33 | 16 | 89 | 1600 | 286 | 273 |
| **GFM F droop increased by 2** | 87.5 | 144 | 31 | 61 | 92 | 1507 | 433 | 279 |
| **GFM F droop increased by 3** | 87.5 | 151 | 31 | 55 | 90 | 436 | 331 | 320 |
| **GFM F droop increased by 4** | 87.5 | 147 | 23 | 60 | 89 | 1758 | 491 | 317 |
| **GFL WF offline** | 87.5 | 14 | 31 | 60 | 8 | 3081 | 479 | 280 |
| **With CMPL** | 87.5 | 55 | 145 | 30 | 99 | 1181 | 413 | 286 |
| **With CMPL and DER** | 87.5 | 24 | 71 | 19 | 119 | 1183 | 327 | 309 |
| **With CMPL and DER, inductor switched out** | 87.5 | 26 | 65 | 34 | 152 | 3195 | 2965 | 321 |
| **With CMPL and DER, long fault** | 87.5 | 45 | 82 | 19 | 131 | 310 | 339 | 300 |
| **With CMPL and DER, alternate fault** | 87.5 | 85 | 24 | 81 | 62 | 1331 | 786 | 404 |

**Table 16 GFM reactive current injection rise and settling time response during fault.**

| SCENARIO | GFM CAPACITY (MVA) | RISE TIME (MS) | SETTLING TIME (MS) |
|---|---|---|---|
| **Base scenario** | 42 | 13 | 7107 |
| **Base scenario** | 87.5 | 89 | 413 |
| **Base scenario** | 175 | 43 | 283 |
| **Base scenario** | 262.5 | 58 | 256 |
| **Base scenario** | 350 | 65 | 261 |
| **GFM F droop increased by 2** | 87.5 | 52 | 405 |
| **GFM F droop increased by 3** | 87.5 | 57 | 1135 |
| **GFM F droop increased by 4** | 87.5 | 62 | 437 |

| | | | |
|---|---|---|---|
| **GFL WF offline** | 87.5 | 77 | 282 |
| **With CMPL** | 87.5 | 11 | 308 |
| **With CMPL and DER** | 87.5 | 49 | 551 |
| **With CMPL and DER, inductor switched out** | 87.5 | 19 | 7269 |
| **With CMPL and DER, long fault** | 87.5 | 16 | 338 |
| **With CMPL and DER, alternate fault** | 87.5 | 17 | 453 |

# 4 Conclusions

## 4.1 Large-scale IBR

- Grid-forming BESS as a black start device can support multiple grid-following support devices, transmission lines and transmission level transformers through the restoration process.
  - Transformer energisation may prove to cause challenges for relays due to second order harmonic voltage distortion spikes which could cause maloperation. Further studies with detailed relay models are recommended to confirm.
- A “rule of thumb” GFM black start device to GFL support device ratio of no less than 1 : 10 is recommended.
  - A ratio of 1 : 10 was shown as viable for both “N” and “N-1” levels of system security.
  - Higher ratios (less GFM or more GFL) can be utilised for “N” level system security criteria rather than “N-1”, with multiple OEMs and technology types being stable under ratios up to 1 : 12.
  - A maximum GFM black start device to GFL support device ratio of 1 : 18 was observed for “N” level system security.
  - When system restart failure was observed, in “N” level studies these were due to failed start-up or tripping during energisation of GFL support devices, and in “N-1” level studies they were due to IBR device protection activation following a fault.
- Commonly observed challenges with IBR-only system restart are:
  - Generating system protection activation.
  - GFL IBR fault ride through mode re-triggering that is attributed to reduced voltage stiffness and is exacerbated by high or low network voltage during system restoration process.
  - Active power oscillations between GFM and GFL IBRs have been observed during the system restoration process.
- It is possible for grid-following support devices to provide the majority of active power output to provide frequency control in a restarted island, dependent on frequency droop settings, minimising loading on the black start device and allowing it to respond to fast transients.
- Transformer energisation is not observed to cause under-voltages below existing system normal under-voltage ride through performance requirements for generating systems in the NEM but will cause FRT mode activation on GFL devices during system restoration.

## 4.2 Bottom-up restoration

- GFM BESS black start device locations close to synchronous generators can facilitate the energisation of synchronous generators significantly larger than the GFM BESS by utilising soft energisation. Soft energisation entails the GFM BESS ramping up voltage while already connected to a synchronous generator from 0 pu rather than energising it by closing a circuit breaker when already at 1 pu voltage.

- Two restarted islands, one comprised of a synchronous generator black start device and the other IBR-only with a GFM BESS black start device, are capable of synchronising to each other and operating stably after interconnection.
- Synchronous generator isochronous mode can be used during synchronisation of two restarted islands without exhibiting control system interaction or network instability.

## 4.3 Technical and regulatory requirements

- Incentives or requirements should be developed to encourage proponents to provide IBR EMT models with sufficient detail for inclusion in system restart studies as support devices, regardless of their participation in system restart ancillary service (SRAS) contracts.
  - IBR support device models should include transformer saturation, surge arresters, frequency dependent line models and node-breaker layout where possible.
  - IBR support device models should include energisation or reconnect functionality of plants, both in inverters and PPCs, to ensure they can be started up after long simulation periods without protection activation and reflect physical start-up.
- Existing voltage protection requirements under clause S5.2.5.4 of the NER [6] are considered adequate for system restart conditions, with switching and energisation events on transmission lines, capacitor banks, inductor banks and transformers not observed to cause network voltages to exceed these requirements.
- Network frequency was observed to operate within 49.5 Hz – 50.5 Hz in alignment with the Frequency Operating Standards (FOS) [7] requirements for system restoration and IBRs should be encouraged to provide continuous frequency protection for 49.5 Hz to 50.5 Hz.
  - Current NER clause S5.2.5.3 minimum access standard [6] requires continuous operation within 49.75 Hz to 50.25 Hz, and operation for at least 10min within 49.0 Hz – 51.0 Hz.
  - Network frequency was observed to settle within 49.75 Hz – 50.25 Hz, the continuous frequency operation band, in under 60 seconds across all stable scenarios. It is not recommended that any additional requirements should be implemented.
- Existing typical system normal settings, and rise and settling times, for GFL IBR support devices do not detract from the stability of viability of system restart scenarios. No additional requirements or incentives should be required from GFL IBR beyond additional modelling.
- It is recommended that GFM IBR black start devices apply system restart site-specific control system settings. System normal inertia and damping constant settings were not observed to cause instability or concern but optimisation of the settings for GFM IBR black start devices may improve the likelihood of a system restart scenario. GFM IBR black start performance may not meet existing NER clause minimum access standard S5.2.5.13 [6] rise and settling times and it is recommended to waive these requirements during system restoration if it improves stability.

## 4.4 Impact of distributed energy resources

- DER and composite load models are suitable to evaluate restarted island stability and capability to handle rooftop PV and load shake-off, but further work is required on the models to correctly evaluate their impact to the system as loads and DER systems come back online when energised.
- Composite load models exhibit constant power consumption and a step-change power response to undervoltage conditions, reflective of domestic devices tripping offline, which contrasts to ZIP load model linear or exponential response to voltage and frequency changes. Composite load models are likely to provide less damping to network voltage and frequency oscillations and are recommended for inclusion in all future system restart studies where domestic loads are considered, or where industrial loads do not have a site-specific EMT model available for use.
- DER did not exhibit any transient instabilities or appear to reduce the stability of an IBR-only island during system restoration.
- Material levels of DER disconnection following a fault were observed, in the order of 20% or greater, and should be considered on a case-by-case basis for future system restoration studies.
  - IBR BESS within the restarted island compensated for DER disconnection, but BESS energy availability would need to be monitored under system restart conditions where large amounts of DER are present.
  - No maximum threshold for the amount of DER that can be hosted was identified, and further studies with DER model reconnect feature is recommended.

# 5 Recommendations

Aurecon's recommendation of future work is consistent with our original research plan proposed in 2021, thereafter the most critical items were included in the 2023-2024 research plan and currently being pursued. The list below includes recommended priority items to be addressed as part of the 2024-25 research work.

- Tools and techniques
  - Power system modelling and simulation tools
    - Integrating the response of protective relays into power system dynamic simulation tools for black start and restoration studies.
- Technical and regulatory requirements
  - Dynamic reactive support requirements during system restoration
  - DER response guidelines considering reconnect behaviour and refined limits to supportable levels of DER.
- End-to-end system restoration in power systems with high share of inverter-based resources
  - Restoration from transmission network
    - Bottom-up restoration:
      The coordination of responses of grid-forming black-start IBRs and synchronous generators and condensers during system built up. This includes assessing the risk of sub-synchronous torsional interaction (SSTI) between inverter controls and rotating masses of synchronous machines, and in particular synchronous generators.
    - Top-down restoration:
      The use of HVDC links, both black start (grid-forming) and non-black start capable HVDC links are suggested.
      The extent to which IBRs, whether grid-forming or grid-following, or synchronous condensers nearby an interconnector can facilitate energising one region from a neighbouring region by providing voltage support.
    - Hybrid restoration:
      This generally refers to the simultaneous use of top-down and bottom-up approaches. This means that system restoration will proceed concurrently with the use of designated black start sources in the region under restoration, as well as the use of interconnectors to supplement restoration from adjacent healthy networks.
- Impact on network control and protection systems
  - Impact of control systems
    - Static reactive power support plant

        - Emergency control schemes such as under-frequency load shedding, over-frequency generator shedding, transient power runbacks[5] and system integrity protection schemes[6].
          Note that the intent of this research item is not to assess the role of these emergency control systems in preventing the occurrence of a blackout, but how they can assist or adversely impact system restoration following a black system event.
    - Impact on protection systems
        - Current-based protection such as overcurrent relays and fuses.
        - Impedance-based protection including distance protection.
        - Low frequency demand disconnection (LFDD) caused by a lower inertia and higher RoCoF.
        - Special protection schemes such as power swing blocking and out of step tripping at the transmission network level.
    - Assessing the need for modifications
        - Whether there is a need to use different settings for certain protection systems, including:
        - Whether there is a need to block certain protection systems during system restoration, and if so
        - Whether there is a need to introduce new relay algorithms/protection philosophies.
        - High-level comparison of relative merits of changing protection system device/operating philosophies across the system against changing the requirements for additional fault current by grid-following and in particular grid-forming IBRs to provide sufficient fault current for correct operation of existing relays.
- The treatment of inverter-based resources during system restoration
    - Grid-following inverters
        - Reactive power control at low or no active power.
        - Impact of reactive plant switching including harmonic filters, in particular for HVDC links, during early stages of system restoration.
        - Managing operating reserves.
    - Grid-forming inverters:
      Grid-forming control strategies and their relative merit for system restoration, including the following technologies. As many control strategies as possible should be considered in

[5] A transient power runback is comprised of a signal being sent to a generating system which will activate a reduction in the active power output of the generating system to a pre-defined level.

[6] System integrity schemes are commonly implemented to manage atypical network events, such as loss of multiple transmission lines, which can lead to significant network impact such as load shedding or cascaded tripping of network elements.

2024-25, but likely due to market availability of products not all control strategies can be evaluated in 2024-25.

  - Droop
  - Virtual synchronous machines
  - Power Synchronisation Control
  - Distributed Phased-Locked Loop
  - Direct Power Control

– Grid-forming inverters:

  Comparison of different storage technologies from a supply/load restoration perspective.

– Distributed energy resources

  - Coordination between transmission and distribution system operator/owner(s).

# Appendix A Restarted island stability boundary results

## A.1 Scenario A

**Apx Table A.1 Scenario A energisation sequence.**

| EVENT TIME (S) | DESCRIPTION |
|---|---|
| **3.000s** | Energise 87.5 MVA grid-forming battery substation |
| **4.000s** | Energise 275 kV line |
| **5.000s** | Energise 275 kV terminal station busbar |
| **5.000s** | Energise 275A busbar reactor |
| **6.000s** | Energise 275 kV line |
| **6.000s** | Energise 275 kV line |
| **7.000s** | Energise terminal station busbar (and 275 kV 190 MVA wind farm terminal busbar) |
| **7.000s** | Energise line to 163.8 MVA grid following battery |
| **10.000s** | Energise 163.8 MVA grid-following battery reticulation network |
| **10.000s** | Energise 163.8 MVA grid-following battery inverter transformers |
| **15.000s** | Energise 163.8 MVA grid-following battery inverters |
| **25.000s** | Energise 275 kV line |
| **30.000s** | Energise 275 kV/132 kV transformer |

Link to study raw result figures: Restarted_island_stability_boundary_results_Appendix A.pdf

## A.2 Scenario B

**Apx Table A.2 Scenario B energisation sequence.**

| EVENT TIME (S) | DESCRIPTION |
|---|---|
| **3.000s** | Energise 350 MVA grid-forming battery substation |
| **4.000s** | Energise 275 kV line |
| **5.000s** | Energise 27k kV terminal station busbar |
| **5.000s** | Energise 275A busbar reactor |
| **6.000s** | Energise 275 kV line |
| **6.000s** | Energise 275 kV line |
| **7.000s** | Energise 275 kV terminal station busbar (and 275 kV 190 MVA wind farm terminal busbar) |
| **7.000s** | Energise line to 163.8 MVA grid following battery |
| **10.000s** | Energise 163.8 MVA grid-following battery reticulation network |
| **10.000s** | Energise 163.8 MVA grid-following battery inverter transformers |
| **15.000s** | Energise 163.8 MVA grid-following battery inverters |
| **25.000s** | 190 MVA wind farm terminal busbar |
| **25.000s** | 190 MVA wind farm ENI line |
| **30.000s** | 190 MVA wind farm turbines |
| **35.000s** | Energise 275 kV line |
| **40.000s** | Energise 275 kV/132 kV transformer |

Link to study raw result figures: Restarted_island_stability_boundary_results_Appendix B.pdf

## A.3 Scenario C

**Apx Table A.3 Scenario C energisation sequence.**

| EVENT TIME (S) | DESCRIPTION |
|---|---|
| **3.000s** | Energise 87.5 MVA grid-forming battery substation |
| **4.000s** | Energise 275 kV line |
| **5.000s** | Energise 275k kV terminal station busbar |
| **5.000s** | Energise 275A busbar reactor |
| **6.000s** | Energise 275 kV line |
| **6.000s** | Energise 275 kV line |
| **7.000s** | Energise terminal station busbar (and 275 kV 190 MVA wind farm terminal busbar) |
| **7.000s** | Energise line to 163.8 MVA grid-following battery |
| **10.000s** | Energise 163.8 MVA grid-following battery reticulation network |
| **10.000s** | Energise 163.8 MVA grid-following battery inverter transformers |
| **15.000s** | Energise 163.8 MVA grid-following battery inverters |
| **25.000s** | 275 kV 190 MVA wind farm connection point busbar |
| **25.000s** | 190 MVA wind farm ENI line |
| **30.000s** | 190 MVA wind farm turbines |
| **35.000s** | Energise 275 kV line |
| **40.000s** | Energise 275 kV/132 kV transformer |

Link to study raw result figures: Restarted_island_stability_boundary_results_Appendix C.pdf

## A.4 Scenario D1

**Apx Table A.4 Scenario D1 energisation sequence.**

| EVENT TIME (S) | DESCRIPTION |
|---|---|
| **3.000s** | Energise 87.5 MVA grid-forming battery substation |
| **4.000s** | Energise 275 kV line |
| **5.000s** | Energise 275k kV terminal station busbar |
| **5.000s** | Energise 275A busbar reactor |
| **6.000s** | Energise 275 kV line |
| **6.000s** | Energise 275 kV line |
| **7.000s** | Energise 275k kV terminal station busbar (and 275 kV 190 MVA wind farm terminal busbar) |
| **7.000s** | Energise line to 163.8 MVA grid-following battery |
| **10.000s** | Energise 163.8 MVA grid-following battery reticulation network |
| **10.000s** | Energise 163.8 MVA grid-following battery inverter transformers |
| **15.000s** | Energise 163.8 MVA grid-following battery inverters |
| **25.000s** | 275 kV 190 MVA wind farm connection point busbar |
| **25.000s** | 190 MVA wind farm ENI line |
| **30.000s** | 190 MVA wind farm turbines |
| **35.000s** | 275 kV 304 MVA wind farm connection point busbar |
| **35.000s** | 304 MVA wind farm ENI line |
| **40.000s** | 304 MVA wind farm transformer |
| **45.000s** | Energise 275 kV line |
| **50.000s** | Energise 275 kV/132 kV transformer |

Link to study raw result figures: Restarted_island_stability_boundary_results_Appendix D1.pdf

## A.5 Scenario D2

**Apx Table A.5 Scenario D2 energisation sequence.**

| EVENT TIME (S) | DESCRIPTION |
|---|---|
| **0.0** | 87.5 MVA grid-forming inverter black start of reticulation |
| **4.0** | Energise 275 kV transmission line |
| **5.0** | Energise 88 Mvar substation reactor |
| **6.0** | Energise 2 x 275 kV transmission line |
| **7.0** | Energise 275 kV transmission line to grid-following BESS |
| **10.0** | Energise main grid transformer at grid-following BESS |
| **15.0** | Energise 163.8 MVA grid-following BESS inverters |
| **25.0** | Energise WF main grid transformer |
| **30.0** | Energise 190 MVA WF turbines |
| **40.0** | Energise WF main grid transformer |
| **45.0** | Energise 304 MVA WF turbines |
| **55** | Energise 275 kV transmission line |
| **60** | Energise 275 / 132 kV transformer |

Link to study raw result figures: Restarted_island_stability_boundary_results_Appendix D2.pdf

## A.6 Scenario E

**Apx Table A.6 Scenario E energisation sequence.**

| EVENT TIME (S) | DESCRIPTION |
|---|---|
| **3.000s** | Energise 350 MVA grid-forming battery substation |
| **4.000s** | Energise 275 kV line |
| **5.000s** | Energise 275k kV terminal station busbar |
| **5.000s** | Energise 275A busbar reactor |
| **6.000s** | Energise 275 kV line |
| **6.000s** | Energise 275 kV line |
| **7.000s** | Energise 275k kV terminal station busbar (and 275 kV 190 MVA wind farm terminal busbar) |
| **7.000s** | Energise line to 163.8 MVA grid-following battery |
| **10.000s** | Energise 163.8 MVA grid-following battery reticulation network |
| **10.000s** | Energise 163.8 MVA grid-following battery inverter transformers |
| **15.000s** | Energise 163.8 MVA grid-following battery inverters |
| **25.000s** | 275 kV 190 MVA wind farm connection point busbar |
| **25.000s** | 190 MVA wind farm ENI line |
| **30.000s** | 190 MVA wind farm turbines |
| **35.000s** | 275 kV 304 MVA wind farm connection point busbar |
| **35.000s** | 304 MVA wind farm ENI line |
| **40.000s** | 304 MVA wind farm transformer |
| **45.000s** | Energise 275 kV line |
| **50.000s** | Energise 275 kV/132 kV transformer |

Link to study raw result figures: Restarted_island_stability_boundary_results_Appendix E.pdf

## A.7 Scenario F

**Apx Table A.7 Scenario F energisation sequence.**

| EVENT TIME (S) | DESCRIPTION |
|---|---|
| **3.000s** | Energise 47.04 MVA grid-forming battery substation |
| **4.000s** | Energise 275 kV line |
| **5.000s** | Energise 275k kV terminal station busbar |
| **5.000s** | Energise 275A busbar reactor |
| **6.000s** | Energise 275 kV line |
| **6.000s** | Energise 275 kV line |
| **7.000s** | Energise 275k kV terminal station busbar (and 275 kV 190 MVA wind farm terminal busbar) |
| **7.000s** | Energise line to 163.8 MVA grid-following battery |
| **10.000s** | Energise 163.8 MVA grid-following battery reticulation network |
| **10.000s** | Energise 163.8 MVA grid-following battery inverter transformers |
| **15.000s** | Energise 163.8 MVA grid-following battery inverters |
| **25.000s** | 275 kV 190 MVA wind farm connection point busbar |
| **25.000s** | 190 MVA wind farm ENI line |
| **30.000s** | 190 MVA wind farm turbines |
| **35.000s** | 275 kV 304 MVA wind farm connection point busbar |
| **35.000s** | 304 MVA wind farm ENI line |
| **40.000s** | 304 MVA wind farm transformer |
| **45.000s** | Energise 275 kV line |
| **50.000s** | Energise 275 kV/132 kV transformer |

Link to study raw result figures: Restarted_island_stability_boundary_results_Appendix F.pdf

## A.8 Scenario G

**Apx Table A.8 Scenario G energisation sequence.**

| EVENT TIME (S) | DESCRIPTION |
|---|---|
| **3.000s** | Energise 36.7 MVA grid-forming battery substation |
| **4.000s** | Energise 275 kV line |
| **5.000s** | Energise 275k kV terminal station busbar |
| **5.000s** | Energise 275A busbar reactor |
| **6.000s** | Energise 275 kV line |
| **6.000s** | Energise 275 kV line |
| **7.000s** | Energise 275k kV terminal station busbar (and 275 kV 190 MVA wind farm terminal busbar) |
| **7.000s** | Energise line to 163.8 MVA grid-following battery |
| **10.000s** | Energise 163.8 MVA grid-following battery reticulation network |
| **10.000s** | Energise 163.8 MVA grid-following battery inverter transformers |
| **15.000s** | Energise 163.8 MVA grid-following battery inverters |
| **25.000s** | 275 kV 190 MVA wind farm connection point busbar |
| **25.000s** | 190 MVA wind farm ENI line |
| **30.000s** | 190 MVA wind farm turbines |
| **35.000s** | 275 kV 304 MVA wind farm connection point busbar |
| **35.000s** | 304 MVA wind farm ENI line |
| **40.000s** | 304 MVA wind farm transformer |
| **45.000s** | Energise 275 kV line |
| **50.000s** | Energise 275 kV/132 kV transformer |

Link to study raw result figures: Restarted_island_stability_boundary_results_Appendix G.pdf

## A.9 Scenario H

**Apx Table A.9 Scenario H energisation sequence.**

| EVENT TIME (S) | DESCRIPTION |
|---|---|
| **3.000s** | Energise 36.69 MVA grid-forming battery substation |
| **4.000s** | Energise 275 kV line |
| **5.000s** | Energise 275k kV terminal station busbar |
| **5.000s** | Energise 275A busbar reactor |
| **6.000s** | Energise 275 kV line |
| **6.000s** | Energise 275 kV line |
| **7.000s** | Energise 275k kV terminal station busbar (and 275 kV 190 MVA wind farm terminal busbar) |
| **7.000s** | Energise line to 163.8 MVA grid-following battery |
| **10.000s** | Energise 163.8 MVA grid-following battery reticulation network |
| **10.000s** | Energise 163.8 MVA grid-following battery inverter transformers |
| **15.000s** | Energise 163.8 MVA grid-following battery inverters |
| **25.000s** | 275 kV 190 MVA wind farm connection point busbar |
| **25.000s** | 190 MVA wind farm ENI line |
| **30.000s** | 190 MVA wind farm turbines |
| **35.000s** | 275 kV 304 MVA wind farm connection point busbar |
| **35.000s** | 304 MVA wind farm ENI line |
| **40.000s** | 304 MVA wind farm transformer |
| **45.000s** | Energise 275 kV line |
| **50.000s** | Energise 275 kV/132 kV transformer |

Link to study raw result figures: Restarted_island_stability_boundary_results_Appendix H.pdf

## A.10 Scenario I

**Apx Table A.10 Scenario I energisation sequence.**

| EVENT TIME (S) | DESCRIPTION |
|---|---|
| **3.000s** | Energise 87.5 MVA grid-forming battery substation |
| **4.000s** | Energise 275 kV line |
| **5.000s** | Energise 275k kV terminal station busbar |
| **5.000s** | Energise 275A busbar reactor |
| **6.000s** | Energise 275 kV line |
| **6.000s** | Energise 275 kV line |
| **7.000s** | Energise 275k kV terminal station busbar (and 275 kV 190 MVA wind farm terminal busbar) |
| **7.000s** | Energise line to 163.8 MVA grid-following battery |
| **10.000s** | Energise 163.8 MVA grid-following battery reticulation network |
| **10.000s** | Energise 163.8 MVA grid-following battery inverter transformers |
| **15.000s** | Energise 163.8 MVA grid-following battery inverters |
| **25.000s** | 275 kV 121 MVA solar farm connection point busbar |
| **25.000s** | 121 MVA solar farm ENI line |
| **30.000s** | 121 MVA solar farm turbines |
| **35.000s** | 275 kV 304 MVA wind farm connection point busbar |
| **35.000s** | 304 MVA wind farm ENI line |
| **40.000s** | 304 MVA wind farm transformer |
| **45.000s** | Energise 275 kV line |
| **50.000s** | Energise 275 kV/132 kV transformer |

Link to study raw result figures: Restarted_island_stability_boundary_results_Appendix I.pdf

## A.11 Scenario J

**Apx Table A.11 Scenario J energisation sequence.**

| EVENT TIME (S) | DESCRIPTION |
|---|---|
| **3.000s** | Energise 87.5 MVA grid-forming battery substation |
| **4.000s** | Energise 275 kV line |
| **5.000s** | Energise 275k kV terminal station busbar |
| **5.000s** | Energise 275A busbar reactor |
| **6.000s** | Energise 275 kV line |
| **6.000s** | Energise 275 kV line |
| **7.000s** | Energise 275k kV terminal station busbar (and 275 kV 190 MVA wind farm terminal busbar) |
| **7.000s** | Energise line to 163.8 MVA grid-following battery |
| **10.000s** | Energise 163.8 MVA grid-following battery reticulation network |
| **10.000s** | Energise 163.8 MVA grid-following battery inverter transformers |
| **15.000s** | Energise 163.8 MVA grid-following battery inverters |
| **25.000s** | 275 kV 121 MVA solar farm connection point busbar |
| **25.000s** | 121 MVA solar farm ENI line |
| **30.000s** | 121 MVA solar farm turbines |
| **35.000s** | 275 kV 452.89 MVA wind farm connection point busbar |
| **35.000s** | 452.89 MVA wind farm ENI line |
| **40.000s** | 452.89 MVA wind farm transformer |
| **45.000s** | Energise 275 kV line |
| **50.000s** | Energise 275 kV/132 kV transformer |

Link to study raw result figures: Restarted_island_stability_boundary_results_Appendix J.pdf

## A.12 Scenario K

**Apx Table A.12 Scenario K energisation sequence.**

| EVENT TIME (S) | DESCRIPTION |
|---|---|
| **3.000s** | Energise 87.5 MVA grid-forming battery substation |
| **4.000s** | Energise 275 kV line |
| **5.000s** | Energise 275k kV terminal station busbar |
| **5.000s** | Energise 275A busbar reactor |
| **6.000s** | Energise 275 kV line |
| **6.000s** | Energise 275 kV line |
| **7.000s** | Energise 275k kV terminal station busbar (and 275 kV 190 MVA wind farm terminal busbar) |
| **7.000s** | Energise line to 163.8 MVA grid-following battery |
| **10.000s** | Energise 163.8 MVA grid-following battery reticulation network |
| **10.000s** | Energise 163.8 MVA grid-following battery inverter transformers |
| **15.000s** | Energise 163.8 MVA grid-following battery inverters |
| **25.000s** | 275 kV 121 MVA solar farm connection point busbar |
| **25.000s** | 121 MVA solar farm ENI line |
| **30.000s** | 121 MVA solar farm turbines |
| **35.000s** | 275 kV 180 MVA wind farm connection point busbar |
| **35.000s** | 180 MVA wind farm ENI line |
| **40.000s** | 180 MVA wind farm transformer |
| **45.000s** | Energise 275 kV line |
| **50.000s** | Energise 275 kV/132 kV transformer |

Link to study raw result figures: Restarted_island_stability_boundary_results_Appendix K.pdf

## A.13 Scenario L

**Apx Table A.13 Scenario L energisation sequence.**

| EVENT TIME (S) | DESCRIPTION |
|---|---|
| **3.000s** | Energise 87.5 MVA grid-forming battery substation |
| **4.000s** | Energise 275 kV line |
| **5.000s** | Energise 275k kV terminal station busbar |
| **5.000s** | Energise 275A busbar reactor |
| **6.000s** | Energise 275 kV line |
| **6.000s** | Energise 275 kV line |
| **7.000s** | Energise 275k kV terminal station busbar (and 275 kV 190 MVA wind farm terminal busbar) |
| **7.000s** | Energise line to 163.8 MVA grid-following battery |
| **10.000s** | Energise 163.8 MVA grid-following battery reticulation network |
| **10.000s** | Energise 163.8 MVA grid-following battery inverter transformers |
| **15.000s** | Energise 163.8 MVA grid-following battery inverters |
| **25.000s** | 275 kV 190 MVA solar farm connection point busbar |
| **25.000s** | 190 MVA solar farm ENI line |
| **30.000s** | 190 MVA solar farm turbines |
| **35.000s** | 275 kV 304 MVA wind farm connection point busbar |
| **35.000s** | 304 MVA wind farm ENI line |
| **40.000s** | 304 MVA wind farm transformer |
| **50.000s** | Energise 275 kV Line |
| **50.000s** | Energise 275kV busbars |
| **55.000s** | Energise 230MVA SVC ENI line |
| **60.000s** | Energise 230MVA SVC |
| **65.000s** | Energise 275 kV/132 kV transformer |
| **70.000s** | Energise 150MVA SVC ENI line |
| **75.000s** | Energise 150 MVA SVC |

Link to study raw result figures: Restarted_island_stability_boundary_results_Appendix L.pdf

## A.14 Scenario M

**Apx Table A.14 Scenario M energisation sequence.**

| EVENT TIME (S) | DESCRIPTION |
|---|---|
| **1.000s** | Energise 87.5 MVA grid-forming battery substation |
| **2.000s** | Energise 275 kV line |
| **3.000s** | Energise 275k kV terminal station busbar |
| **3.000s** | Energise 275A busbar reactor |
| **6.000s** | Energise 275 kV line |
| **6.000s** | Energise 275 kV line |
| **12.000s** | Energise 275 kV line |
| **14.000s** | Energise 275 kV terminal station busbars |
| **14.000s** | Energise 230 MVA SVC ENI line |
| **16.000s** | Energise 230 MVA SVC |
| **18.000s** | Energise 275k kV terminal station busbar (and 275 kV 190 MVA wind farm terminal busbar) |
| **18.000s** | Energise line to 163.8 MVA grid-following battery |
| **18.000s** | Energise 163.8 MVA grid-following battery reticulation network |
| **20.000s** | Energise 163.8 MVA grid-following battery inverter transformers |
| **20.000s** | Energise 163.8 MVA grid-following battery inverters |
| **35.000s** | 275 kV 190 MVA wind farm connection point busbar |
| **35.000s** | 190 MVA wind farm ENI line |
| **40.000s** | 190 MVA wind farm turbines |
| **45.000s** | 275 kV 304 MVA wind farm connection point busbar |
| **45.000s** | 304 MVA wind farm ENI line |
| **50.000s** | 304 MVA wind farm transformer |
| **60.000s** | Energise 275 kV line |
| **60.000s** | Energise 275 kV/132 kV transformer |

Link to study raw result figures: Restarted_island_stability_boundary_results_Appendix M.pdf

## A.15 Scenario N

**Apx Table A.15 Scenario N energisation sequence.**

| EVENT TIME (S) | DESCRIPTION |
|---|---|
| **1.000s** | Energise 37.5 MVA grid-forming battery substation |
| **2.000s** | Energise 275 kV line |
| **3.000s** | Energise 275k kV terminal station busbar |
| **3.000s** | Energise 275A busbar reactor |
| **6.000s** | Energise 275 kV line |
| **6.000s** | Energise 275 kV line |
| **12.000s** | Energise 275 kV line |
| **14.000s** | Energise 275 kV busbars |
| **14.000s** | Energise 230 MVA SVC ENI line |
| **16.000s** | Energise 230 MVA SVC |
| **18.000s** | Energise 275k kV terminal station busbar (and 275 kV 190 MVA wind farm terminal busbar) |
| **18.000s** | Energise line to 163.8 MVA grid-following battery |
| **18.000s** | Energise 163.8 MVA grid-following battery reticulation network |
| **20.000s** | Energise 163.8 MVA grid-following battery inverter transformers |
| **20.000s** | Energise 163.8 MVA grid-following battery inverters |
| **35.000s** | 275 kV 190 MVA wind farm connection point busbar |
| **35.000s** | 190 MVA wind farm ENI line |
| **40.000s** | 190 MVA wind farm turbines |
| **45.000s** | 275 kV 304 MVA wind farm connection point busbar |
| **45.000s** | 304 MVA wind farm ENI line |
| **50.000s** | 304 MVA wind farm transformer |
| **60.000s** | Energise 275 kV line |
| **60.000s** | Energise 275 kV/132 kV transformer |

Link to study raw result figures: Restarted_island_stability_boundary_results_Appendix N.pdf

# Appendix B Restarted island fault study

## B.1 Scenario A1

Link to study raw result figures: Fault_Study_Appendix A1.pdf

## B.2 Scenario A2

Link to study raw result figures: Fault_Study_Appendix A2.pdf

## B.3 Scenario B1

Link to study raw result figures: Fault_Study_Appendix B1.pdf

## B.4 Scenario B2

Link to study raw result figures: Fault_Study_Appendix B2.pdf

## B.5 Scenario C1

Link to study raw result figures: Fault_Study_Appendix C1.pdf

## B.6 Scenario C2

Link to study raw result figures: Fault_Study_Appendix C2.pdf

## B.7 Scenario D1

Link to study raw result figures: Fault_Study_Appendix D1.pdf

## B.8 Scenario D2

Link to study raw result figures: Fault_Study_Appendix D2.pdf

## B.9 Scenario E1

Link to study raw result figures: Fault_Study_Appendix E1.pdf

## B.10 Scenario E2

Link to study raw result figures: Fault_Study_Appendix E2.pdf

# Appendix C Grid-forming BESS frequency control

## C.1 Scenario A

Link to study raw result figures: GFM_F_Droop_2.0Perc_Appendix A.pdf

## C.2 Scenario B

Link to study raw result figures: GFM_F_Droop_3.0Perc_Appendix B.pdf

## C.3 Scenario C

Link to study raw result figures: GFM_F_Droop_3.5Perc_Appendix C.pdf

## C.4 Scenario D

Link to study raw result figures: GFM_350MVA_F_Droop_3.5Perc_Appendix D.pdf

# Appendix D GFM voltage control sensitivity

## D.1 Scenario A

Link to study raw result figures: GFM_V_Droop_1.0Perc_Appendix_A.pdf

## D.2 Scenario B

Link to study raw result figures: GFM_V_Droop_3.0Perc_Appendix_B.pdf

## D.3 Scenario C

Link to study raw result figures: GFM_V_Droop_5.0Perc_Appendix_C.pdf

## D.4 Scenario D

Link to study raw result figures: GFM_V_Droop_7.0Perc_Appendix_D.pdf

## D.5 Scenario E

Link to study raw result figures: GFM_V_Droop_9.0Perc_Appendix_E.pdf

## D.6 Scenario F

Link to study raw result figures: GFM_V_Droop_11.0Perc_Appendix_F.pdf

# Appendix E Grid-forming BESS Inertia and Damping Constants Sensitivity

## E.1 Scenario A

Link to study raw result figures: GFM_BESS_D_5_H_1_Appendix A.pdf

## E.2 Scenario B

Link to study raw result figures: GFM_BESS_D_5_H_2_Appendix B.pdf

## E.3 Scenario C

Link to study raw result figures: GFM_BESS_D_5_H_3_Appendix C.pdf

## E.4 Scenario D

Link to study raw result figures: GFM_BESS_D_5_H_8_Appendix D.pdf

## E.5 Scenario E

Link to study raw result figures: GFM_BESS_D_5_H_10_Appendix E.pdf

## E.6 Scenario F

Link to study raw result figures: GFM_BESS_D_6_H_8_Appendix F.pdf

# Appendix F Grid-following BESS Frequency Control

## F.1 Scenario A

Link to study raw result figures: GFM_F_Droop_1.7Perc_Appendix A.pdf

## F.2 Scenario B

Link to study raw result figures: GFM_F_Droop_3.0Perc_Appendix B.pdf

## F.3 Scenario C

Link to study raw result figures: GFL_F_Droop_3.0Perc_GFM_350MVA_Appendix C.pdf

## F.4 Scenario D

Link to study raw result figures: GFL_F_Droop_4.0Perc_Appendix D.pdf

# Appendix G Island synchronisation study results

## G.1 Scenario A

Link to study raw result figures: Island synchronisation study_Appendix_A.pdf

## G.2 Scenario B

Link to study raw result figures: Island synchronisation study_Appendix_B.pdf

## G.3 Scenario C

Link to study raw result figures: Island synchronisation study_Appendix_C.pdf

# Appendix H Network active power oscillations – GFM size sensitivity

## H.1 Scenario A

Link to study raw result figures: GFM 42.3MVA_Appendix_A.pdf

## H.2 Scenario B

Link to study raw result figures: GFM 87.5MVA_Appendix_B.pdf

## H.3 Scenario C

Link to study raw result figures: GFM 175MVA_Appendix_C.pdf

## H.4 Scenario D

Link to study raw result figures: GFM 262.5MVA_Appendix_D.pdf

## H.5 Scenario E

Link to study raw result figures: GFM 350MVA_Appendix_E.pdf

# Appendix I Network active power oscillations – frequency droop sensitivity

## I.1 Scenario A

Link to study raw result figures: GFL Droop 2.4_Appendix_A.pdf

## I.2 Scenario B

Link to study raw result figures: GFL Droop 3.6_Appendix_B.pdf

## I.3 Scenario C

Link to study raw result figures: GFL Droop 4.8_Appendix_C.pdf

## I.4 Scenario D

Link to study raw result figures: GFL Droop 1.2_Appendix_D.pdf

# Appendix J Composite load model and DER model studies

## J.1 Scenario A

Link to study raw result figures: CMPL Second Location 3phg 0.00001ohm XR 3 0.12s (Inductor Off)_Appendix_A.pdf

## J.2 Scenario B

Link to study raw result figures: CMPL Second Location 3phg 0.00001ohm XR 3 0.12s (Inductor On)_Appendix_B.pdf

## J.3 Scenario C

Link to study raw result figures: CMPL Stable 2phg 0.1ohms XR 3 0.12s_Appendix_C.pdf

## J.4 Scenario D

Link to study raw result figures: CMPL DER 3phg 0.00001ohms XR 3 0.12s_Appendix_D.pdf

## J.5 Scenario E

Link to study raw result figures: CMPL 2phg 0.1ohms XR 3 0.12s Full Duration_Appendix_E.pdf

## J.6 Scenario F

Link to study raw result figures: ZIP 2phg 0.1ohms XR 3 0.12s_Appendix_F.pdf

# Glossary

| ABBREVIATION | DEFINITION |
|---|---|
| **AC** | Alternating Current |
| **AEMO** | Australian Energy Market Operator |
| **BESS** | Battery Energy Storage System |
| **CSIRO** | Commonwealth Scientific and Industrial Research Organisation |
| **DC** | Direct Current |
| **DER** | Distributed Energy Resources |
| **EMT** | Electromagnetic Transient |
| **EMTDC** | Electromagnetic Transient Direct Current |
| **FACTS** | Flexible AC Transmission System |
| **FNQLD** | Far North Queensland |
| **FOS** | Frequency Operating Standards |
| **FRT** | Fault Ride Through |
| **GFL** | Grid Following (inverter) |
| **GFM** | Grid Forming (inverter) |
| **G-PST** | Global Power System Transformation |
| **HVRT** | High Voltage Ride Through |
| **IBR** | Inverter Based Resource |
| **km** | Kilometre |
| **kV** | Kilovolt |
| **LVRT** | Low Voltage Ride Through |
| **MVA** | Megavolt Amperes |
| **Mvar** | Megavolt Amperes Reactive |
| **MW** | Megawatt |
| **MWh** | Megawatt-hour |
| **NEM** | National Electricity Market |
| **NER** | National Electricity Rules |
| **NQLD** | North Queensland |
| **NQREZ** | North Queensland Renewable Energy Zone |
| **NSP** | Network Service Provider |
| **OEM** | Original Equipment Manufacturer |
| **PPC** | Power Plant Controller |
| **PSCAD** | Power System Computer Aided Design |
| **PV** | Photovoltaic |
| **REZ** | Renewable Energy Zone |

| | |
|---|---|
| **SCR** | Short Circuit Ratio |
| **SF** | Solar Farm |
| **SRAS** | System Restart Ancillary Services |
| **SVC** | Static Var Compensator |
| **SynCon** | Synchronous Condenser |
| **WF** | Wind Farm |

# References


[1] Aurecon, “The Role of Inverter-Based Resources During System Restoration,” CSIRO, 2023.

[2] M. Myers, “2023-27 Powerlink Queensland Revised Revenue Proposal,” PowerLink, Queensland, Novenber-2021.

[3] AEMO, “PSS®E models for load and distributed PV in the NEM,” 2022.

[4] AEMO, “Behaviour of distributed resources during power system disturbances,” 2021.

[5] CSIRO Energise Insight, “Household types and energy use,” 2018.

[6] AEMC, *National Electricity Rules, Version 209,* 2024.

[7] Relibility Panel AEMC, *Frequency Operating Standards,* 2023.

[8] M. Myers, “2023-27 Powerlink Queensland Revenue Proposal,” PowerLink, Queensland, November-2021.

**As Australia's national science agency and innovation catalyst, CSIRO is solving the greatest challenges through innovative science and technology.**

CSIRO. Unlocking a better future for everyone.

**Contact us**

1300 363 400
+61 3 9545 2176
csiro.au/contact
csiro.au

Document prepared by

**Aurecon Australasia Pty Ltd**
ABN 54 005 139 873
Aurecon Centre
Level 8, 850 Collins Street
Docklands, Melbourne VIC 3008
PO Box 23061
Docklands VIC 8012
Australia

**T** +61 3 9975 3000
**F** +61 3 9975 3444
**E** melbourne@aurecongroup.com
**W** aurecongroup.com

aurecon
Bringing ideas to life